Terms and Conditions of Use of Digitised Theses from Trinity College Library Dublin

Copyright statement

All material supplied by Trinity College Library is protected by copyright (under the Copyright and Related Rights Act, 2000 as amended) and other relevant Intellectual Property Rights. By accessing and using a Digitised Thesis from Trinity College Library you acknowledge that all Intellectual Property Rights in any Works supplied are the sole and exclusive property of the copyright and/or other IPR holder. Specific copyright holders may not be explicitly identified. Use of materials from other sources within a thesis should not be construed as a claim over them.

A non-exclusive, non-transferable licence is hereby granted to those using or reproducing, in whole or in part, the material for valid purposes, providing the copyright owners are acknowledged using the normal conventions. Where specific permission to use material is required, this is identified and such permission must be sought from the copyright holder or agency cited.

Liability statement

By using a Digitised Thesis, I accept that Trinity College Dublin bears no legal responsibility for the accuracy, legality or comprehensiveness of materials contained within the thesis, and that Trinity College Dublin accepts no liability for indirect, consequential, or incidental, damages or losses arising from use of the thesis for whatever reason. Information located in a thesis may be subject to specific use constraints, details of which may not be explicitly described. It is the responsibility of potential and actual users to be aware of such constraints and to abide by them. By making use of material from a digitised thesis, you accept these copyright and disclaimer provisions. Where it is brought to the attention of Trinity College Library that there may be a breach of copyright or other restraint, it is the policy to withdraw or take down access to a thesis while the issue is being resolved.

Access Agreement

By using a Digitised Thesis from Trinity College Library you are bound by the following Terms & Conditions. Please read them carefully.

I have read and I understand the following statement: All material supplied via a Digitised Thesis from Trinity College Library is protected by copyright and other intellectual property rights, and duplication or sale of all or part of any of a thesis is not permitted, except that material may be duplicated by you for your research use or for educational purposes in electronic or print form providing the copyright owners are acknowledged using the normal conventions. You must obtain permission for any other use. Electronic or print copies may not be offered, whether for sale or otherwise to anyone. This copy has been supplied on the understanding that it is copyright material and that no quotation from the thesis may be published without proper acknowledgement.

Synthesis and Biological Activity of 9-Azapaullone, its *N*-oxide and *N*-benzyl Derivatives

A thesis submitted to the University of Dublin for the degree of Doctor of Philosophy

by

David Power B. A. (Mod.)

Under the supervision of

Prof. Stephen Connon

2011

Trinity College Dublin

Declaration

I declare that this work has not been submitted as an exercise for degree at this or any other university, and that it is entirely my own work. Due acknowledgements and references are given to the work of others. I agree that the
Library may lend or copy this thesis upon request

Power

Summary

Cancer is a serious and life-threatening disease that accounts for 13 % of deaths each year. It is a complicated process with many factors and variations observed, however research has uncovered many new strategies for the treatment of this disease. A recently initiated strategy is molecular targeted therapy; this involves the targeting of relevant biomolecules such as receptors and enzymes that have a role to play in the development of cancer. This strategy has yielded several new drugs that are currently approved for treatment of patients.

One such strategy involves the targeting of an important cellular system, the cell cycle. This is a system that controls the rate of cell division, and it is often deregulated in cancer. For this reason it is an apt choice for therapeutic intervention; to target the kinases (named Cyclin-dependent kinases, CDKs, which form complexes with their cyclin partners) that are involved in this system. A class of compounds, named paullones, have been demonstrated to be effective inhibitors of these kinases. The present work was concerned with synthesising novel paullones shown below and evaluating their ability to inhibit CDKs.

83

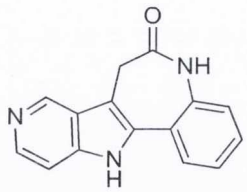

82

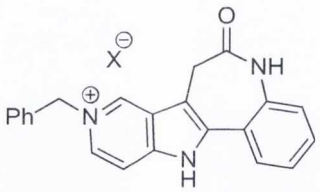

84

Of the compounds that were synthesised and tested for their inhibitory activity against a panel of CDKs and other relevant kinases, *N*-oxide **83** was found to have remarkable selectivity for CDK9/cyclin T, which is a kinase involved in transcription and has been connected with viral diseases such as HIV. This improved selectivity is a new finding for this class of inhibitor.

Publication:

Concise synthesis and CDK/GSK inhibitory activity of the missing 9-azapaullones, D. P. Power, O. Lozach, L. Meijer, D. H. Grayson and S. J. Connon, *Bioorg. Med. Chem. Lett.*, 2010, **20**, 4940–4944.

Acknowledgements

First and foremost, my sincerest thanks are offered to Professors Stephen Connon and David Grayson, for all their sound advice and encouragement throughout this long endeavour.

Also to all in the Connon group, past and present for a great shared experience during my time there: Ciaran, Shay, Eimear, Sarah, Barbara, Conor, Aldo, Ollie, Jen, Sarah, Alessandro, Cormac, Carole and everyone else that's been in lab 0.14 over the years. Special thanks to Jen and Sarah for proof-reading, it was a tremendous help.

To the technical staff in the school of chemistry for making everything run smoothly, Drs John O'Brien and Manuel Ruether, Martin Feeney, Peggy, Brendan, Dorothy, Teresa and Fred.

Lastly, to my family and friends for all their love and support.

Abbreviations

AIBN	Azobisisobutyronitrile
atm	Atmosphere
ATP	Adenosine 5'-triphosphate
Boc	*tert*-Butoxycarbonyl
br s	Broad singlet
cat.	Catalyst
CAK	Cyclin activating kinase
CDK	Cyclin dependent kinase
CDKi	Cyclin dependent Kinase Inhibitor
CoMSIA	Comparative Molecular Similarity Indices Analysis
COSY	Correlation Spectroscopy
d	Doublet
DBU	1,8-Diazabicyclo[5.4.0]undec-7-ene
DCM	Dichloromethane
dd	Double doublet
DMAP	Dimethyl amino pyridine
DMF	*N*,*N*-dimethylformamide
DMSO	Dimethyl sulfoxide
DNA	Deoxyribonucleic acid
dt	Doublet triplet
equiv.	Equivalents
ESI	Electrospray Ionisation
GI_{50}	50% growth inhibition
GSK	Glygogen synthase kinase
HMBC	Heteronuclear Multiple Bond Coherence
HSQC	Heteronuclear Single Quantum Coherence
HRMS	High Resolution Mass Spectroscopy
Hz	Hertz
IC_{50}	50% Inhibitory Concentration
IPA	iso-propyl alcohol
IR	Infrared

J	Coupling constant
m	Multiplet
M	Molar
m	Meta
mCPBA	*m*-Chloroperoxybenzoic acid
MPLC	Medium Pressure Liquid Chromatography
MW	Microwave
NOE	Nuclear Overhauser effect
NMR	Nuclear magnetic resonance
NCI	National Cancer Institute
o	Ortho
p	Para
PPA	Polyphosphoric acid
pRB	Retinoblastoma protein
*p*TSA	*p*-Toluenesulfonic acid
q	Quartet
QSAR	Quantitative Structure-Activity Relationships
RaNi	Raney Nickel
RT	Room temperature
s	Singlet
t	Triplet
TBAF	Tetrabutyl ammonium fluoride
TEA	Triethylamine
TFA	Trifluoroacetic acid
THF	Tetrahydrofuran
TIPS	Triisopropylsilyl
TLC	Thin-layer chromatography
TMS	Trimethylsilyl
TOCSY	Total Correlation Spectroscopy

Table of Contents

Introduction

Introduction

1.1 Cancer and the Cell Cycle

All cells can grow and divide; thus producing progeny that are an exact replica. First, they must grow in size until they are large enough to produce two sufficiently sized daughter cells, then they replicate their DNA. This genetic information constitutes the instruction manual that a cell requires to function throughout its lifespan. Once this has been done accurately, with errors and damage repaired if possible, the physical splitting apart of the cell into two separate entities can commence. Cells in multicellular organisms need to retain this innate function for growth and repair, but tight regulation must be exercised over the type and number of cells within the organ, which ultimately determines the size of the organism. If this regulation fails the cells will continue to grow and divide under their own autonomy, regardless of external factors such as sufficient space and the supply of nutrients in the micro-environment surrounding the cell, and this malfunction is the basis for many human tumours. The cell cycle is the 'clock' by which cells regulate the timing of the important function of division and incorporates strict checkpoints that must be traversed to complete a cell's default mission of grow and divide.

Due to the strict regulation in the integrity of the genome and division, mutations that take hold and cause cancer should be very rare events, however it takes only one cell out of a vast number to lose or relax the controlling mechanisms for the disease to take hold. Thereupon the rate of mutation in nascent cancer cells needs to become much higher than normal cells, and they must be able to bypass the increasingly slack controls to allow for a cascade of detrimental changes to proceed. The ultimate result is a disease that affected 11.3 million new patients in 2007 and which is predicted to rise to 15.5 million by 2030. It accounts for 13% of deaths worldwide: 7.4 million in 2004, 7.9 million in 2007 and is projected to reach 11.5 million in 2030, attributed to an ageing population despite improvements in available treatment.[1]

1.1.1 Hallmarks of Cancer

The 'hallmarks of cancer' is a seminal review by Weinberg and Hanahan,[2] it is very informative in helping the reader understand where a particular piece of research fits in the hugely complicated and expansive field of cancer research (Figure 1.1). Accordingly it is used by many researchers, as evidenced by the enormous number of citations it has received. [3]

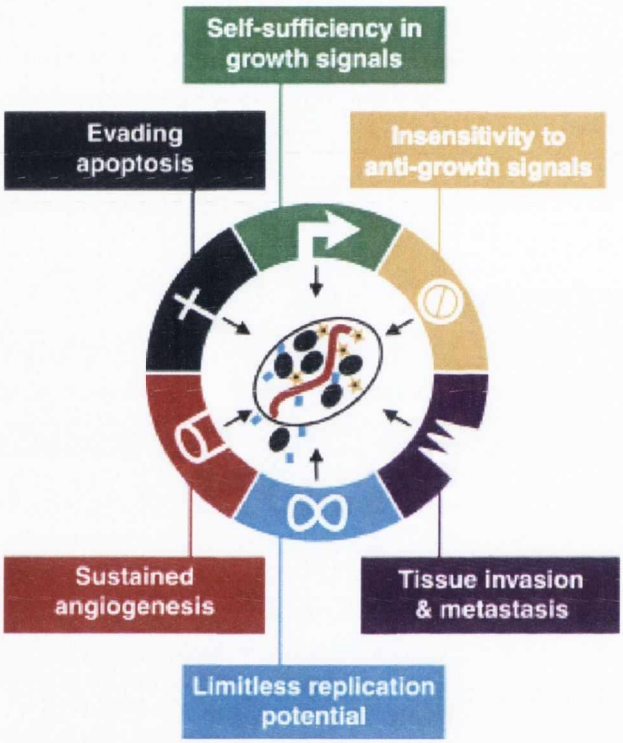

Figure 1.1: The six hallmarks of cancer.[2]

Most if not all cancer cells can acquire every one of the following features in any order, the mechanism for different tumours will vary, though certainly it is a multi-step process to reach a malignant state. A diagram depicting the six hallmarks is shown in Figure 1.1.

1) ***Self-sufficiency in Growth Signals*****:** All normal cells must receive growth signals from outside if they are to divide, otherwise they will remain in a quiescent (resting, non-dividing) state. In contrast, cancer cells can acquire the ability to synthesise or co-

opt their neighbouring cells to produce growth factors to which they can respond; to over-express the growth factor receptors or express receptors that are constitutively active; or effectors downstream of these receptors can become disrupted, *i.e.* the intracellular signalling pathways (see Section 1.1.2).

2) *Insensitivity to Antigrowth Signals*: In normal tissue anti-growth factors are in place to prevent cells dividing under their own autonomy. Most of the components of this system converge on the preliminary stage (named G1) of the cell cycle. In this stage, the cell is monitoring the levels of antigrowth signals, either in preparation of entry to the cell cycle or remaining in a quiescent state. This hallmark is of particular interest to the current work, and the components will be discussed further later (Sections 1.1.2 and 1.1.3).

3) *Evading Apoptosis*: While the two preceding hallmarks were concerned with the proliferation of cells, cancer cells need also to avoid the inherent cell-death mechanisms (apoptosis) that would prevent their expansion. Survival and death factors from outside the cell, disruptions and stresses encountered inside the cell such as DNA damage initiate apoptosis, which results in the cellular structure and components broken down and engulfed by surrounding cells. This feature is connected to the first two, as it is one of the resulting states a cell can attain; the other states are proliferation, senescence and differentiation.

4) ***Limitless Replication Potential*:** A distinct system is in place to prevent a rapid expansion in cell populations; it is separate from the cell signalling pathways involved in the first three hallmarks. A normal cell can divide 60-70 times, and this number of division is counted by telomeres; guanine rich sequences at the end of chromosomes which loses 50-100 base pairs per division, until eventually the telomeres fail in their normal role of protecting the end of the chromosomes. Cancer cells can maintain the telomeres by a number of methods, thus becoming immortal.

5) ***Sustained Angiogenesis*:** Nearly all cells need to be in close proximity to blood capillaries to receive the oxygen and nutrients they require to grow and survive. Creating blood capillaries is a tightly regulated process, which a rapidly growing tumour must circumvent if it is to continue expanding.

6) ***Tissue Invasion and Metastasis*:** Metastasis is when cancer cells acquire the ability to leave the tissue in which they formed and travel to other organs, either migrating to adjacent sites or by entering blood and lymph vessels to reach distant sites. It is when tumours have metastasised that patients receive the poorest prognosis.

In addition, for cancer cells to acquire each of these capabilities, another enabling characteristic is needed: ***Genomic Instability***. Under normal circumstances the six hallmarks are very difficult to acquire due to the innate system of checks-and-balances that cells possess. Conversely, genomic instability is attributed to loss of proteins that are required to monitor the integrity of the genome, most notably p53, thus allowing abnormalities to accrue and exacerbate the situation. The cell cycle is intimately linked to this deterioration *via* a number of checkpoints: control of proliferation, correct replication of the genome and an even splitting of the duplicated genome into both daughter cells.

One criticism however is that several hallmarks listed are the same whether the tumour is benign or malignant, except for tissue invasion, metastasis and sustained angiogenesis, and understanding how and why that difference exists is a major on-going endeavour.[3] Particular attention is required to validate research and show that there is no doubt about the significance of a particular target or system to the progression of the disease, and therefore avoid focusing on a feature that could prove to be inconsequential.

Through the first half of this chapter, some of the causes and effectors of these hallmarks will be described in more detail, especially where it highlights the difficulties and challenges for medicinal chemistry. It is a pertinent endeavour to identify drugable targets whose modulation could reverse and alter a very complex process. In the next section some of this complexity will be illustrated.

1.1.2 Signal Transduction in Cancer

Signal transduction or cell signalling consists of the pathways through which messages from outside the cell (the messengers include small molecules or peptides interacting with trans-membrane or intracellular receptors) are transmitted to the internal mediators and effectors resulting in a change in cellular function. Complexity arises from the many different proteins involved in a single pathway, the ability of different pathways to influence each other and the variable endpoints of a particular pathway in different cells. It is abnormal signal transduction in cancer that most attention has been focused on, in the hope that novel drugable targets can be identified.

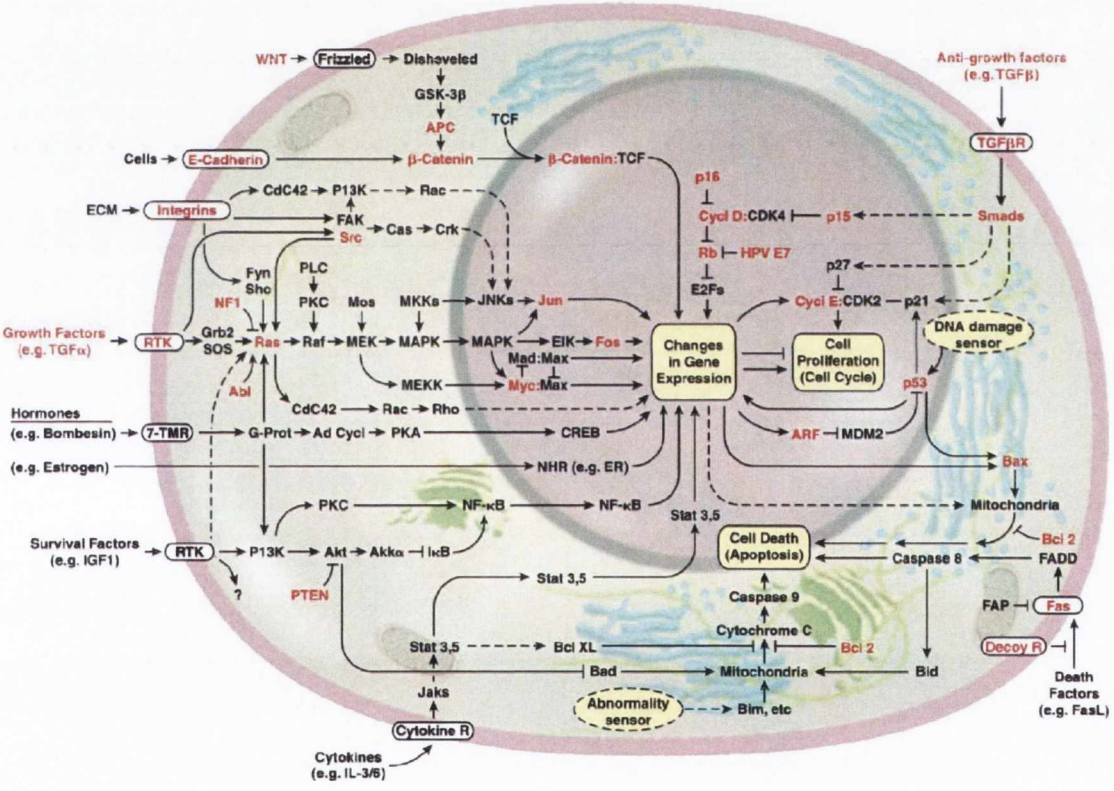

Figure 1.2: An overview of the important signal transduction pathways in cancer.[2] Genes known to be altered in cancer cells are highlighted in red.

Figure 1.2 is a schematic of the some of the signal transduction pathways as known in 2000.[2] It is a complex diagram and since then more details have been elucidated, but there are a few important genes to note, such as dual 'braking system' of the tumour suppressor proteins, p53, and retinoblastoma (Rb).[4] p53 has been found to be mutated in

most common tumour types,[4] and in the diagram it is seen to operate as a junction switch between the cell cycle and apoptosis. Its main role is to trigger cell death by inhibiting the cell cycle and initiating apoptosis if any DNA damage sustained is considered irreparable. Also, loss of p53 can give a developing tumour more than one advantage; allowing it to bypass apoptotic pathways even in the face of such adverse conditions as DNA damage, genomic instability, or lack of oxygen and nutrients.[5] These unfavourable conditions would normally eliminate the cell within 24 hours, this is in contrast to the long times for a tumour to initiate and develop.[2] Loss of pRb on the other hand, allows a cell to ignore the anti-growth signals that normal somatic cells constantly experience and preventing them dividing under their individual autonomy. Also, deregulation of the pRb pathway is thought to be important for CDK inhibitors to be tumour selective.[6]

It is the alterations in these essential components that are the basis of most cancers. The altered genes are classified as either oncogenes or tumour suppressor genes. An oncogene is a gene that when mutated or overexpressed, helps turn a normal cell into a tumour cell, *e.g.* EGFR, HER2. A tumour suppressor is a gene that when mutated causes a loss or reduction in function that allows a cell to become cancerous, *e.g.* RB, p53. The different oncogenes (green) and tumour suppressors (red) are shown in Figure 1.3.

To take as an example of the diverse causes of tumours, the grey line (Wnt-β-catenin pathway) in Figure 1.3 below, this pathway is responsible for the regulation of stem cell numbers. It is thought that tumours derive from excessive and abnormal stem cell division. This is due to the observation that stem cells are more like cancer cells in their undifferentiated nature and ability to divide more frequently than normal cells.[7] An example of this includes the progenitor cells in intestinal crypts that generate the cells of the villi, these function to replace those that are shed during the processes of digestion and absorption, and it is observed that colorectal cancer cells resemble these original progenitor cells.[8]

As a medicinal chemist the challenge arises in obtaining a good understanding of the pathways, including the biological components (gene, transcription factor, protein or enzyme) contained within them, and their importance in the development of human

tumours. More importantly, is realising the best strategy for effective chemotherapy. It is most improbable that there is a 'silver bullet' to cure every cancer type, and more likely for the treatment to consist of a combination of drugs chosen as a result of an examination of the tumour type and the patient's genes. Hence the medicinal chemist's role is to provide a diverse toolkit for clinicians to employ in the treatment of cancer.

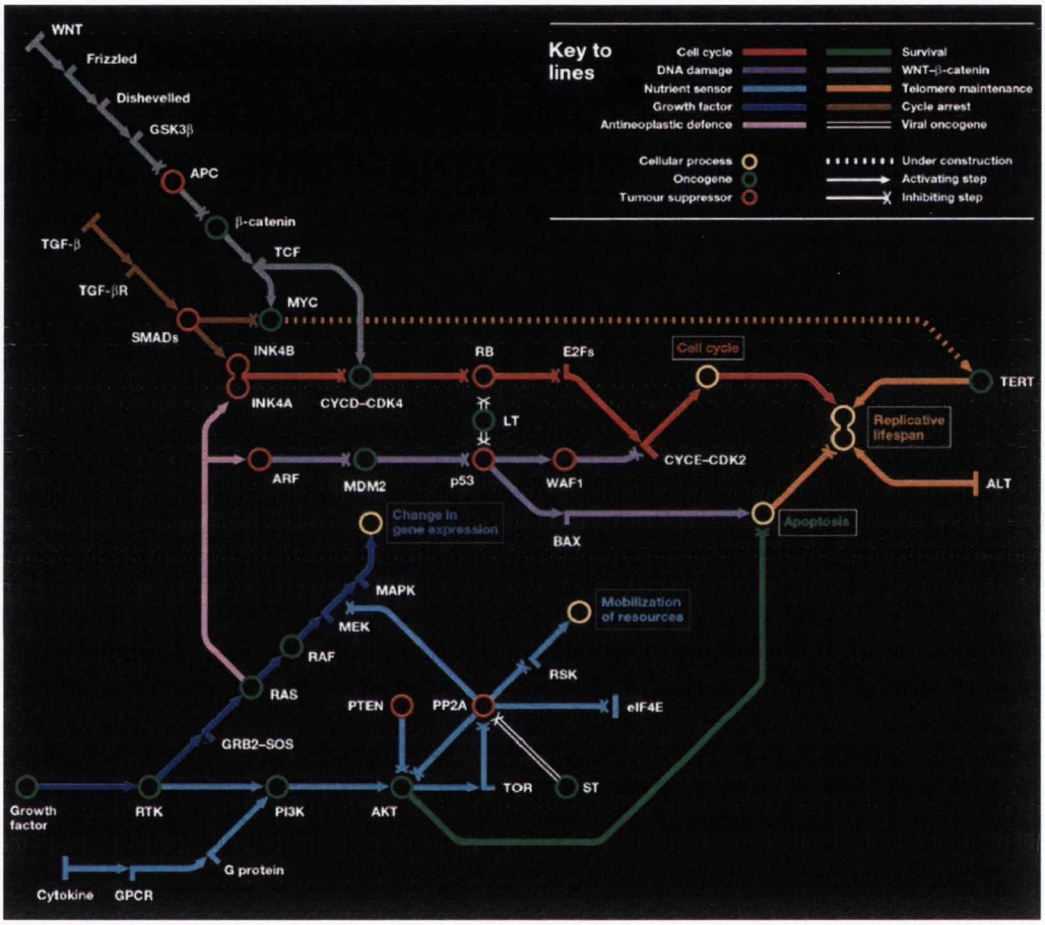

Figure 1.3: Subway map; with oncogenes and tumour suppressor genes indicated.[9]

For similar reasons, it would be wrong to focus solely on any one line/signalling pathway, as a tumour needs to acquire several abilities above the normal remit of somatic cells to be considered malignant, as evidenced by the previously discussed hallmarks, such as the ability to invade other tissues and promotion of angiogenesis to overcome the inherent hypoxic conditions in large solid tumours. However, since the cell cycle is at the heart of many of the pathways and implicated in half the hallmarks it

can be considered a very relevant target. Therefore, finding inhibitors of the kinases that are its effectors is potentially a very productive strategy.

1.1.3 Cell Cycle

The cell cycle is more than a timing mechanism at the centre of the complex wiring diagram that is signal transduction; it is a sequence of checkpoints that must be traversed and ultimately determines the fate of a cell.

The cell cycle is divided into four phases (Figure 1.4), with an additional resting state (quiescence), named G0 for when a cell is not actively dividing. The G0 phase is a state in which a progenitor cell remains until instructed to produce new cells as required by a tissue. There are two fundamental processes involved in the cell cycle: mitosis and DNA replication. Mitosis (M phase) is the physical splitting of an enlarged cell into two daughter cells, each with an identical set of genetic information. This is preceded by DNA replication which takes place during the S (Synthesis) phase. These processes are separated from each other by two gaps. The gaps (G1 and G2) serve as spacers that allow the cell to accumulate information and determine the feasibility of the subsequent process.

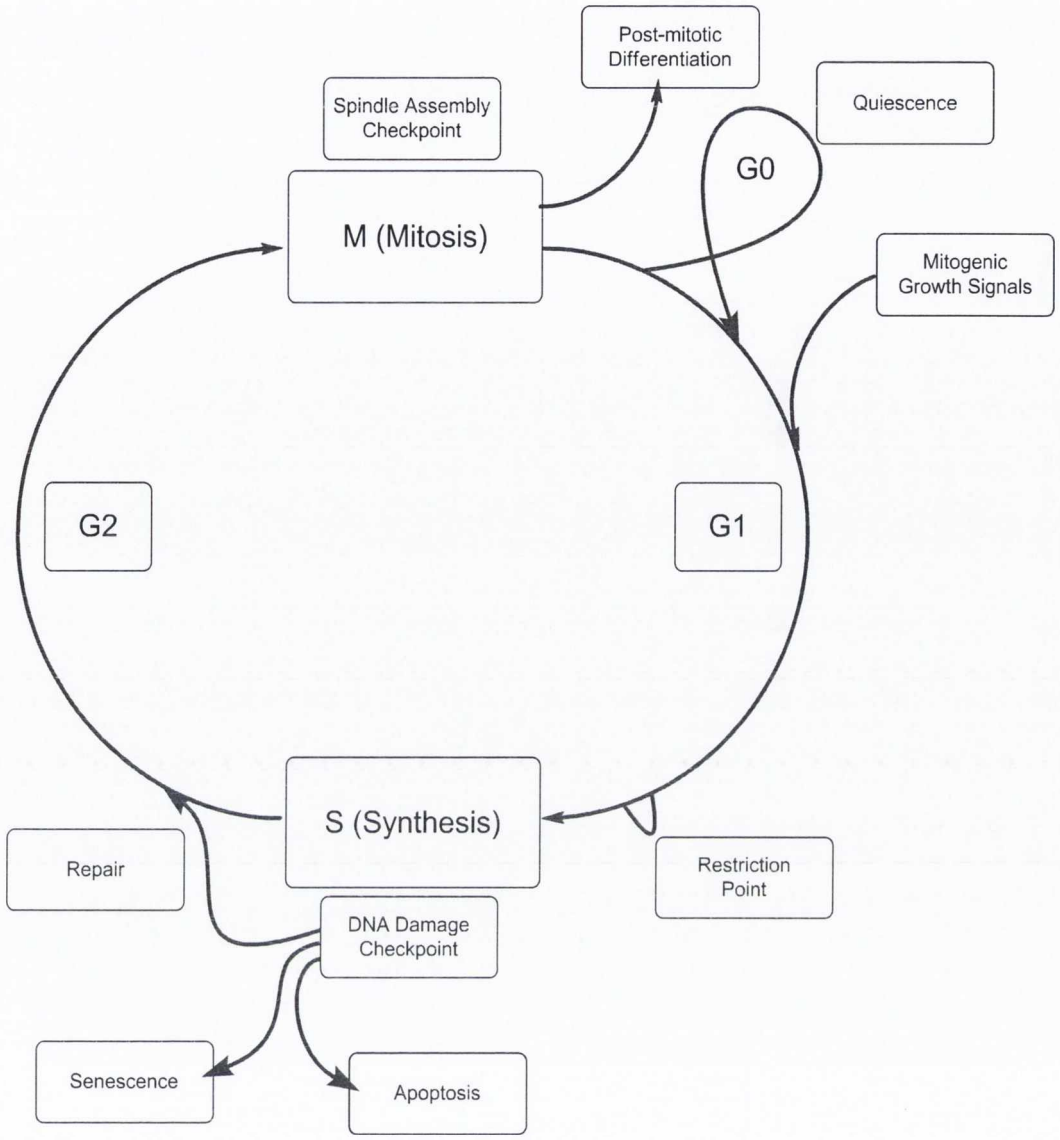

Figure 1.4: An overview of the cell cycle.

Beginning in the G1 phase of the cell cycle, the cell is receiving and interpreting a multitude of growth and anti-growth signals, from internal and external sources (surrounding tissue and neighbouring cells), if it is determined that the cell can divide then it passes through the **restriction point** into the S phase, where DNA is replicated ready for mitosis. The restriction point is a point of no return, the cell stops responding to external growth stimulus.[10] After DNA replication, a process of quality control is completed to ensure DNA was replicated accurately, this is termed the **DNA damage checkpoint**. The DNA damage may be repaired, or if the damage is too extensive, senescence or apoptosis can result.

Once an accurate copy of the genome is obtained, the cell prepares for mitosis. Each of the chromosomes now occurs in a pair of identical copies that are still bound together, sister chromatids. The chromatid pairs must be separated from each other, and each half moved to the two newly forming daughter cells. This process is achieved by a complex multi-protein assembly and a checkpoint governing the integrity of this system, termed the **spindle assembly checkpoint**, is in place to prevent an abnormal distribution of chromatids when cell division completes. The final result is two daughter cells that have a definite place and function in a tissue.

1.1.4 Cyclin-dependent Kinases (CDKs)

Controlling the progress through the cell cycle and the checkpoints are protein complexes consisting of a kinase (serine/threonine specific) and a non-catalytic component, named Cyclin-Dependent Kinase (CDK) and cyclin respectively. Typically the kinase requires association of the cyclin component before it can bind ATP and phosphorylate its substrates. The concentrations of the cyclins vary throughout the cell cycle, whereas the levels of the CDKs involved directly with the cell cycle remain relatively static.

1.1.4.1 Interphase CDKs: CDK4, CDK6 and CDK2

Interphase is the term for the portion of the cell cycle not in mitosis phase *i.e.* it includes G1, S and G2. Cyclin Ds are produced as a result of external growth signals received through cell surface receptors and also in response to the availability of nutrients, these bind preferentially to CDK 4 and 6, and the resulting complexes phosphorylate Rb[11] (as shown in Figure 1.5). Rb (Retinoblastoma protein) must be further phosphorylated[12] to allow for the transcription of genes necessary for DNA replication, this transcription is promoted by transcription factor E2F. The additional phosphorylation is carried out by CDK2 and cyclin E complexes.[13] There is a positive feedback loop active here; full release of E2F allows for additional cyclin E to be transcribed and synthesised.[14] It is this feedback and the formation of fully phosphorylated Rb that signals the passing of the restriction point and entry in the S

phase. Subsequently Rb must be kept phosphorylated for the remainder of the cell cycle, this is accomplished by the CDK/cyclin complexes that are active during those stages as indicated in the diagram.

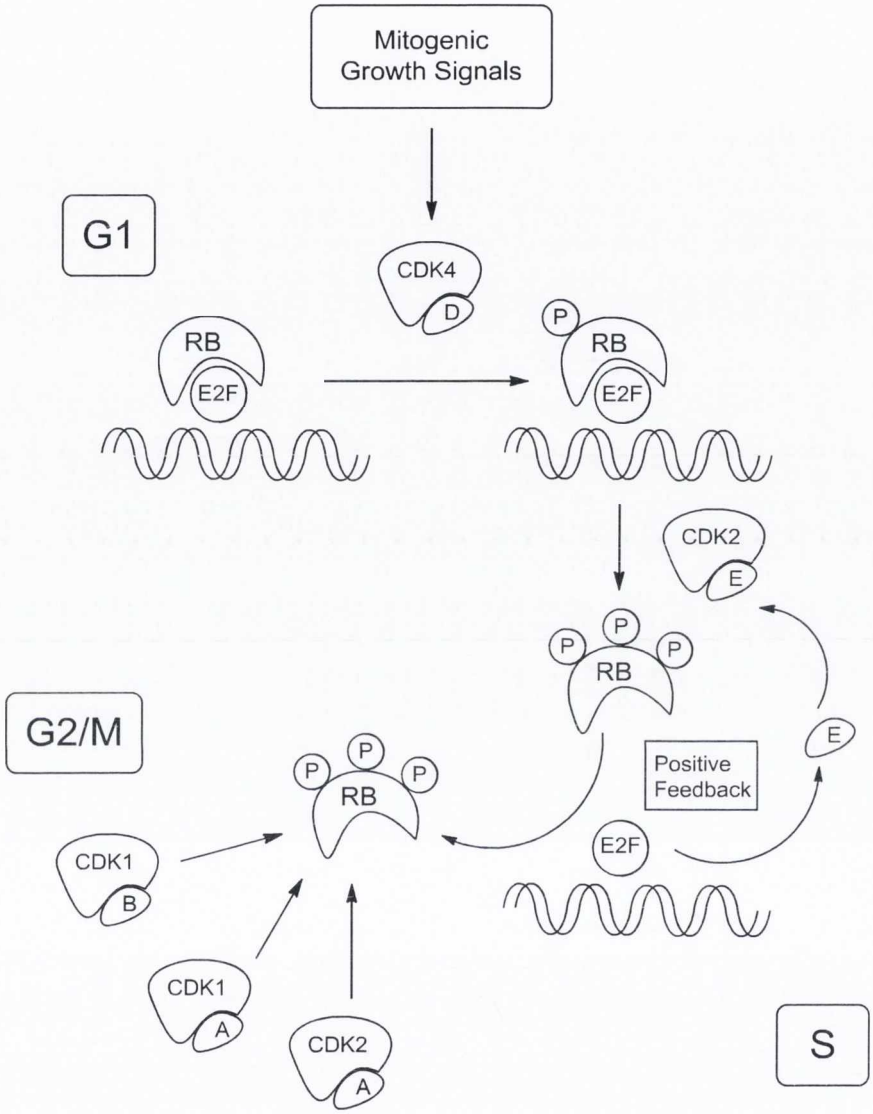

Figure 1.5: Interphase CDKs involved in the G1/S transition.

1.1.4.2 DNA damage checkpoint

At the end of the G1 and during the S/G2 phases, an important endeavour is ensuring the integrity of the genome, the components involved in its regulation and latterly the fidelity of the newly synthesised DNA. Early in the cell cycle p53 is the most important intermediary,[15] promoting the transcription of a CDK inhibitor (p21) that blocks the

activity of CDK2 and thus prevents entry into S phase. Later, a related pathway results in the deactivation of a phosphatase (Cdc25) necessary for the function of CDK1 is in effect.[16] Both pathways result in cell cycle arrest, though the ultimate result may be apoptosis, if repair cannot be accomplished. The checkpoints and the various DNA damage repair (DDR) mechanisms are of on-going interest because it is thought that while a defect in one is not detrimental to a cancer cell, disrupting additional systems proves to be fatal e.g. PARP inhibitors.[17]

1.1.4.3 Mitotic CDK: CDK1

CDK1 has over seventy-five substrates, though this number is likely an underestimate,[18] most of which are involved in mitosis, the events in preparation for this process and the accuracy by which the duplicated genome is divided evenly between the two new cells. It is therefore the most important CDK from the first embryonic division onwards, (targets and functions reviewed in Ref 19). In addition, recent research has shown that it can assume the role of the interphase CDKs.[20]

In G2 CDK1 (also CDK2) is activated by an increase in the concentration of cyclin A, this initiates the process of mitosis, chromosome condensation and microtubule formation. When the nuclear membrane breaks down, cyclin A is degraded to be replaced by cyclin B. CDK1/cyclin B complex continues the progression through mitosis. Before mitosis is completed CDK1 activity is switched off, caused by the degradation of cyclin B promoted by APC-C (Anaphase-Promoting Complex or Cyclosome). It is essential that CDK1 remains switched off, or otherwise cells cannot exit mitosis and continue on with the cell cycle.[21]

1.1.4.4 Spindle assembly checkpoint

Cell division is a complex process and cells are most vulnerable during this stage of the cell cycle to disruption and cell death. This accounts for the success of anti-mitotic agents such as taxanes and vinca alkaloids, which act by disrupting the microtubule frame-work, thus activating the spindle assembly checkpoint and eventually resulting in cell death. Much attention has been focused on this checkpoint, as microtubules are

essential to cellular function and it is hoped that ways to modulate their activity in cancer cells without affecting healthy cells may be found.

1.1.4.5 Transcription CDKs: CDK7, CDK8 and CDK9

Transcription is the process of synthesising messenger RNA using the DNA in the genome as a code. This mRNA is then used as a template by the ribosomes to synthesise new proteins. It is a continual process, and an important part of signal transduction is the timely activation, inhibition or destruction of relevant proteins. The mRNA is synthesised by a multi-protein complex called RNA polymerase II, which must bind several transcription factors in order to begin replication. These transcription factors include TFIIH and P-TEFb that contain CDK7/cyclin H and CDK9/cyclin T respectively. The role of the CDK/cyclin component is the phosphorylation of RNA pol II to allow initation of transcription and then the efficient elongation of the nascent mRNA (Figure 1.6). CDK8/cyclin C also forms part of the RNA pol II complex and provides a distinct layer of regulation.[22]

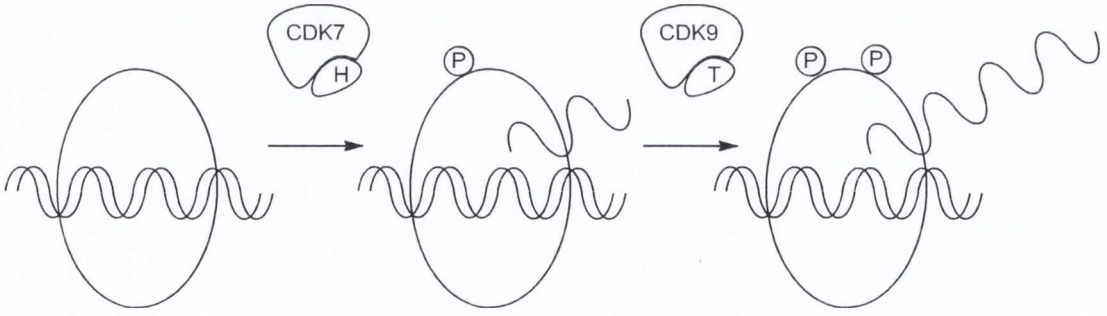

Figure 1.6: Initiation and elongation in transcription.

The transcription CDKs are of most interest as potential targets for anti-viral drugs,[23] because the replication of viruses is very much dependent on efficient synthesis of mRNA. Also, some cancers have acquired the ability to over-synthesise anti-apoptotic proteins and limiting this excess could be a possible therapy (see Sections 1.3.1.1 and 1.3.1.2).

1.1.4.6 CDK5

CDK5 does not appear to have a role in the cell cycle, and its distribution is concentrated in the CNS. In embryos, CDK5 is important in neuronal development, including the migration and differentiation of neurons.[24] In adult cells CDK5, in conjunction with its activators p35 and p39, has several roles that are clinically relevant.[25] In neurodegenerative diseases, such as Alzheimer's disease, CDK5/p25 (p25 is a truncated form of p35) phosphorylates tau, a microtubule protein polymer, this together with phosphorylations by other kinases leads to the precipitation of hyperphosphorylated tau, a feature of Alzheimer's and tauopathies (see Section 1.4.6.1).

1.1.4.7 CDK10 and CDK11

Less is known about these two CDKs, also they are very rarely included in kinase assay panels, though this could change due to some observations that have recently come to the fore. There is a direct link between low levels of CDK10 in patients and the occurrence of tamoxifen resistance in the treatment of hormone-dependent breast cancers.[26] Loss of one allele of CDK11 (haplo-insufficiency) leads to skin tumour development in mice.[27] These results highlight the value of selective CDK inhibitors rather than pan-CDK inhibitors, where (off-target) toxicity is a major issue hindering progress in clinical trials.

1.1.5 Regulation of CDKs

CDKs require the binding of a regulatory subunit, either a cyclin or a related protein, to function. In addition several other methods of regulation are in operation and dependent on the CDK in question, and individual CDKs may respond differently to the same inhibitor or activator.

1.1.5.1 Endogenous CDK inhibitors

There are two families of endogenous inhibitory proteins of CDKs; INK4 (INhibitor of CDK4) and CIP (CDK Inhibitory Protein; CIP1/WAF1, KIP1/p27, KIP2). INK4 (4 forms, A-D) inhibit the activity of CDKs by competing with the cyclin for its binding site on the CDK, while CIP inhibits by wrapping around the CDK/cyclin complex, causing a conformational change and blocking the ATP binding site.

An important difference (see Figure 1.7) is observed when CIP binds to either CDK4/6 or CDK2, CDK4/6 remain active while CDK2 is inactivated. As previously mentioned, there is a feedback effect necessary for the cell cycle to continue past the restriction point and the G1/S transition, the positive feedback loop with the expression of cyclin E is one part, while the sequestration of CIP by CDK4/6 is another part, and finally when CDK2 becomes fully active it can phosphorylate CIP and signal for its destruction.

Both sets of inhibitors are as a result of anti-mitogenic signalling, which is a constant message being received by cells. It is only when growth signalling exceeds this threshold that the cell cycle can occur. For example the accumulation of INK4A (p16) is thought to be the major factor for keeping somatic cells senescent, *i.e.* towards the end of a cell's lifespan, after the cell has divided a 'safe' number of times, and to decrease the probability of DNA damage occurring with superfluous replications the cell cycle becomes dormant.[28] Another important role is arresting the cell cycle in response to DNA damage CIP1 (also known as WAF1 or p21) is formed in response to the detection of DNA damage by ATM-p53 pathway.[29]

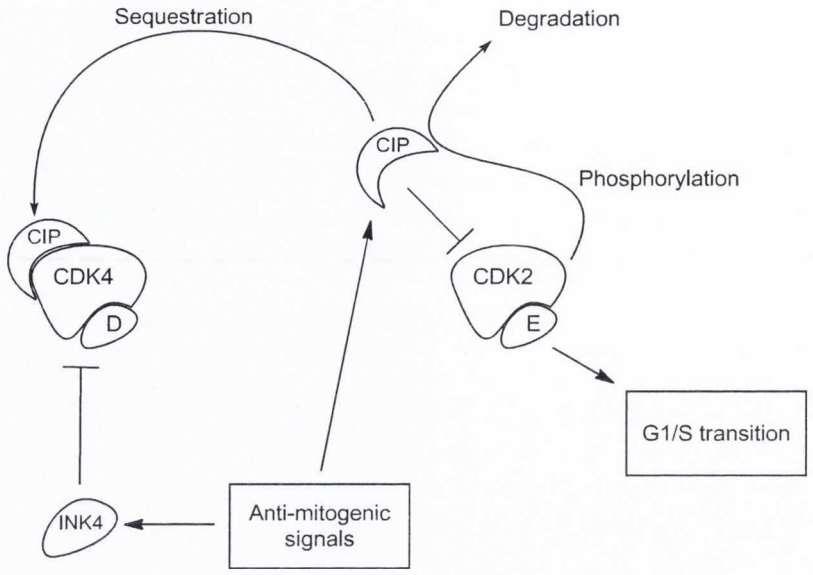

Figure 1.7: Distinction between the two groups of CDK inhibitors.

1.1.5.2 Phosphorylation and dephosphorylation

CDK activity is also regulated by phosphorylation and/or dephosphorylation. CDK7/cyclin H (also named CAK; CDK Activating Kinase) in addition to its transcription role, adds an activating phosphate to the other CDKs,[30] and is required for the assembly of CDK1/cyclinB complex.[31] WEE1 and MYT1 add phosphates that inhibit CDK1/2 activity, which can be removed by a CDC25 (Cell Division Cycle) phosphatase to restore activity. The balance between MYT/WEE and CDC25 is the means by which a cell is prevented from early entry into mitosis, before DNA replication has occurred successfully, due to this and because these are observed to be often over-expressed and deregulated in cancer, they are considered to be very relevant targets.[16] For CDK5, the binding of its non-catalytic subunit is sufficient for activity.[25]

1.1.6 Prevalence of Disrupted Cell Cycle Components in Cancer

Table 1 illustrates the prevalence of mutations in the components of the cell cycle, percentages represent the proportion of the tumours that have any or all of the listed components mutated and those components in bold highlight any malfunctioning component that results in a poor prognosis for patients. For example, 90% of sarcomas have CDK6, cyclin D1, INK4A, cyclin E1 or KIP1, with KIP1 indicating a poor outcome in patients.

Table 1: Prevalence of a disrupted cell cycle and impact on prognosis.[32]

Tumour	Altered Components			
	RB	CDK	Cyclin	Inhibitor
>80% Pituitary	RB		D1, D3	INK4, **KIP1**
>90% Head and Neck	p130	4	**D1**	INK4, **KIP1**
>90% Lymphoma	RB	6	D1-3, **E1**	INK4, **KIP1**
>20% Melanoma	**p130**		D1, E1	**p16**
>90% Liver	RB	2, 4	D1, **E1**	INK4, p15, **KIP1**
70% Prostate	**RB**		D1, E1	INK4, **KIP1**
>90% Testes/Ovary	RB	4	D1,2, E1	INK4, KIP1
>90% Glioma/blastoma	RB,	4, 6	E1	INK4, KIP1
>80% Breast	RB, p130	4	D1, **E1**	INK4, **KIP1**
>90% Lung	**RB, p130**	4	D1, **E1**	**INK4, KIP1**
>90% Pancreas			**D1,3**	INK4, **KIP1**
>90% Gastrointestinal		2, 4	D1,2, **E1**	INK4, **KIP1**
>80% Endometrium	**RB, p130**	4	**D1**, E1	INK4, KIP1
70% Bladder	**RB**		D1, **E1**	INK4, **KIP1**
>90% Leukaemia	**RB**	4	D1, E1	INK4, KIP1
>80% Osteosarcoma	RB	4	E1	**INK4**
90% Other Sarcomas		6	D1, E1	INK4, **KIP1**

1.2 Targeted Anti-cancer Drugs

Targeted therapy has been a very active research field in the past decade. It involves the design and discovery of molecules that are active against the various proteins involved in the cell-cycle and the surrounding signal transduction pathways. It differs from traditional chemotherapy where cytotoxic compounds that target all rapidly dividing cells are employed. The expansion in interest in targeted therapy is reflected in the market sales; between 2005 and 2010 US sales in targeted therapies more than doubled and overtook the sales of traditional cytotoxics to a significant degree, though likely in part due to the high-cost of these new to market drugs.[33]

The goal of targeted therapy is to find agents that target biological (macro-) molecules that are found to function abnormally in cancer cells, and can be purposely targeted without affecting the normal versions in healthy cells. A large part of the potential effectiveness of this approach is being able to tailor the treatment to a particular patient and the factors causing and exacerbating their disease and prognosis *i.e.* 'personal medicine'. The major obstacle that needs to be overcome is validation of the chosen targets. Proof-of-concept is made more difficult by cancers being based on multiple alterations, as evidenced by the 'hallmarks of cancers', resistance mechanisms are common and prediction of the outcome in a complex tissue where cell types may have similar pathways but operating differently or modified in different ways by cancer.

There are several types of agent used in targeted therapy: a) hormones and hormones inhibitors are used in those tumours that respond to them, b) antibodies to stimulate the immune system to recognise and destroy cancer cells *e.g.* rituximab and alemtuzumab, c) recognition elements such as antibodies or peptides with a cytotoxic or radionuclide attached to them that will be delivered and released where the attached ligand binds *e.g.* ^{131}I-tositumomab and gemtuzumab ozogamicin (contains highly toxic calicheamicins), d) small molecule inhibitors. Presently monoclonal antibodies are the most developed and widely used in treatment, but also the most expensive, annual treatment cost are $50,000-100,000 per patient.[33]

Formerly, the more important biological targets were G-Protein Coupled Receptors (GPCRs), ligand-gated ion channels, voltage-gated ion channels, nuclear receptors and enzymes. Kinases have in the last three decades emerged as significant vectors in an array of diseases and are now second to GPCRs as the most relevant target currently.[34] However, the first target for an anti-cancer targeted therapy to pass the proof-of-concept stage and enter the clinical setting was the estrogen receptor, a nuclear receptor, which is essential for the proliferation of hormone-dependent breast tumours.

Currently the most important and well-established targets in anti-cancer targeted therapy are the receptors for growth factors for example the EGFR family of receptors that includes EGFR and HER2, and VEGF receptors. These are transmembrane receptors with a tyrosine kinase domain inside the cell (RTK, Receptor Tyrosine Kinase). The signal transmitted by the EGFR receptor is carried through several important pathways, but due to the propensity of these receptors to occurrences of over-expression and constitutive activation are linked to uncontrolled proliferation;[35] while the VEGF receptor is important in angiogenesis.

Two strategies exist to target these receptors; either to target the protein surface outside the cell with antibodies or to target the TK activity. Monoclonal antibodies predominate, in particular bevacizumab (Avastin, Genentech/Roche), though there are several small-molecule kinase inhibitors on the market (Figure 1.8) including erlotinib (**1**) (Tarceva, Genentech/Roche) and gefinitib (**2**) (Iressa, AstraZeneca) for EGFR and HER2 respectively; the less selective sorafenib (**3**) (Nexavar, Bayer) and sunitinib (**4**) (Sutent, Pzifer) active against other relevant RTKs including VEGF and PDGF (Platelet-derived Growth Factor) receptors.

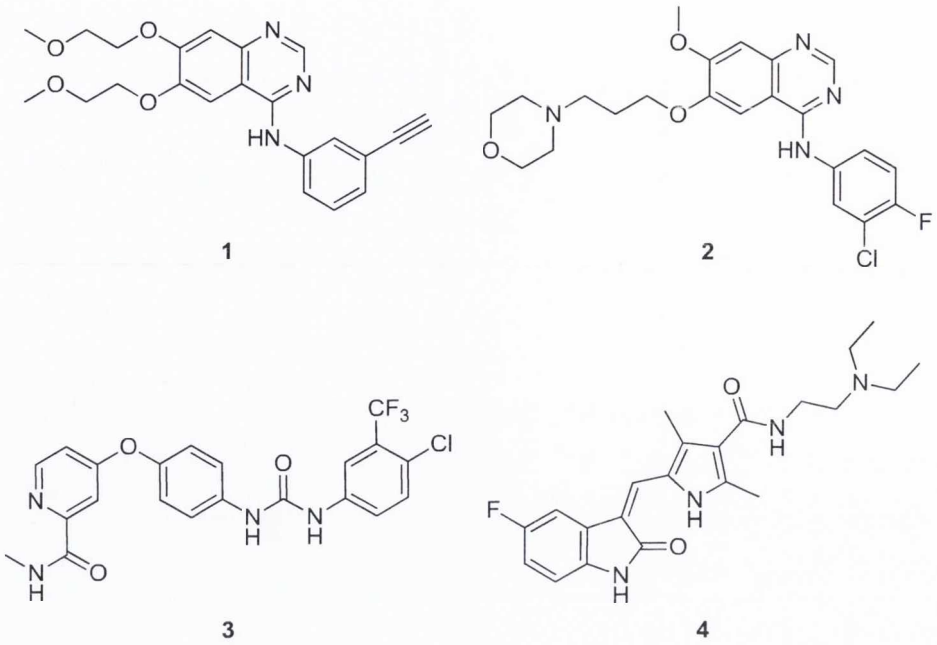

Figure 1.8: Structures of small-molecule targeted therapeutics.

Much work is ongoing to find other molecular targets for the treatment of cancer, not all of the components described previously have specific inhibitors or are thought to be suitable therapeutic targets. An assumed role for a medicinal chemist would be to take any leads generated, along with the structure of the target, and attempt to design more selective and hopefully more active compounds, as well as help to evaluate a target's potential worth in treating disease.

1.2.1 Kinase Inhibitors as Treatments for Cancer

The last decade has witnessed an explosion of interest in kinase inhibitors. Prevailing wisdom had dismissed the endeavour of finding selective kinase inhibitors as difficult, which is understandable considering that the then available inhibitors such as staurosporine, cyclosporins and rapamycin were not particularly selective. The success of imatinib (**5**, Figure 1.9) (Gleevec/Glivec, Novartis) in trials and its subsequent approval in 2001 brought a lot of attention to the area and it is now a commonly cited touchstone in the success of kinase inhibitors in treating cancer. It has the biggest

market share among small-molecule targeted therapies (not just kinase inhibitors), accounting for 11% of total sales of targeted therapies ($1.1 billion) in 2009.[33]

Imatinib is found to be effective against chronic myeloid leukaemia (CML) - a disease that results from translocation between two chromosomes (9 and 22), forming the 'Philadelphia chromosome' and giving rise to a fusion protein called BCR-ABL. This kinase is always active and is the main causative factor of CML, stimulating myeloid cells to proliferate continuously. In essence this is a perfect target, in that the majority of patients with CML have this alteration and its activity has been found to be dispensable in normal untransformed cells. However, **5** is not completely selective, it also inhibits another RTK, c-KIT, this fact has been beneficial in the treatment of gastrointestinal stromal tumours.[36] Two further inhibitors have been developed that are used when resistance to **5** occurs: dasatinib (**6**) (BMS) and nilotinib (**7**) (Norvartis).

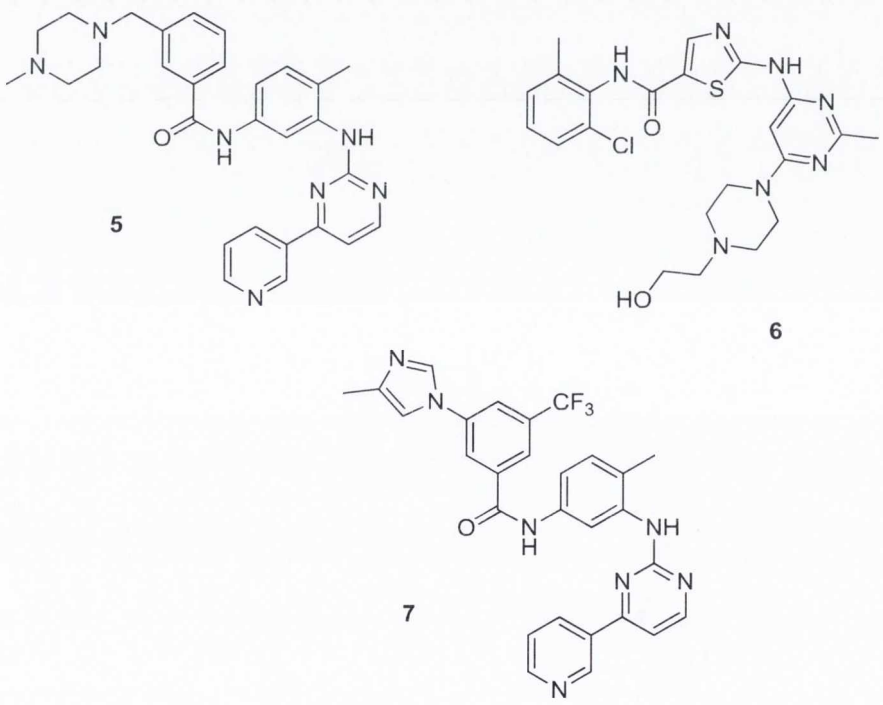

Figure 1.9: Three drugs currently approved for the treatment of CML.

1.3 Small-molecule Cell Cycle Inhibitors

Numerous inhibitors of the cell cycle mechanism have been found, many of which are useful for probing the function of the various enzymes and proteins associated with the cell cycle. This remains an ongoing process, but it is hoped that some could potentially be developed as antiproliferative agents. A problem arises in choosing which CDK is the best target to pursue. The simplest answer is that inhibition of each of them could have a marked response in cancer cells, either the interphase, mitotic or transcription CDKs. More difficult is determining those that will prove to be the most effective targets in targeted therapy. Despite a growing collection of published clinical data, a consensus has yet to be reached.[37]

For interphase CDKs CDK4/6, several observations point to their potential: removal of cyclin D prevents breast cancer caused by Erbb2 (Her2) and Hras in animal studies;[38,39] also CDK4 loss prevents skin tumours induced by Myc;[40] over expression of cyclin D1 and loss of INK4A are common features in cancer. As Her2 inhibitors have already been approved for clinical use, small-molecule CDK4 selective inhibitors that would have a similar effect as lowering the amount of cyclin D present, could see similar success, or could be combined with the already approved treatments.

A potential problem with solely selective CDK4 inhibitors is that CDK2 has a compensatory function, it can also bind cyclin D and carry out the necessary functions in early G1 phase; conversely including CDK2 inhibition does not seem to provide any additional benefit. This depends on the tumour type; some melanomas have high levels of CDK2, which is responsible for a significant proportion of their growth.[41] Another factor that should be considered is that while none of the interphase-CDKs are essential, each has additional activities in different subsets of tissue types, and would be expected to cause off-target effects.[42]

At present CDK1 inhibitors seem to offer the greatest potential, though their apparent indispensability to the cell cycle means that they may be employed more as a cytotoxic agent than a targeted therapy.

1.3.1 CDK Inhibitors

1.3.1.1 Flavopiridol

Flavopiridol (**8**, Figure 1.10) is one of the oldest and most studied CDK inhibitors, in both a clinical setting and in solid tumours.[43,44] It is a semi-synthetic flavone, derived from rohitukine, a naturally occurring alkaloid. It is a pan-CDK inhibitor with greatest selectivity for CDK9/cyclin T and has been shown to cause arrest at multiple transitions in the cell cycle: sub G1, G1/S and G2/M. The outcomes of its inhibition include decrease in cyclin D1 expression, decrease in transcription including anti-apoptotic factors, an accumulation of p53. Its high selectivity for CDK9 and lowering of anti-apoptotic proteins has earned it success in treating tumours dependent on these, such as Chronic Lymphocytic Leukemia (CLL).

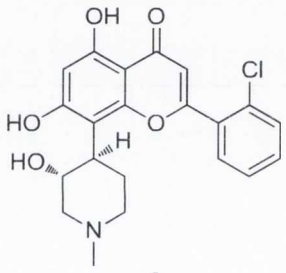

8

Figure 1.10: Flavopiridol

Treatment with **8** appears to be considerably dose and administration schedule dependent, having very mixed outcomes.[45] In early clinical testing the response could be poor and side-effects ranged from severe, including arterial and venous thromboembolic events, to more manageable side-effects such as fatigue and neutropenia. In more recent protocols a bolus dose followed by a short infusion period was used to treat patients.[46] The response rate was much improved, most notably in CLL including those cancers with resistance to previous treatment and with mutations usually indicating a poor prognosis. Though acute tumour lysis syndrome was observed as a Dose-Limiting Toxicity (DLT), this adverse effect could be remedied by excluding patients with high leukocyte cell counts. An observation that suggests the reason for the discrepancy between animal studies and clinical trials is the very high (>90%) binding

of **8** to plasma proteins in humans, thus when pharmokinetics were more thoroughly considered improvements in outcomes were produced.

Another promising feature that is being explored is the combination of **8** with cytotoxic agents, in particular those that cause mitotic arrest. This has resulted in a greatly increased incidence of cell death, for example a combination of **8** with paclitaxel/carboplatin in treating NSCLC.[47]

Analogues of **8** have been synthesised, and some are already in phase I/II clinical trials. Of a series of flavones (Figure 1.11), designated P276-00 (Nicholas Piramal), the best has similar levels of kinase activity to **8** but is two to three times more potent *in vitro*.[48] P276-00 is very selective for CDK4/cyclinD, CDK9/cyclin and CDK1/cyclinB out of all the other CDKs and other kinases. It was found to reduce levels of cyclin D and CDK4, also causing complete dephosphorylation of Rb and an increase in caspase-3 activity; altogether providing a good rationale for mode of action. In cell-line and xenograph studies it was found to be more potent than cisplatin, and could even elicit a response in cells from cisplatin resistant tumours.[49] It causes arrest in G1 for normal cells but does not lead to any significant cell-death.

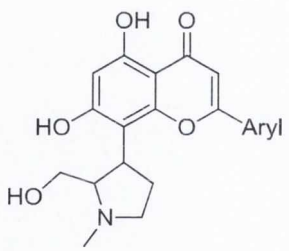

Figure 1.11: General structure of P276-00 series of flavones.

1.3.1.2 Tri-substituted purines

Several tri-substituted purines have had success in pre-clinical and clinical trials: *(R)*-roscovitine (**9**), purvalanol A (**10**) and olomucine (**11**) (Figure 1.12); also some newer generation purines, *(S)*-CR8 (**12**) and NU-6140 (**13**) (Figure 1.13).

(R)-Roscovitine (**9**, seliciclib, CYC-202) is the most studied and well-established example of this structural class of inhibitors. It is a competitive inhibitor selective for

CDK1/2/7/9, less so for CDK4/6. It has completed phase I trials and is at the phase II stage, though it is not faring as well as predicted from pre-clinical studies, where favourable results and pharmacokinetics were observed. In a recently published phase I trial:[50] the compound could be orally administered twice daily for 5-7 days every 3 weeks; it was well tolerated with toxicities being mostly transient and reversible, very few symptoms were noted below 400 mg per dose, with disruption to liver and kidney function, hypokalemia, rash and fatigue being observed at greater doses. However the response in patients was limited to a temporary stabilization of disease progression, this was suggested to be due to low plasma concentration of the drug with the doses employed in the study; the concentrations were much lower than those that elicited adequate response in xenograph models.

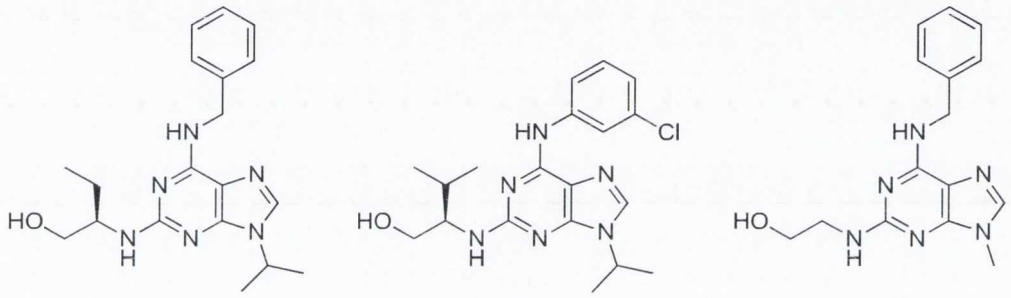

Figure 1.12: Tri-substituted purines

Due to the low potency of **9**, newer analogues have been synthesised including **12** and **13**. Analogue **12** was first synthesised for a study to find CDK inhibitors that are taken up by dopamine transporters. Subsequently, it was found to have a higher potency (at least 10-fold and as much as a 50-fold increase in some cell types) than **9** against several tumour cell-line cultures, with its activity assigned mainly to CDK9 inhibition and a reduction in anti-apoptotic proteins.[51] Both enantiomers were tested separately, with each having distinct advantages; the authors favoured the *S* enantiomer due to a lesser effect on GSK3 (Glycogen Synthase Kinase-3). While **13** was discovered by structure based design.[52] It was tested alone and in combination with paclitaxel, and high levels of apoptosis were observed, especially when **13** was used after paclitaxel.[53] Also a link was proposed between CDK1 inhibition, the levels of anti-apoptotic protein survivin, and the success of treatment with paclitaxel. In both cases the potency

problem with **9** was addressed by developing more potent compounds, though neither took into consideration the avoidance of rapid clearance from the body, which had a significant effect on the pharmokinetics of **9**.

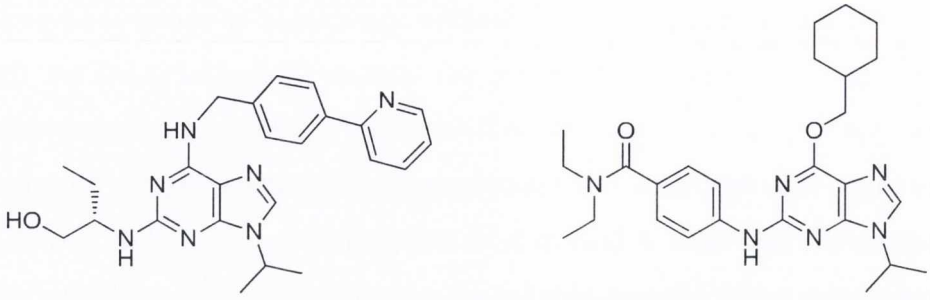

12 **13**

Figure 1.13: Newer generation tri-substituted purines in pre-clinical trials.

1.3.1.3 SNS-032

SNS-032 (**14,** Figure 1.14) (formerly BMS-387032) is a pan-CDK aminothiazole inhibitor with selectivity for the transcription CDKs 7 and 9 in the low nanomolar range, also CDK 2 over both CDK1 and CDK4. An important capability of this compound is that it sensitises non-small cell lung carcinoma (NSCLC; a particularly resilient solid tumour type) at concentrations of 500 nM to radiotherapy *in vitro*, including cells that are quiescent and hypoxic.[54] Conversely it has poor bioavailability when administered orally due to Pgp-mediated efflux, thus a number of analogues (**15, 16**) have been designed to overcome this problem, these molecules are currently at the pre-clinical stage.[55,56]

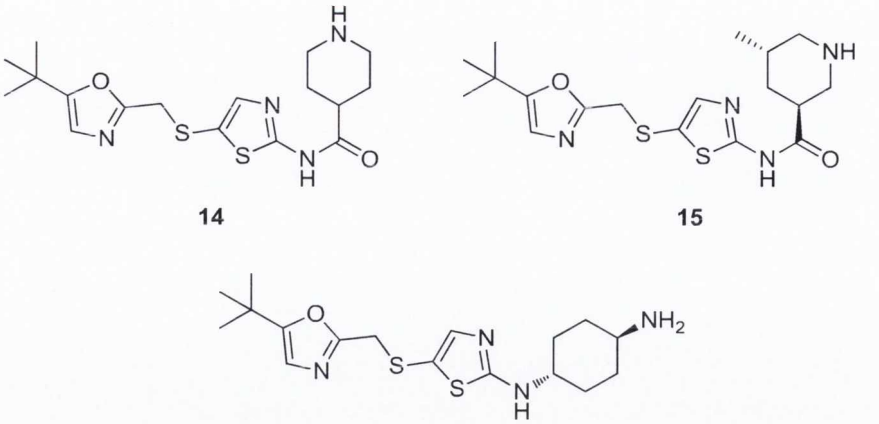

Figure 1.14: SNS-032 and analogues.

1.3.1.4 AT7519

AT7519 (**17**, Figure 1.15) is a pan-CDK competitive inhibitor developed by Astex using structure-based drug design with CDK2 as the target. It is selective for CDK2 out of the cell cycle CDKs, but is more active against CDK5 and inhibits the other CDKs and GSK-3 with IC_{50} values below 200 nM. The compound causes inhibition of the proliferation of tumour cell lines in the nanomolar range; this inhibition is independent of the presence of Rb, thus eliminating CDK4/6 as the effective target. Also it was found to lower transcription as a result of CDK9 inhibition. Against HCT116 xenographs, complete regression was observed in most of the testing undertaken.[57]

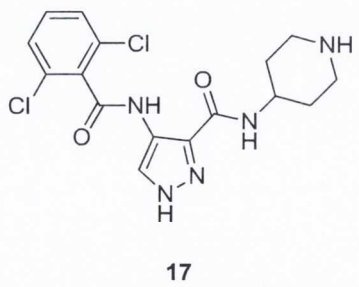

Figure 1.15: AT7519

1.3.1.5 R547

R547 (**18**, Figure 1.16) is a pan-CDK inhibitor with IC_{50} values of 1-3 nM for CDK1/2/4, thus having one of the highest set of activities for the cell cycle CDKs. It gave excellent results in preventing the growth of several cancer cell lines *in vitro* and xenographed HCT116 tumour cells,[58] and has completed a phase I clinical trial.

18

Figure 1.16: R547

1.3.1.6 PD-0332991

PD-0332991 (**19,** Figure 1.17) is a highly CDK4/6 selective inhibitor, developed by Pfizer that entered phase I/II clinical trials in 2004. It has IC_{50} for CDK4 of 11 nM and for CDK6 of 16 nM, with CDK2/cyclin B inhibition reported as greater than 5 μM.[59] Inhibition of cellular proliferation in xenographs can result in regression of the tumour, but is dependent on the presence of Rb.[60] It is also being tested in combination with dexamethasone (anti-inflammatory steroid) and bortezomib (proteasome inhibitor) for the treatment of multiple myeloma; and in combination with letrozole (Femara; an aromatase inhibitor) for advanced breast cancer. The success or otherwise of this compound will determine the case for CDK4/6/cyclin D selective inhibitors.

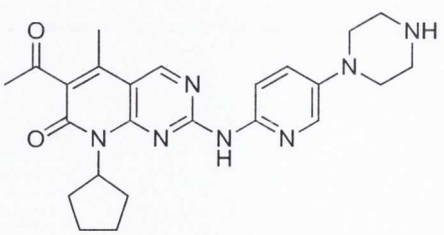

19

Figure 1.17: PD-0332991

1.3.1.7 RO-3306

RO-3306 (**20,** Figure 1.18) is selective for CDK1 and CDK2, which is expected since they have similar structures, but is much less selective for CDK4. This was evidenced as complete arrest at the G2/M transition and a slowdown in the S phase, but no arrest in G1. At present this inhibitor and other members of the class are at the pre-clinical stage, and are able to produce a high degree of tumour cell death *in vitro*.[61] This result supports the theory of CDK1 as being essential and non-redundant for mitosis. [62]

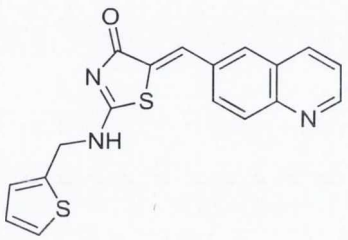

20

Figure 1.18: RO-3306

1.3.2 Non-CDK Cell Cycle Inhibitors

In addition to the research and testing of CDK inhibitors, several other related kinases that play a part in the cell cycle are also under investigation. (Reviewed in ref 14 and 63)

1.3.2.1 DNA damage checkpoint inhibitors

While CDC25 phosphatase has a role to play here, investigation has also focused on the kinases that are higher up in the DNA damage response pathway, namely the checkpoint kinases CHK1 and CHK2.[63]

1.3.2.2 Mitotic spindle assembly checkpoint inhibitors

Besides CDK1 as the main kinase acting at this checkpoint, the activity of several other associated kinases have also been implicated in cancer; these are aurora kinases, PLKs (Polo-Like Kinases) and BUB1(B) (Budding Uninhibited by Benzimidazoles).[14,63] In addition as mentioned previously the physical process of mitosis has been targeted by traditional cytotoxic drugs, the vinca alkaloids and taxanes.

1.3.2.3 CDC25 inhibitors

CDC25 inhibitors are a relatively recent development, the phosphatases themselves have been known to be present in humans for over two decades, though the importance of the link between over-expression of CDC25 genes and tumorigenesis is uncertain.[14] Speculation is split between whether it is preferable to inhibit or promote the activity of these phosphatases. Inhibition should bring the cell cycle back under control but to what extent is unknown. In addition after toxic stress has halted the cell cycle it would prevent a recommencement of the cycle prematurely. Activation pushes the abnormal cells forward into a mitosis that would prove destructive, although this remains more speculative than certain, but CHK1 inhibitors seem the more likely candidate for this strategy.

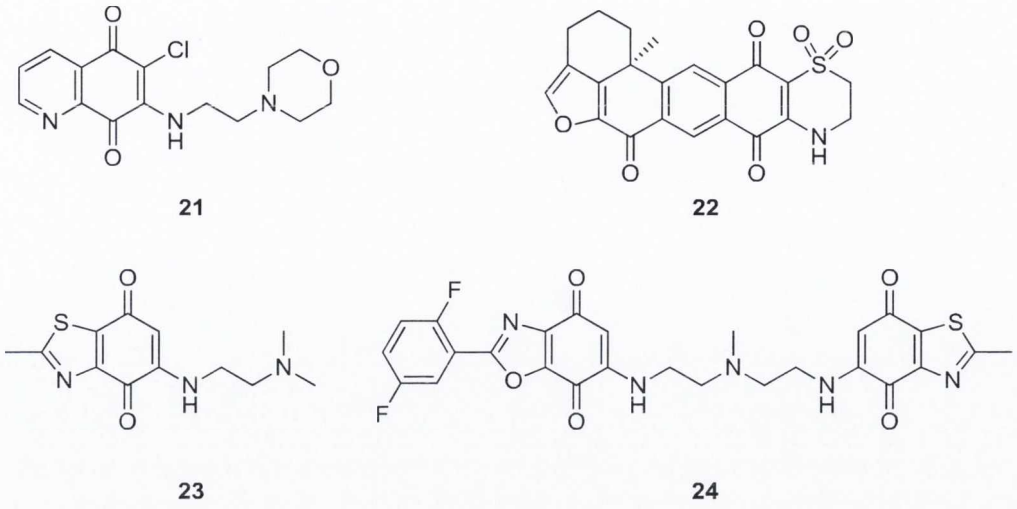

Figure 1.19: CDC25 phosphatase inhibitors.

The compounds at present are limited mostly to quinones (**21-24**, Figure 1.19). The quinones are capable of oxidising a cysteine residue at the catalytic site. Other inhibitors include phosphate group mimics. The number of compounds that are active *in vivo* is limited, and only an inhibition of growth is displayed rather than cell killing *i.e.* it is a transient inhibition of the cell cycle.

1.4 Paullones

1.4.1 Overview and Discovery

Paullones (paullone, **25**; 7,12-dihydroindolo[3,2-d][1]benzazepine-6(5H)-ones) are a class of synthetic small molecule CDK inhibitors. They are competitive inhibitors, occupying the same space as ATP in the active site of the kinases, and are highly selective for CDKs. To date more than 280 derivatives have been synthesised,[64] and tested for their anti-proliferative properties and also in several other relevant diseases.

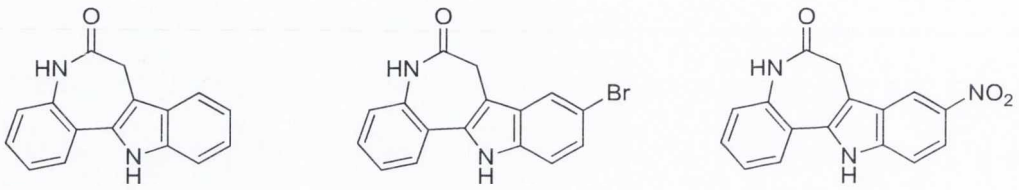

25 **26** **27**

Figure 1.20: Earliest paullone derivatives.

Kenpaullone (**26**, Figure 1.20) was the first of the class identified as having significant CDK inhibitory activity. It was discovered using the COMPARE program to search a database of chemicals screened by the National Cancer Institute (NCI) for molecules having a similar activity profile to flavopiridol. Typically when a molecule is submitted to the NCI for testing, it is screened against a panel of 60 cancer cell lines, thus a 'fingerprint' for each compound is generated. The expectation then is that compounds with similar modes of action have a similar activity profile against the various cancer cell lines. Paullone **26** was named after the inventor of the COMPARE program, Ken Paull. It has modest anti-proliferative activity *in vitro*, but more success was achieved by replacing the bromine with a nitro group, to give the molecule named alsterpaullone (**27**) which is one of the more active in cellular cultures to date.

1.4.2 Cellular Targets of Paullones

1.4.2.1 Identification of cellular targets:

In an effort to discover all the targets of paullones, Kunick *et al.* used a strategy of immobilising a paullone on agarose beads, incubating the beads with cellular extracts and any resulting bound protein isolated and identified.[65] The two paullones used: 'gwennpaullone' (**28**) and 'C3-paullone' (**29**) were based on **26** but contained a linker attached at the C-2 and C-3 positions respectively (Figure 1.21). The choice of attachment position was based on homology modelling (docking the paullone structure in a model of CDK1/cyclinB, which was based on a crystal structure of CDK2/cyclinA) that indicated this part of the paullone structure as being orientated toward the opening of the active site of CDK1. When the bound proteins were isolated by SDS-PAGE, three proteins were identified: GSK-3α, GSK-3β and a previously unknown target, mitochondrial malate dehydrogenase (mMDH). Interestingly, immobilised **28** did not bind CDK5 from the cellular extracts (porcine brain, rat tissues, xenopus eggs or sea urchin eggs) even when GSK-3s were removed in a pre-treatment, nor even when purified CDK5/p25 or CDK1/cyclinB were used (unbound **28** binds both of these in the sub micro-molar range[66]), whereas purvalanol immobilised on sepharose did. It was speculated that while the linker is tolerated for GSK-3, it hinders CDK binding.

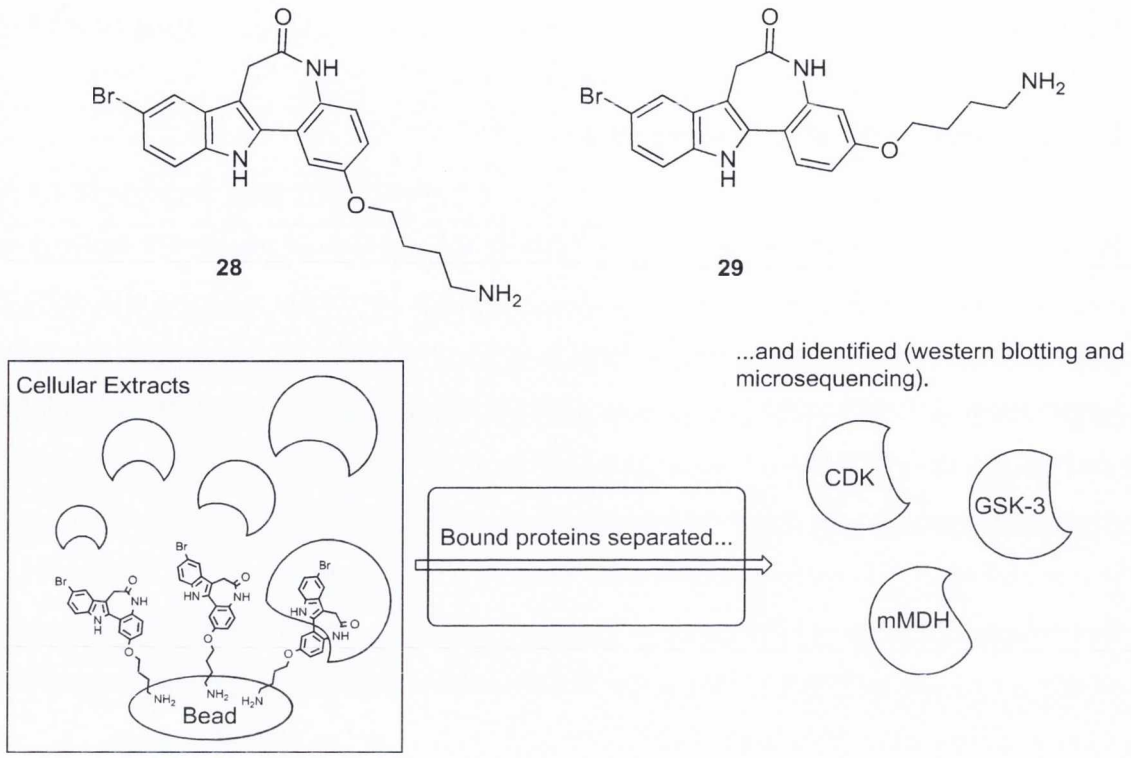

Figure 1.21: Identification of intracellular targets of paullones.

1.4.2.2 Targets: CDKs

Paullones are selective for CDKs when compared to several other relevant kinases that are involved in growth factor signal transduction (Table 2). The typical selectivity profile of paullones toward cell cycle CDKs is CDK1>CDK2>>CDK4. Early work on paullones neglected transcription CDKs including CDK9, so it is omitted from this data.[67,68]

Table 2: Activity profile of kenpaullone (**26**)[67] and alsterpaullone (**27**)[68] against a panel of relevant kinases.

Kinase	IC_{50} (μM)	
	26	**27**
CDK1/cyclin B	0.4	0.035
CDK2/cyclin E	7.5	0.2
CDK4/cyclin D	>100	>10
CDK5/p35	0.85	0.04
GSK-3α	-	0.004
GSK-3β	-	0.004
Erk1	20	22
Erk2	9	4.5
c-raf	38	>10
MAPKK	>100	>100
c-Jun NH_2-terminal kinase	>100	>100
PKC (8 isoforms)	>100	>100
cAMP-dependent kinase	>100	>100
cGMP-dependent kinase	>100	>100
Casein Kinase 1	>100	>100
Casein Kinase 2	20	>100
Insulin RTK	>1000	>100

1.4.2.3 Target: GSK-3α/β

Paullones also have significant activity towards glycogen synthase kinase-3, in fact many have better IC_{50}'s for GSK-3s than CDKs. GSK-3 is a kinase encoded by two genes GSK-3α and GSK-3β; with the two versions having 97% similarity at the primary sequence level and some but not complete redundancy in function between them. GSK-3s are ubiquitous in all cells and also termed pleiotropic *i.e.* they are involved in multiple distinct pathways affecting diverse cellular functions. Two of the functions will be discussed further in Sections 1.4.6.1 and 1.4.6.2, where paullones have been tested in their ability to effect change at the cellular function level; these functions are GSK-3's role in insulin signal transduction (type II diabetes) and microtubule regulation (tauopathies, Alzheimer's disease).

Further functions of GSK-3s have a definite but somewhat undefined links to cancer. This link is observed through several pathways and a multitude of substrates. GSK-3 is directly linked to the cell cycle by counting cyclin D among its substrates.[69] In addition it is involved in two clinically very relevant pathways in the occurrence of cancer. GSK-3 has a role in the (canonical) WNT signalling pathway (reviewed in ref [70]): WNTs are glycoproteins secreted by cells that interact with a cell surface receptor to transmit a signal, *via* the activation of β-catenin (transcription factor), leading to the expression of a set of genes involved in cell growth, differentiation, migration and cell fate. In normal circumstances, GSK-3 in complex with several other proteins phosphorylates β-catenin, signalling for its ubiquitinylation and subsequent degradation. This results in low levels of β-catenin unable to carry out its normal role of transactivating genes, and remains so until WNT signalling occurs. It has been observed that the proteins involved in this process, namely axin, β-catenin and APC have mutation in the corresponding genes in many cancers *e.g.* APC (Adenomatous Polyposis Coli) is mutated in more than 85% of colon cancers.[67]

As part of the body's response to abnormal cells such as cancer cells or those infected by viruses, macrophages release cytokines that bind to a receptor on the cell surface and initiate a cell response usually leading to apoptosis. One of these cytokines, TNF (Tumour Necrosis Factor) has a pathway whose ultimate outcome is mediated by GSK-3, though the actual connection remains unclear. What is certain is that either inhibition or removal of GSK-3 leads to an increase in TNF mediated apoptosis,[71] contrarily there remains uncertainty whether the TNF response in cancer is a potential therapy or harmful overall.[72]

For paullones that can be considered more selective for the relatively more abundant GSK-3s than for CDKs, many concerns and questions remain unanswered. One interesting observation is that regulation of GSK-3 in the canonical WNT signalling pathway and in insulin signalling occur in different ways, *i.e.* phosphorylation near the *N*-terminus does not occur and serve to inhibit GSK-3 function in WNT signalling.[73] Also the therapeutic window for the different systems seems to allow room for selectivity and the previously mentioned incomplete redundancy between the two forms of GSK-3.

1.4.2.4 Target: mMDH

Mitochondrial Malate Dehydrogenase is an enzyme that catalyses a reversible reaction converting oxaloacetate to malate, its catalytic activity is NAD+/NADH dependent (Scheme 1.1). It is required in gluconeogenesis, where glucose is synthesised from pyruvate in a multi-step process. This pathway operates in liver cells when blood glucose levels are low. mMDH also acts in the malate-aspartate shuttle, this transfers a reducing equivalent of NADH from the cytosol to the mitochrondria, as the NAD^+/NADH molecule itself does not penetrate the mitochondrial membrane.

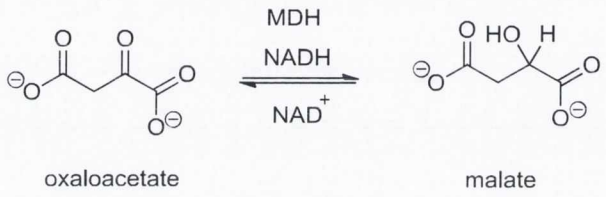

Scheme 1.1: Reaction catalysed by Malate Dehydrogenase.

The earlier work described in Section 1.4.2.1 with polymer bound **28** had determined that **25** and **27** exhibited mMDH in the micromolar range. More recent work involved synthesising more potent and selective paullone inhibitor of mMDH to evaluate its contribution to the overall anti-proliferative activity of the class, a summary of the results is given in Figure 1.22.[64]

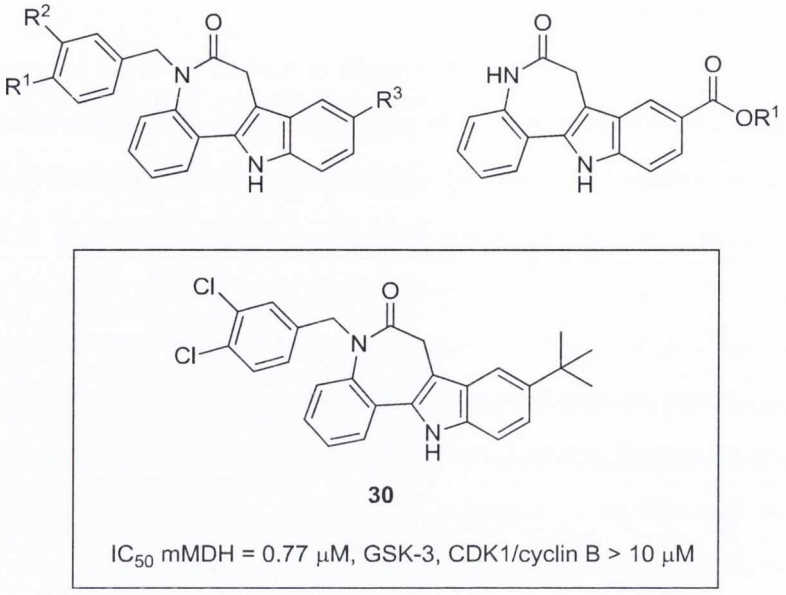

Figure 1.22: mMDH selective paullone inhibitors; **30** was found to have the highest activity as indicated.

It was noted that many of these novel inhibitors were lipophilic and a good relationship was observed when plotting pIC_{50} (mMDH) against predicted logP. Selected compounds from both series were tested *in vitro* and only weak anti-proliferative activity was observed at 10 μM in a 60 cell line test performed by the NCI. Therefore, mMDH has only minimal impact on paullones anti-proliferative activity. One of the reasons that justified this study was the observation that **27** causes the activation of caspases that typically respond to an insult in the mitochondrial membrane and hence a link with MDH was suspected. This mode of action will be discussed further in the next section (1.4.3).

1.4.3 Mode of Action

In a study of how alsterpaullone (**27**) can cause apoptosis,[74] it was found that the CDK inhibition was not enough to induce apoptosis, rather it was as a result of mitochondrial membrane perturbation followed by caspase activation. Firstly it was found that concentrations of at least 1 μM of **27** (compared with an IC_{50} (CDK1/cyclinB) of 0.035 μM and a GI_{50} of 0.49 μM) were required to induce apoptosis, and secondly a series of experiments were performed to determine exactly how this outcome was achieved.

Apoptosis is mediated by a group of cysteine proteases (caspases), working in parallel and in sequence. There are two proposed pathways through which apoptosis occurs: the extrinsic is a result of extra-cellular signalling acting on receptors in the cell membrane and transduced by caspase 8, and the intrinsic pathway which occurs when there is damage to mitochondria and mediated by caspase 9. There is some cross-talk between the two pathways and furthermore recent research suggests it is not as simple a picture as previously described. In the case of **27**, a loss in mitochondrial membrane potential is observed, followed by activation of caspase 9, and then caspase 8 and other effector caspases. The membrane potential change occurs even if a general or specific caspase inhibitors are used to pretreat the particular leukaemia cell line employed in these experiments. At that stage other pathways such as through known pro/anti apoptotic proteins (bcl-2, bcl-XL and XIAP) or occurring through the p53 pathway, were tested and dismissed.

The cell cycle effects caused by **27** include sub G1 accumulation, decrease in cell population in the S-phase, reduced rate of phosphorylation of Rb, G2/M arrest and loss of cyclin D3. Despite these changes if the tested cell line was pretreated with caspase inhibitor (ZVAD, a synthetic peptide) no apoptosis was observed. However, this does not prove conclusively a lack of a link and the actual mode of action remains elusive. The questions that remain yet unanswered include; what is the basis for the membrane potential change? is there any link with the cell cycle effects? or what is the target that confers anti-proliferative or apoptosis inductive properties of paullones if not their action as CDK inhibitors?

1.4.4 Structure-Activity Relationships (SAR)

Structure-activity relationships are an important part of medicinal chemistry and in developing new drug molecules. It involves taking the lead compound and synthesising a small number of analogues that vary in structure, then measuring their activity and comparing them with the biological activity of the lead compound in the hope of deriving a meaningful relationship between structure and activity. Thus, in an effect to identify the structural features that were important for CDK inhibition, early work involved synthesising paullones that were lacking the various groups suspected to be important in binding to the enzyme. A summary is provided in Figure 1.23.

At the outset, the position of the electron withdrawing group was determined as being required in the 9- position and that it must be electron withdrawing, an electron donating group leads to a definite decrease in enzyme inhibition.[67] Another factor is that for example 10-bromopaullone (**31**) leads to a decrease in selectivity for CDKs and has similar potencies against protein kinase C and casein kinase 2 as various CDKs. However a discrepancy arises in that **31** has a superior GI_{50} to **26**, (Table 3). That it was discarded at this stage appears to be due to the COMPARE correlation with flavopiridol (**8**) being low (0.16) suggesting its activity did not arise solely from CDK inhibition and thus falling outside the remit of the work.

Table 3: Comparison of **26**, **31** and 11-bromopaullone (**32**); also included paullone (**25**).[67]

Compound	IC_{50} (CDK1/cyc B) (μM)	pGI_{50} (mean) (M)
8	0.3	7.2
26	0.4	4.3
31	1.3	4.8
32	1.3	4.3
25	7.0	4.5

Subsequent work demonstrated the importance of the indole proton (H-12) and the amide proton (H-5) of the lactam ring, which were both speculated as forming hydrogen bonds.[75] To test the hypothesis the two protons were replaced individually with either simple alkyl (methyl, ethyl, benzyl...) or bulky boc groups. Selected data is shown in Table 4. It is clear that the more important group is H-5, and because an ethyl group fares worse than methyl (entries 2 and 3), this suggests that this part of the molecule occupies a region of the binding site where there is little room to spare; it seems that H-12 is of lesser importance but still necessary (entry 4). Additionally the importance of the lactam oxygen was investigated (entries 5-7), although the data is less clear, the kinase assays indicate poorer activity when this is modified but *in vitro* testing in the cell line listed (HCT-116) suggest otherwise, an especially stark contrast when the oxygen was replaced by a sulphide (entry 6).

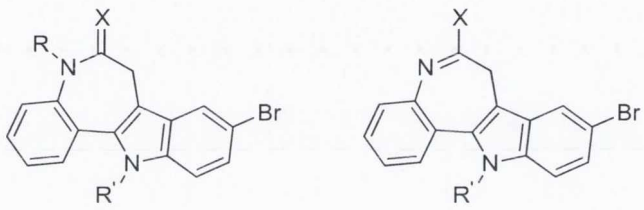

Table 4: CDK1/cyclinB inhibiton and *in vitro* anti-proliferative activity of selected paullones.[75]

Entry	R	R'	X	IC_{50} (CDK1/cyc B) (μM)	pGI_{50} (HCT-116) (M)
1	H	H	O	0.4	5.7
2	Et	H	O	470	4.9
3	Me	H	O	20	4.7
4	H	Et	O	23	4.5
5	H	H	S	2.3	ND
6	-	H	-SMe	43	5.7
7	-	H	-NHOH	1.0	5.2

These constrictions made for a very rigid structure; the only place that substituents could be successfully appended was the 'A' ring at the 2- and 3- positions, as modelling

suggests it is orientated out of the binding cleft. Two lines of thought were followed to either place a group capable of forming a covalent bond or a hydrogen bond. Invariably the covalent strategy involves epoxide groups with variable chain lengths.[76] This line of enquiry was very limited in exposition as the attachment of such groups gave a similar activity profile and individual activities in line with **26**, the existence of a covalent bond was not proved conclusively and further work was deemed necessary. The evidence purported was based on a modelling study showing the close proximity of the epoxide to an aspartate residue, though without an improvement in activity it seems unlikely that there was a bond. A greater improvement in inhibition efficacy was observed after the attachment of aliphatic nitriles, most notably adding 2-cyanoethyl substituent to **27** producing one of the most active compounds to date (IC_{50} (CDK1/cyc B) = 0.23 nM).[77] The reason given for this increase in activity was a possible hydrogen bond with a lysine residue.

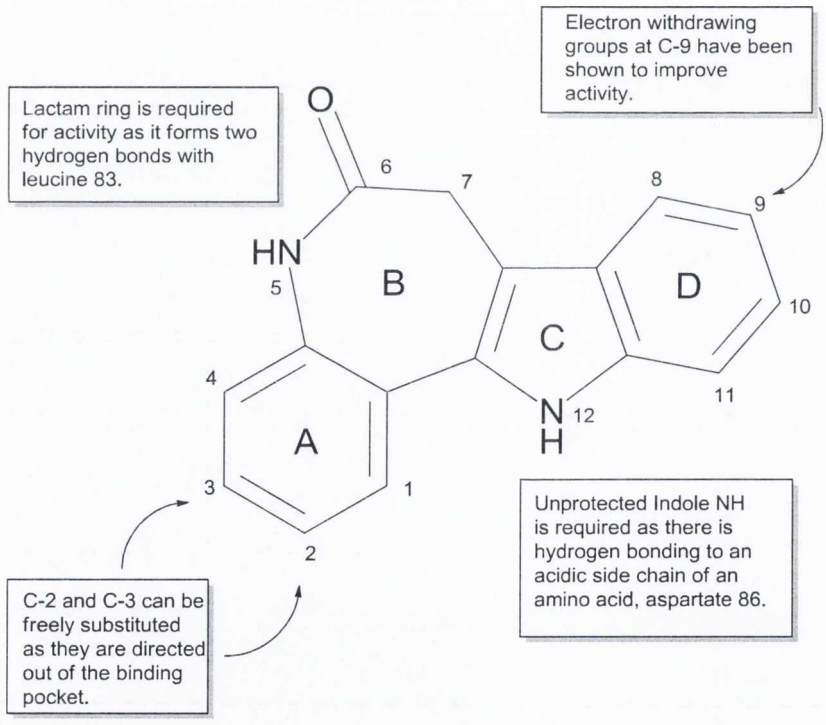

Figure 1.23: A summary of the SAR of the paullone class as CDK inhibitors.

It should be noted that while SARs are well established when enzyme inhibition of CDKs is the activity of interest, the structural requirements of paullones for anti-proliferative activity are not so well defined *i.e.* a paullone that has significant CDK

inhibition activity, may fail to produce any worthwhile *in vitro* anti-proliferation activity and this perplexing trend is observed across the class. This trend will be discussed further in the next section.

1.4.5 Quantitative Structure-Activity Relationships (QSAR)

After a sufficiently varied collection of paullones had been synthesised, attempts were made to quantify the features that account for good CDK inhibitory activity. In a quantitative structure-activity relationship (QSAR) study, the biological activity is expressed as a function of physio-chemical parameters that can be largely divided into three categories: hydrophobicity, steric and electronic parameters (these can either be experimentally determined or theoretically calculated). An equation is generated by regression analysis and validated by statistical analysis to determine how well the equation fits the biological data. The final test is to take the derived equation and use it to determine the biological activity of unknown or new compounds to check for accuracy.

When the IC_{50} values for a small set of paullones against CDK1/cyclin B were expressed in terms of various parameters of their C-9 substituent,[78] one parameter was found to feature significantly in the derived equations, Hammett coefficient σ_m, other parameters could be included but gave inferior statistical results to a simple equation containing σ_m as the lone variable. This indicated that inductive effects in the 'D' aromatic ring were most important, but this result only served to quantify what was already known; that increasingly electron withdrawing groups at C-9 lead to better activity. It is not surprising that steric effects do not contribute at all, since there was little variation in the bulkiness of substituents of the compounds in the training set, thus they must all fit without experiencing steric clashes in the binding site. An attempt was made to express the biological activity, GI_{50} for cancer cell-line HCT-116, in terms of the inhibition of the CDK1/cyclin B or the C-9 parameters, however no correlation could be made.

CoMSIA is a 3D variant of QSAR and depends on the alignment of the electrostatic/steric structures of the group of compounds in question to determine the pharmacophore. Compared to the previous strategy it creates a more complete picture of the biologically relevant structure of the inhibitors and allowed space within the binding site of the target protein. In an extensive study with a large training set, the IC_{50}'s for CDKs 1, 5 and GSK-3 were employed in turn.[79] The paullones were docked and aligned in the binding site of CDK1/cyclin B using **26** as template, thus the model is optimised for this complex over the complexes involving CDK5 or GSK-3. The three models derived predicted the test set quite well, though not unexpectedly slightly worse for CDK5 and GSK-3. The strength of CoMSIA is the generation of 3D contours that show favourable and unfavourable interactions for each of the kinases, thus a comparison can be made and differences should inform future design. CDK1 and CDK5 are very similar in their requirements because of near identical active sites, while differences between them and GSK-3 were observed that could prove useful but to date have not been addressed further.

1.4.6 Potential Therapeutic Uses

For the most part paullones were originally positioned as anti-cancer agents but this functionality still remains in development, it has not progressed beyond the *in vitro* cell-line testing stage. In the meantime several other potential uses have been investigated.

1.4.6.1 Alzheimer's disease

Alzheimer's disease (AD) is a neurodegenerative disease that causes a diminution of neuron form and function in the brain. The disease is currently without effective cures; the available drugs are limited solely to those having the ability to relieve symptoms without preventing the progression of the disease. Current drugs target the observed deficiency in the cholinergic transmission system, and most fall into the category of acetylcholine esterase (AChE) inhibitors (donepezil, rivastigmine, galantamine and tacrine), with memantine being the exception (a non-competitive inhibitor of NMDA, a glutamate ionotropic receptor). Much work is underway to correct this scarcity.[80]

Unlike currently available treatments that resolve deficiencies in neurotransmitters, which is considered an end-point rather than a causative factor,[79] novel therapies revolve around the two major pathological features that are linked to the observed destruction: neurofibrillary tangles and amyloid plaques. Amyloid plaques have drawn the most attention[81] and therapies based on the formation, aggregation and downstream effects of amyloid β –peptide (Aβ) are in development, for example BACE and γ-secretase inhibitors.

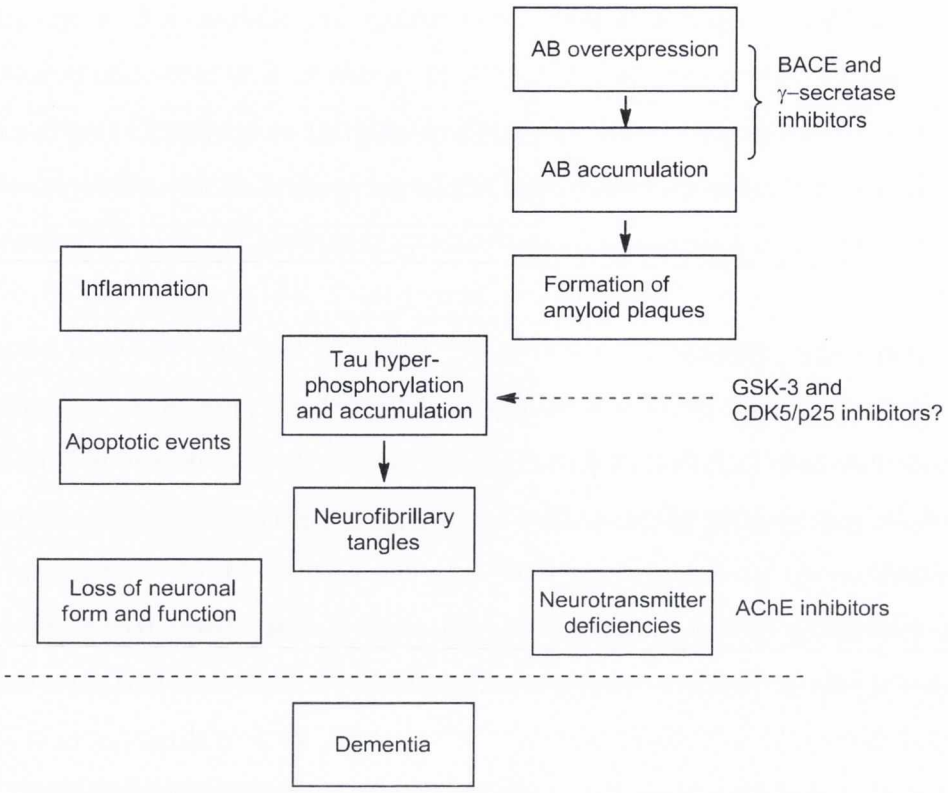

Figure 1.24: Overview of the causative and resulting features of the dementia associated with Alzheimer's disease and some of the therapeutic interventions.

Early work on paullones explored their potential in Alzheimer's disease, with the work focused on tau hyperphosphorylation,[68] but subsequently an interesting link was made with the amyloid pathway that occurs upstream (see below). Hyperphosphorylated tau is the major component of the neurofibrillary tangles (NFTs or PHFs, paired helical filaments) associated with Alzheimer's disease and other related tauopathies. Tau's normal role is to stabilise microtubules especially those in neurons. CDK5/p25 and GSK-3β are two of the kinases involved in the phosphorylation of tau isoforms, and hence **27** was demonstrated to prevent the phosphorylation of specific residues by GSK-3β, as demonstrated with the use of antibodies specific for those particular epitopes. Although the effect of the NFTs on disease progression remains uncertain, more attention is being refocused on this topic at present.[82] Despite suggestions that the precipitation of tau may be an endpoint after a caspase response, the fact remains that neuron death coincides with NFT formation either as a cause or effect.

More promisingly, **26** was shown to reduce the levels of Aβ in cells.[83] This is again tied to GSK-3 inhibition, but this time it involves GSK-3's role in association with presenilin-1. Presenilin-1 is part of the multi-protein complex γ-secretase. β-Secretase (BACE) cleaves a transmembrane peptide called APP (Amyloid Precursor Protein), then APP is cleaved again but this time by γ-secretase to produce Aβ peptides that are released into the intercellular space where they then polymerise and form plaques. The exact nature of the relationship between GSK-3s and presenilins is unclear, but in additional tests with animal cells expressing the APP gene **26** could reduce the levels of Aβ by 50% at 2 μM and > 90% at 5 μM. γ-Secretase has another important substrate besides APP, Notch, which is involved in differentiation and GSK-3 inhibition (lithium only demonstrated) activity did not impact on the processing of this protein. Also the CDK activity of **26** was ruled out, by using *(R)*-roscovitine which has poor GSK-3 inhibitory activity and no changes were observed in the levels of Aβ.

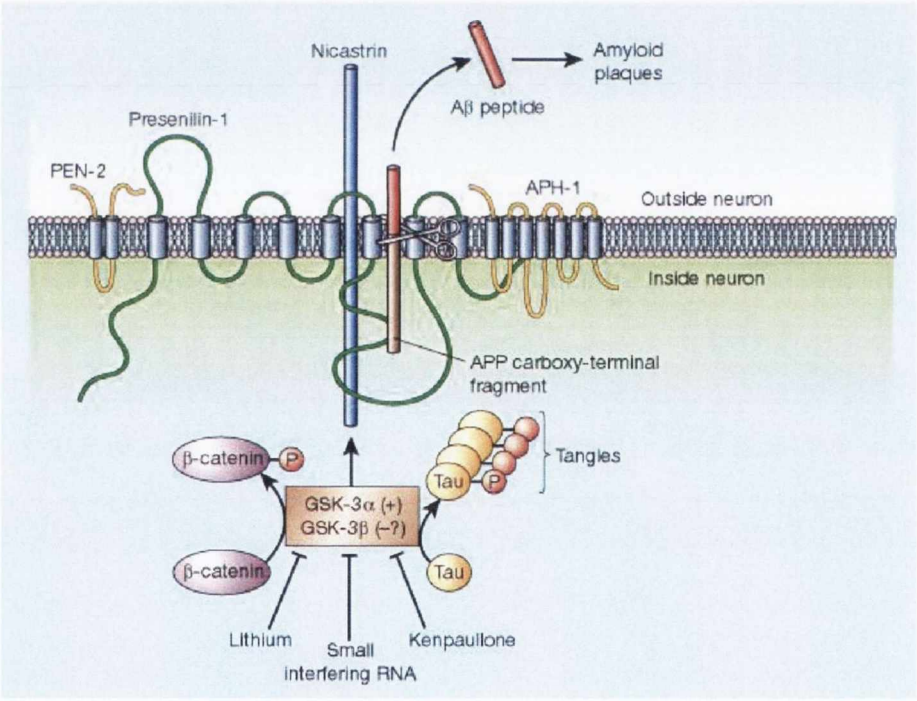

Figure 1.25: Multiples substrates of GSK-3's in Alzheimer's disease?[84]

1.4.6.2 Protection of Insulin-Producing Pancreatic Beta Cells

Diabetes Mellitus is a disease that affects 220 million people worldwide and that is predicted to rise to above 360 million by 2030.[85] The disease is classified into two types: Type I is a failure of the body to produce insulin, Type II results from an insensitivity of cells to respond to insulin. Most occurrences of the disease are type II, and type II is tied to obesity and physical inactivity, thus it is controllable to some extent without drug intervention provided it is diagnosed and managed appropriately from an early stage. However failure to take preventative action causes irreversible damage to eyes, heart and kidneys. In later stages of the type II disease, it begins to resemble type I with the loss of the pancreatic β-cells that produce insulin. It is this loss of pancreatic β-cells that Kunick *et al.* were hoping to prevent when employing paullone inhibitors of GSK-3.[86] GSK-3 has a role to play in apoptosis of pancreatic β cells.

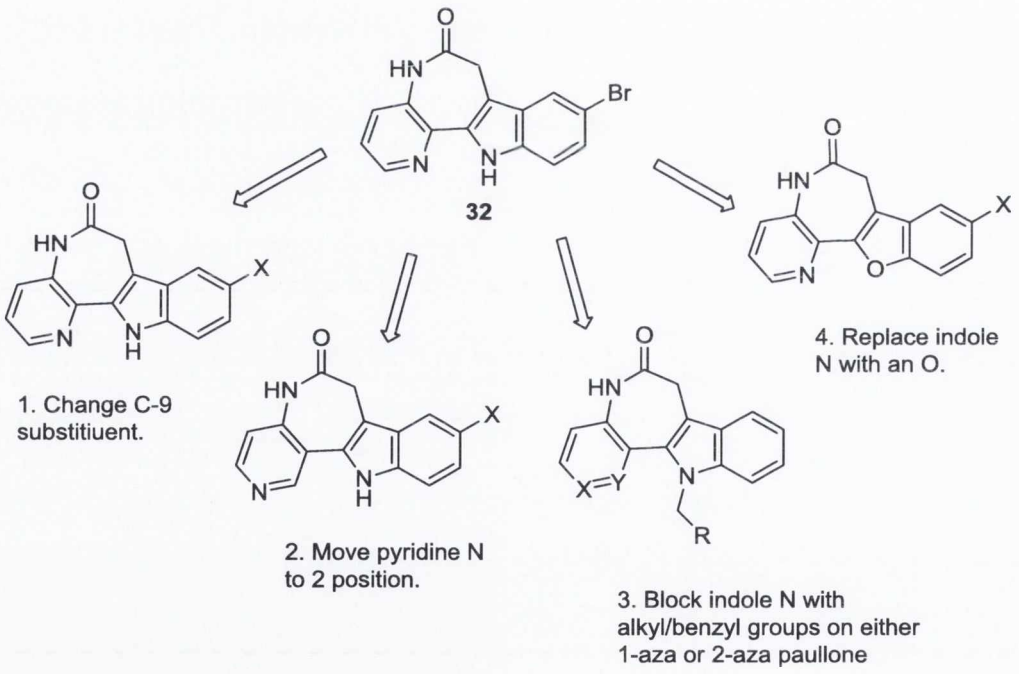

Scheme 1.2: Outline of changes made to lead compound, **32**.

1-Azakenpaullone (**32**) was identified as a selective GSK-3 inhibitor,[87] a 100-fold increase in selectivity for GSK-3β was observed over that of CDK1/cyclin B or CDK5/p25. Taking this compound as a lead structure, two simple modifications were

explored: changing the substituent at the C-9 position and the position of the nitrogen in the A ring of the paullone structure (Scheme 1.2; changes 1 and 2). Both electron withdrawing and donating groups were tested; with electron withdrawing groups exhibiting better activity. The 2-aza set of derivatives had good activity but were less selective than the 1-aza derivatives. Replacing the pyridine ring with another electron deficient ring (benzonitrile) gave a compound of good activity. 1-Aza-9-cyanopaullone (**33**; named cazpaullone) and 1-aza-9-trifluoromethylpaullone (**34**) (Figure 1.26) were found to be the most active out of all the compounds with both having an IC_{50} (GSK-3α/β) of 0.008 μM and IC_{50}'s for CDKs in the micromolar range.

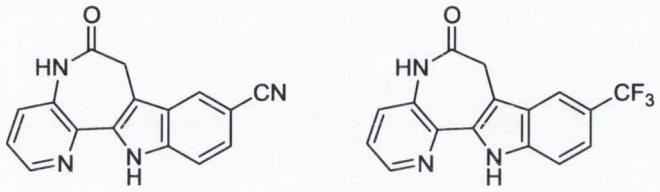

33 **34**

Figure 1.26: Most selective and active paullone based GSK-3 inhibitors.

One strategy that failed to provide any noteworthy new compounds was based on the known crystal structure of **27** bound to GSK-3β (Figure 1.27), which indicated that there was a water molecule between H-12 and a glutamate/glutamine residue, it was decided to take advantage of this difference with the binding pocket of CDKs, where there is a direct hydrogen bond between H-12 and an aspartate side-chain. Accordingly, H-12 was either blocked with an alkyl group to displace the water, or the nitrogen replaced with oxygen that would allow for re-orientation of the water molecule, something that was thought to be impossible in the CDK binding pocket thus increasing selectivity (Scheme 1.2; changes 3 and 4). Interestingly the alkylated compounds retained some activity and selectivity against GSK-3 but the more rationally designed benzofurans had no observable activity.

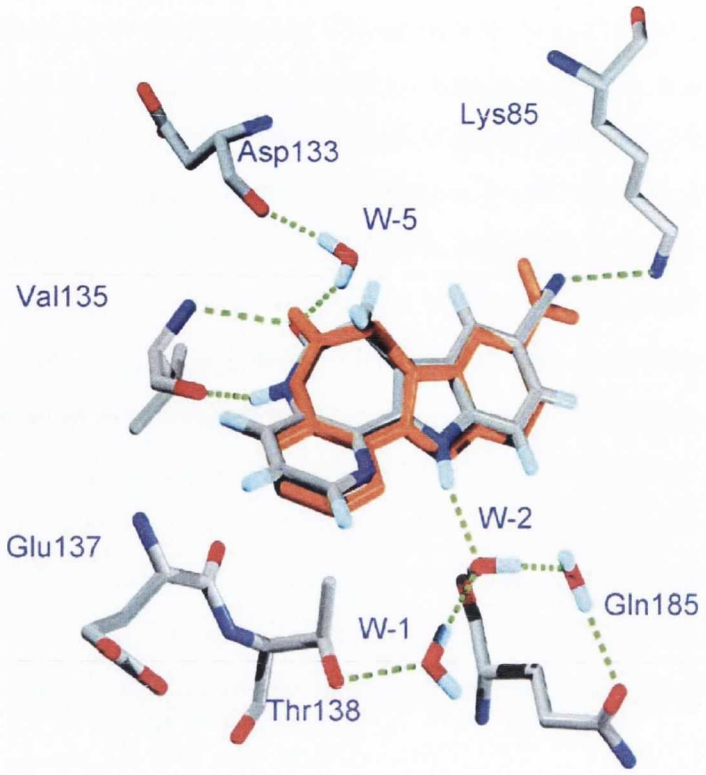

Figure 1.27: Crystal structure of **27** (coloured orange) bound to GSK-3β, with **33** overlaid.[86]

To determine if the compounds inhibited GSK-3 inside cells, an assay to measure the levels of phosphorylated β-catenin was used. For the determination of the ability of the newly synthesised paullones to prevent apoptosis and promote cell division, rat pancreatic β-cells were isolated, which were then exposed to varying levels of a glucose/palmitate mixture that prevents the growth of cells and at high concentrations triggers apoptosis, *i.e.* glucolipotoxicity. Analogue **33** proved to be the best out of all the compounds synthesised, able to reduce the levels of apoptosis by 50% at 2 μM. It appears to have a narrow therapeutic range as concentrations in excess of 1 μM appeared to suppress metabolic activity, as evidenced in tests to determine the ability to promote replication in pancreatic β-cells: at 0.5 μM a 2.5 fold increase in replication was observed that compares well with another GSK-3β inhibitor CHIR9902, however at 2 μM no increase in replication was observed. Interestingly, it was found that **32** and **33** activated the expression of Pax4, a β cell specific transcription factor, which seems to have an effect on the rate of apoptosis. Also, it was found that **27** has a similar effect on its expression levels, even though it is not selective for GSK-3 and does not appear to

have been included in this preliminary biological testing, it still has impressive activity against GSK-3 (IC_{50} 0.004 μM). Two other specific GSK-3 inhibitors CHIR99021 and 6BIO did not have a similar effect.

While the GSK-3 selective paullones have been demonstrated to achieve what they were designed to do, several questions remain to be answered by future work, such as the target(s) that cause the change in Pax4 levels and if this is beneficial for therapy.

1.4.6.3 Anti-Leishmania Activity

Recent work in expanding the potential uses of paullones involved screening a library of previously synthesised compounds and evaluating their ability to inhibit the amastigote stage (obligate parasite of macrophages) of leishmania parasites,[88] in the hope of finding new drugs. Visceral leishmaniasis is an emerging disease in developing countries which can be fatal, and the current treatment regimes are limited by severe side-effects, high cost and parasite resistance.

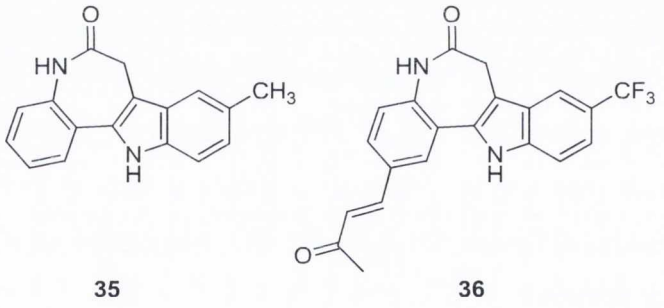

Figure 1.28: Two lead structures identified in preliminary testing.

Two compounds acting as lead for the development are shown in Figure 1.28. Analogue **35** has the poorer activity but is not toxic against macrophages, while **36** has good parasite growth inhibitory activity (extracellular, in an acidic growth medium) but with some toxicity. Replacing the trifluromethyl substituent with methyl in compound **36** gave a compound with both beneficial effects, however no inhibition of the growth of parasites was observed in infected macrophages. A *tert*-butyl group in the 9 position gave a compound that did overcome this challenge and caused a very good inhibition of parasite growth inside cells, except it was highly toxic to the macrophages. A

breakthrough was made when the methyl group of the unsaturated ketone was replaced with an (hetero-)aryl group (compounds **37-41,** Figure 1.29), furnishing compounds that could inhibit the growth of more than 70% of the parasites in infected macrophages at concentrations of 5 μM.[88]

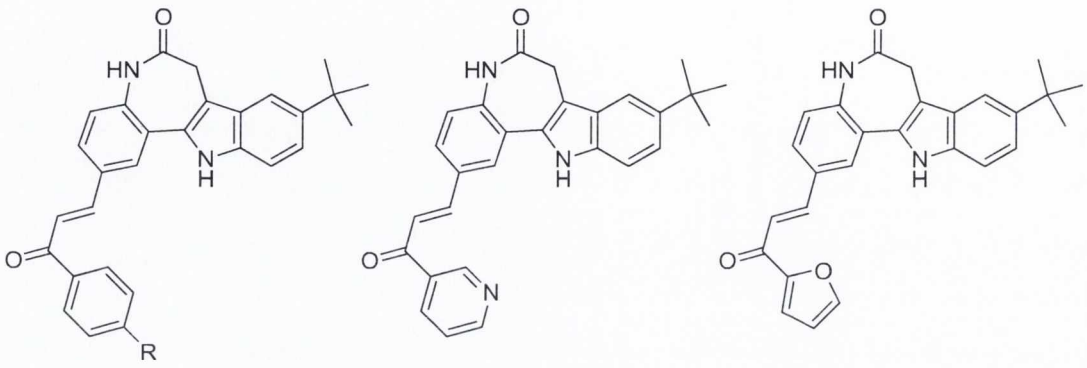

37 R = H
38 R = Cl
39 R = OMe

40 **41**

Figure 1.29: Compounds with improved intracellular anti-parasitic activity.

It was noted by the authors that these active compounds bore a similarity to the already well established chalcone based antileishmanial agents such as licochalcone A (**42**, Figure 1.30). When a molecule was synthesised that is a fragment of **39** (**43**), this produced an inferior inhibitor but still with significant activity in the assay involving extracellular parasites, although the data for this compound acting against infected macrophages is not reported.

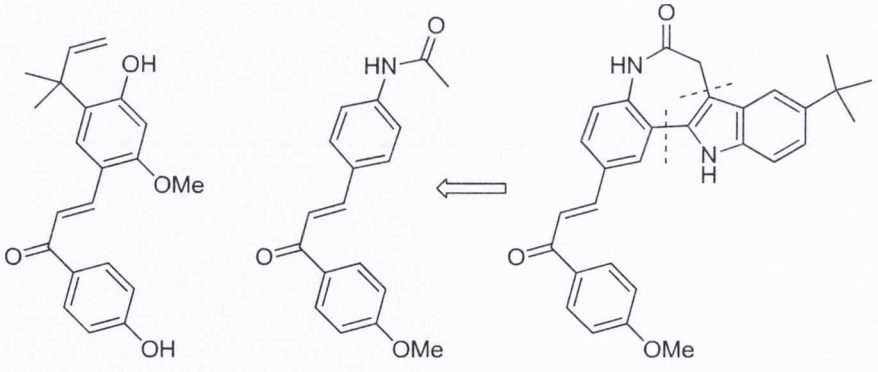

42 **43** **39**

Figure 1.30: Comparison with chalcone based antileishmanial compounds.

1.4.7 Transition Metal Complexes

Early work on synthesising transition metal complexes with modified paullones as ligands, used either gallium[89] (**44**) or ruthenium[90] (**45**, **46**) as the metal (Figure 1.31). The goal behind synthesising such complexes is that they were expected to have increased solubility, with the activity of the ligand attenuated or a synergistic effect observed between the toxic metal and ligand. With these initial complexes a slight to moderate increase in activity was observed over the unbound ligand. Of special note was the gallium complex, which had significant activity against melanoma cells, this tumour cell type had not been previously mentioned as being particularly sensitive to paullones.

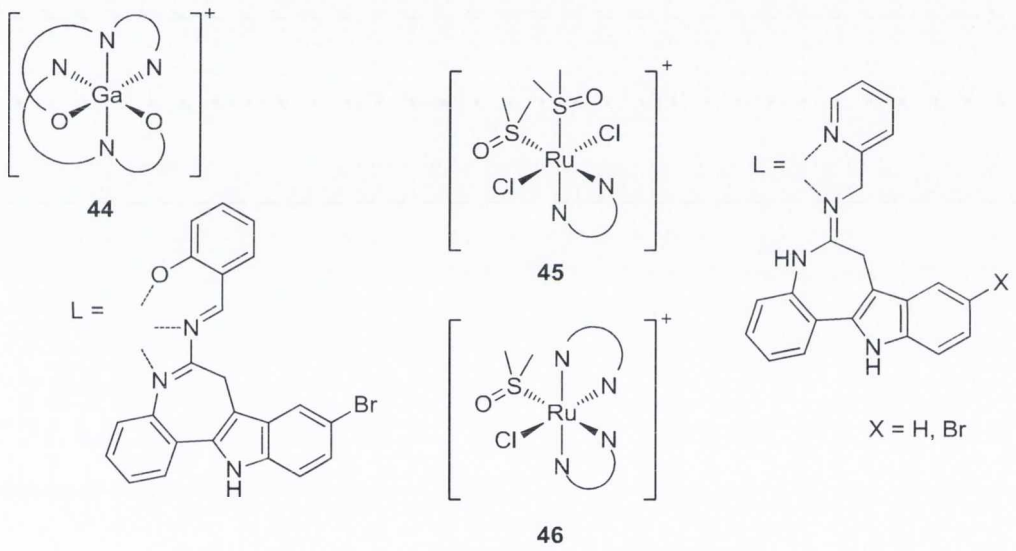

Figure 1.31: Gallium and ruthenium complexes.

A more detailed medicinal chemistry study[91] involved osmium and ruthenium arene complexes, complexed with two paullone ligands that have two distinct points of attachment on the paullone molecule (**47**, **48**). Also depicted in Figure 1.32 is a complex with an alternative point of attachment to the paullone molecule that was investigated in an additional study (**49**).[92] A potential mode of action was investigated by monitoring the ability of these complexes to bind to a nucleotide, 5'-GMP, but it was not found to be a significant factor. Unfortunately for these complexes stability and hydrolysis was a serious issue.

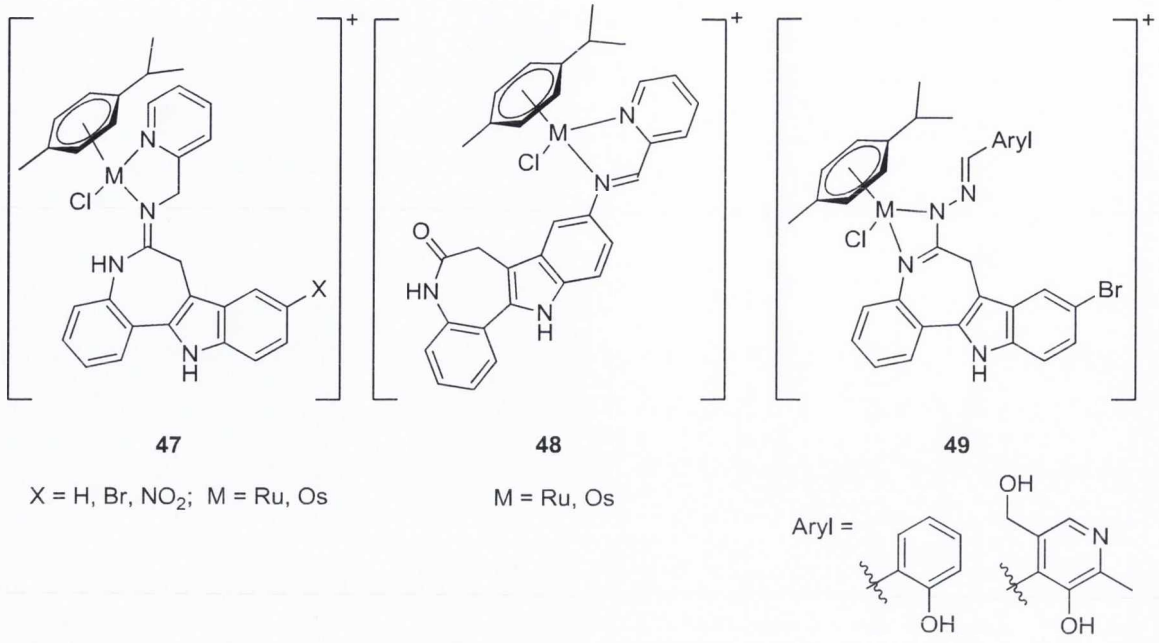

Figure 1.32: Osmium and ruthenium arene complexes.

More recent work involved copper complexes (Figure 1.33),[93] which have produced remarkable results, matching even **27** for anti-proliferative activity *in vitro*. Even more interesting is that the ligand is based on **26**, which has only moderate activity when not modified and complexed in the manner shown. Also of interest is that the ligand on the most active complex (**52**) was found to be insoluble to the extent that a reliable comparison could not be made between the anti-proliferative activity of the unbound and bound paullones.

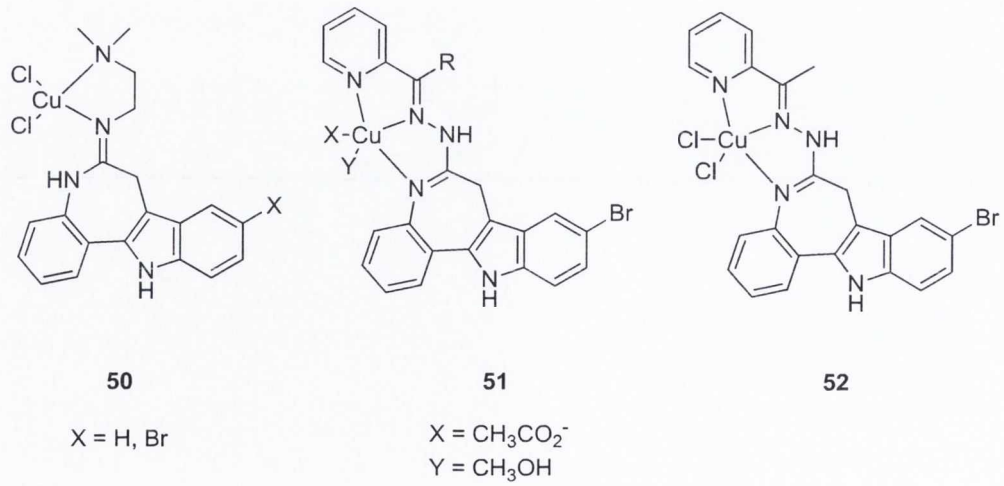

Figure 1.33: Copper complexes of paullones.

One piece of information that could be considered lacking from each of the papers published so far in this area, is enzyme kinetic experiments with CDKs or other related kinases, because the actual target is unknown. It had been demonstrated that DNA cross-linking is unlikely, though intercalation was not ruled out.

1.4.8 Paullone Syntheses

From the time that paullones were identified as potential anti-cancer compounds, several syntheses have been reported besides the original method by Kunick, which was based on the Fischer indole synthesis (method A; Section 1.4.8.1). All of the strategies thus far described are outlined in Scheme 1.3.

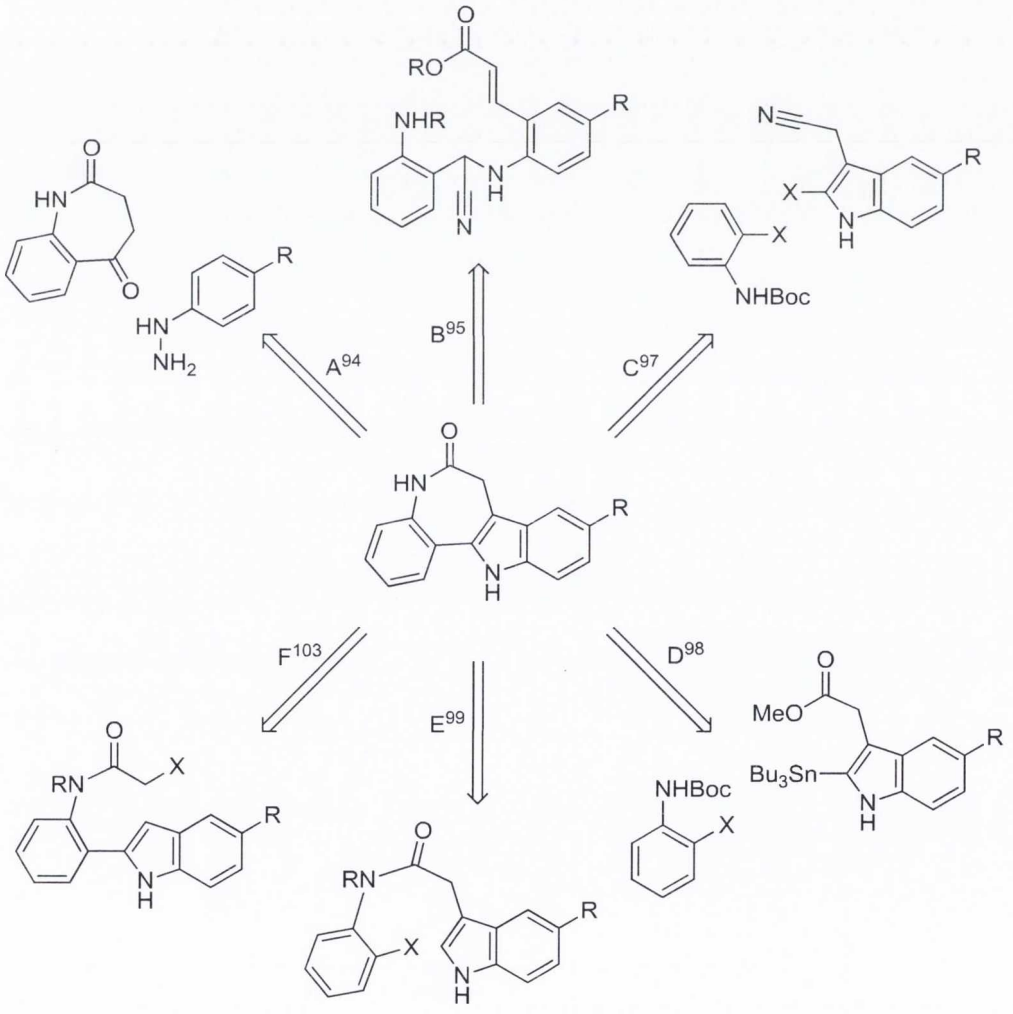

Scheme 1.3: Retrosynthetic outline of reported syntheses.

1.4.8.1 Method A

This was the original methodology for synthesising paullones, it was first described by Kunick[94] and involves a Fischer indole reaction as shown in Scheme 1.4. Two alternatives are used to effect this final step, either to use strong acid (typically conc. sulphuric acid) or to heat the hydrazone in diphenyl ether under reflux. The complete sequence has the advantage that it allows for the formation of large quantities of the ketone starting material, which can then be reacted with a variety of hydrazines to quickly access a large quantity of paullones. As a drawback, each time a change in the substitution pattern on the A ring is required, it necessitates the synthesis of a new ketone over several steps.

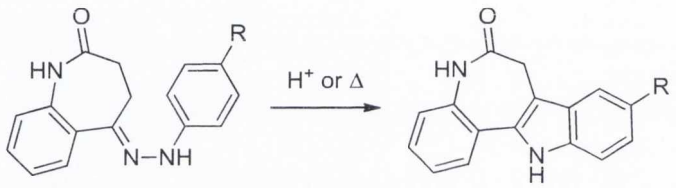

Scheme 1.4: Final step involving a Fischer indole reaction.

1.4.8.2 Method B

Ferenc and Opatz reported a paullone synthesis[95] based on their previous work involving C-deprotonation of α-aminonitriles.[96] It is a short synthesis to give a very desirable product, an indole-3-acetate (Scheme 1.5). The Strecker reaction was carried out in ethanol with potassium *t*-butoxide as base; it gave a complicated mixture of desired α-aminonitrile **54**, corresponding indole **55** and imine **56**. Despite this, the complete synthesis is four steps in total and provides the paullone in an overall yield of 35%.

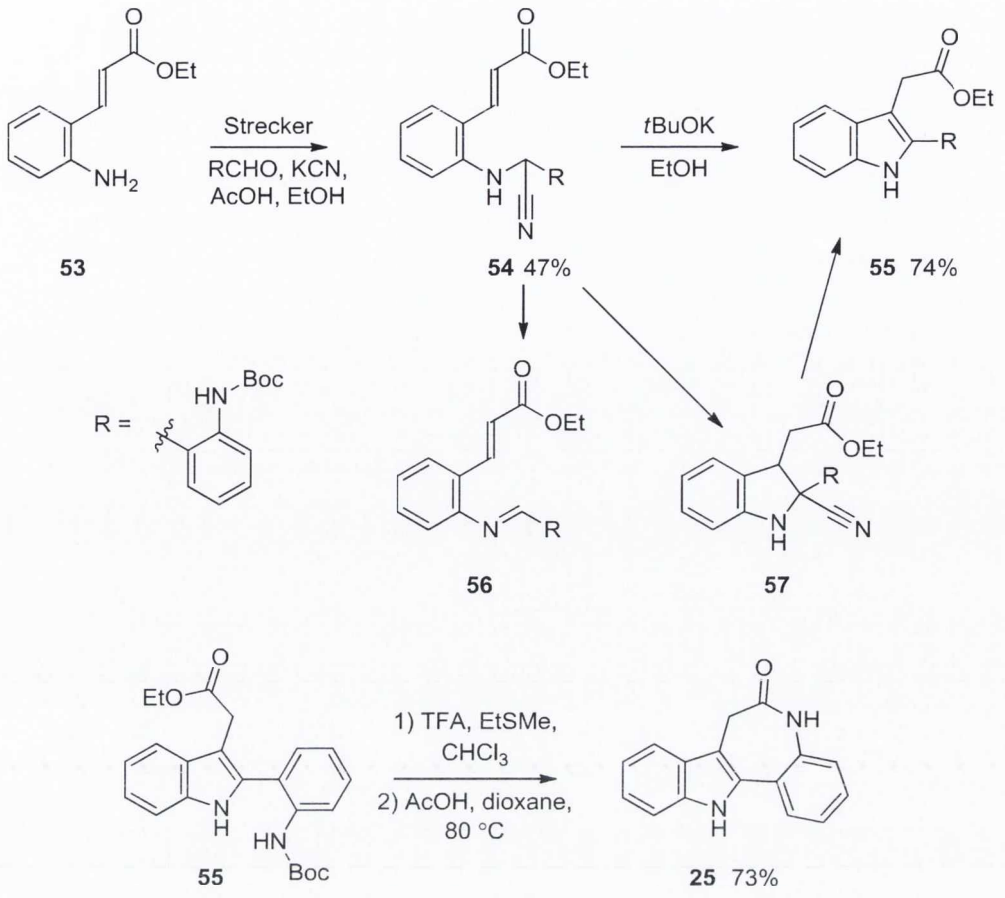

Scheme 1.5: Deprotonation of α-aminonitrile **54** and subsequent cyclisation to give indole-3-acetate **55** and subsequently **25**.

1.4.8.3 Methods C and D

Ostensibly, these two methods are very similar in concept but differing in execution (Scheme 1.6). While method C[97] uses a one-pot borylation/Suzuki-Miyaura coupling strategy and method D[98] uses a radical cyclisation followed by a Stille coupling, both involve intermolecular palladium catalysed coupling reactions to form the same bond in the products.

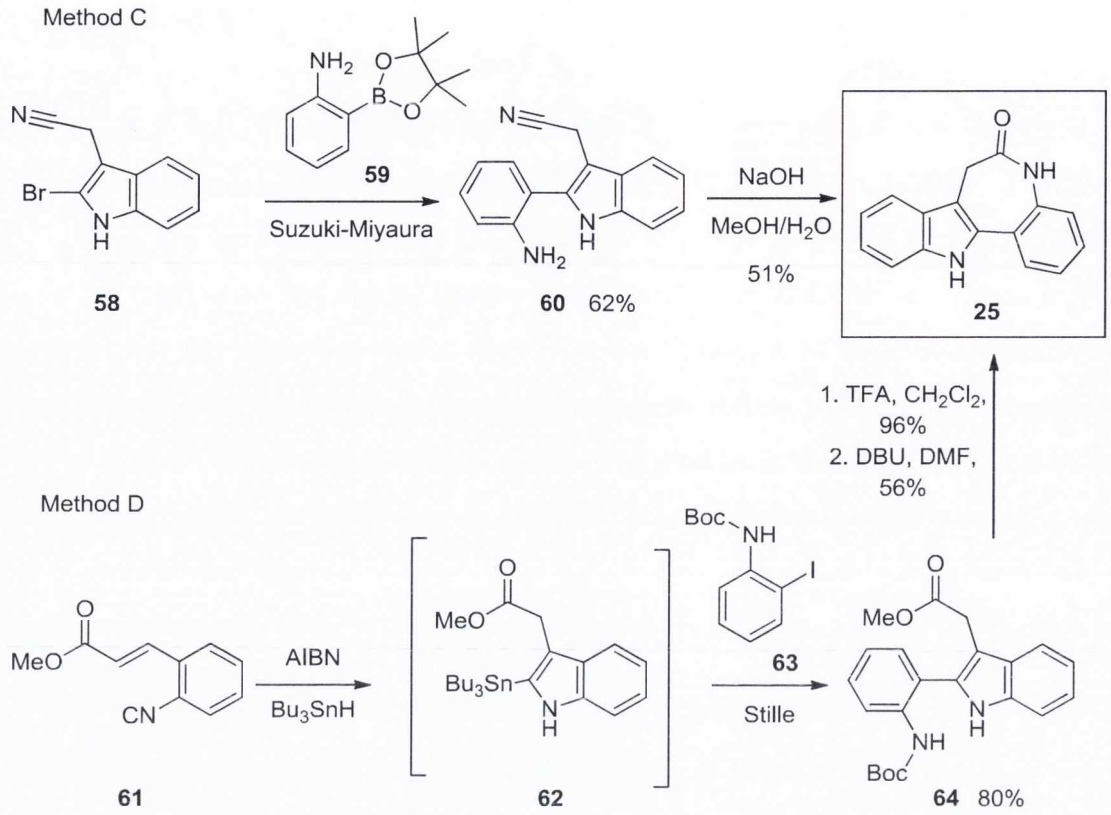

Scheme 1.6: Comparison of methods C and D.

1.4.8.4 Method E

The main difference between this method and the preceeding methods C and D is that the coupling is achieved intramolecularly as depicted in Scheme 1.7.

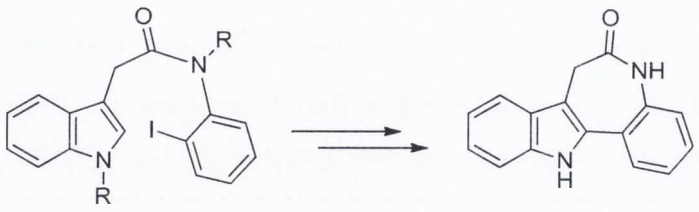

Scheme 1.7: Outline of intramolecular method E.

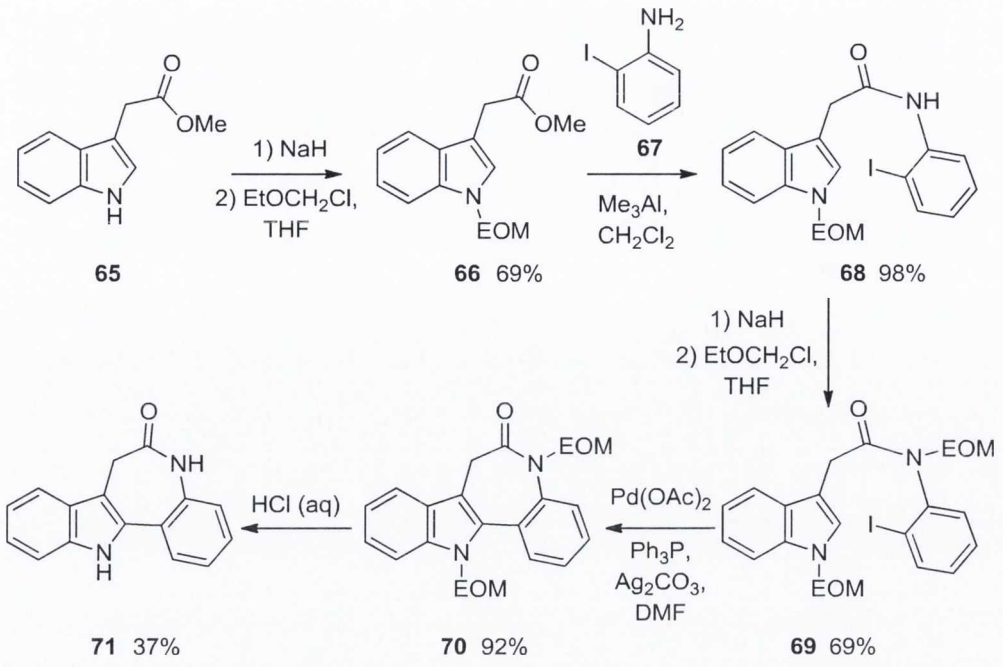

Scheme 1.8: Synthesis of paullone by an intramolecular coupling reaction.

Joseph *et al.* pioneered[99] this strategy (Scheme 1.8), and others have followed closely behind.[100,101] At present this is the most flexible synthetic strategy, with the A ring entering the route near the end of the synthesis. This was further evidenced when this chemistry was used to create novel and diverse compounds related in structure to paullones (Figure 1.34).[102]

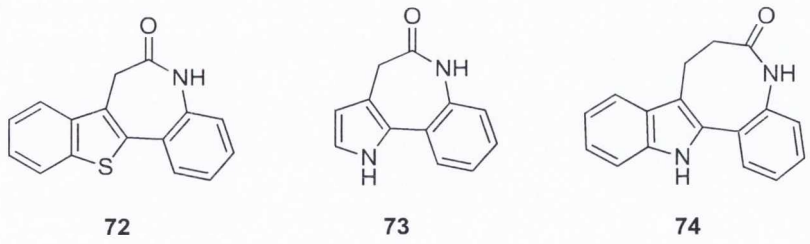

Figure 1.34: Diversification in the paullone structure.

1.4.8.5 Method F

Bremner and Sengpracha employed an intramolecular radical reaction and an intramolecular Heck reaction in their six step synthesis (eight when including addition

and removal of a required benzyl protecting group, yields 62% and 40% respectively), published in 2005 (Scheme 1.9).[103] It was not without problems, the intramolecular radical reaction involving **80** gave two products, depending on which end of the double bond the radical reacted with. The desired product (**81**) was the major product in most examples given, and the yields improved when the higher boiling solvent mesitylene was used in place of toluene. In addition there is the possibility of lactam cyclisation on N-1 rather than C-3 particularly noticeable for the substrate bearing the electron donating methoxy group.

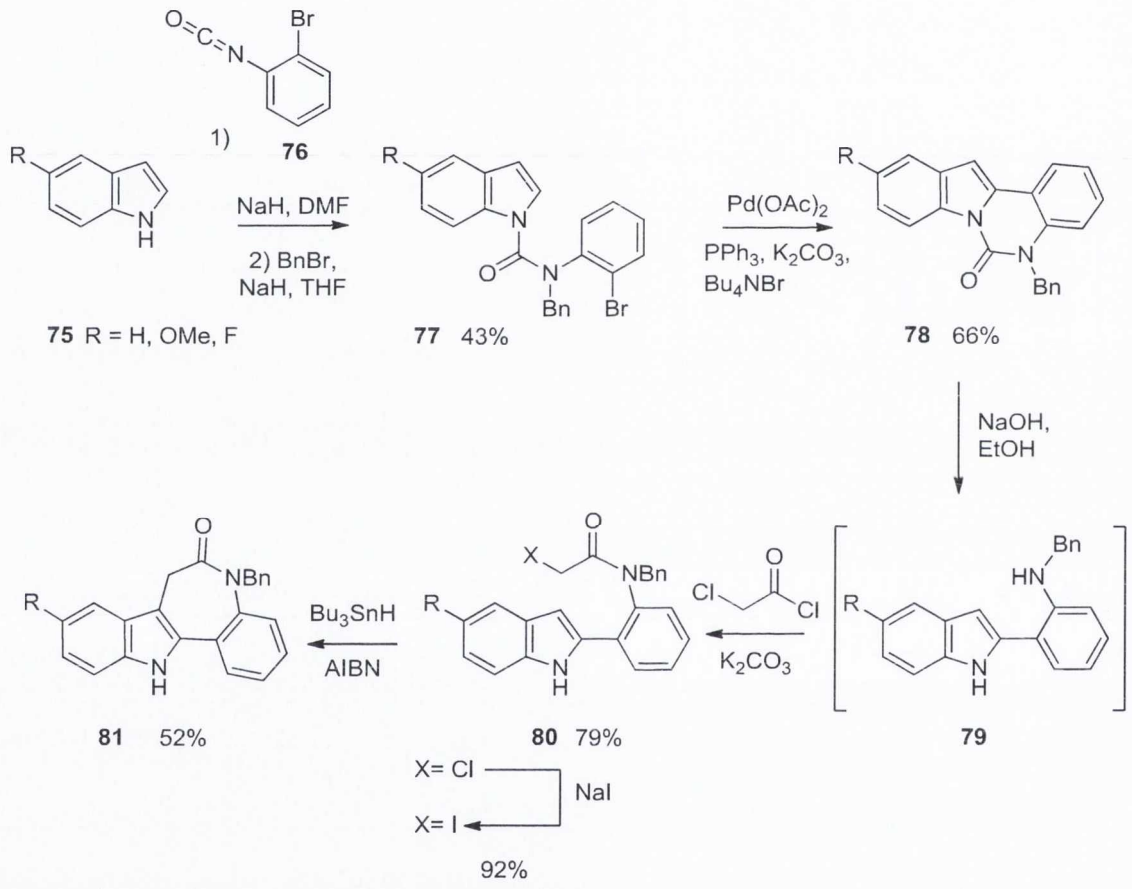

Scheme 1.9: Method F (Yields given for R = H).

1.5 Aim of thesis

The primary aim of this thesis was the synthesis of 9-azapaullone (**82**; Figure 1.35). This molecule was chosen because the pyridine nitrogen was considered an interesting substitute for the nitro group of alsterpaullone, and also it was expected to increase solubility of paullones especially when **82** is employed as a salt. The solubility of paullones is poor in aqueous media, and this was suspected as a hindrance to their testing and biological activity.

Figure 1.35: Target compounds of the current work.

In addition, two other compounds were proposed, the *N*-oxide (**83**) and *N*-benzyl (**84**) derivative of **82**. *N*-oxide **83** was chosen to test the hypothesis that there is a requirement for a hydrogen bond acceptor at the 9- position of the paullone structure. A comparison between the biological activity of **83** and **82** should be helpful in this regard. It was thought that the phenyl ring of **84** should have a noticeable impact either as a sterically demanding group or its lipophilicity would be a suitable compliment to this area of the binding site.

Results and Discussion

2.0 Retrosynthetic Analysis

9-Azapaullone (**82**) was designated the main target molecule; two proposed syntheses are outlined in Schemes 2.1 and 2.2. With only two published syntheses of the paullone core when the present work commenced, the initial options were limited. With Kunick's strategy depending on a Fischer indole synthesis, (Section 1.4.8.1; method A) and believed to be difficult if not impossible to utilise with 4-pyridyl hydrazones, it was rejected at first. The other option included the synthesis of a nitrile (**85**) and a subsequent one-pot hydrolysis/lactamisation, (Section 1.4.7.3; method C), and it was this strategy we chose to begin with.

It was envisaged that nitrile **85** could be obtained from the reduction of a nitro compound, **86**. Before this transformation, the nitrile functional group could be introduced *via* the sequential quaternisation and substitution of dimethylamine **87**. The dimethylamine functionality of **87** was expected to be accessible from azaindole **88**, by completion of a Mannich reaction using Eschenmoser's salt.

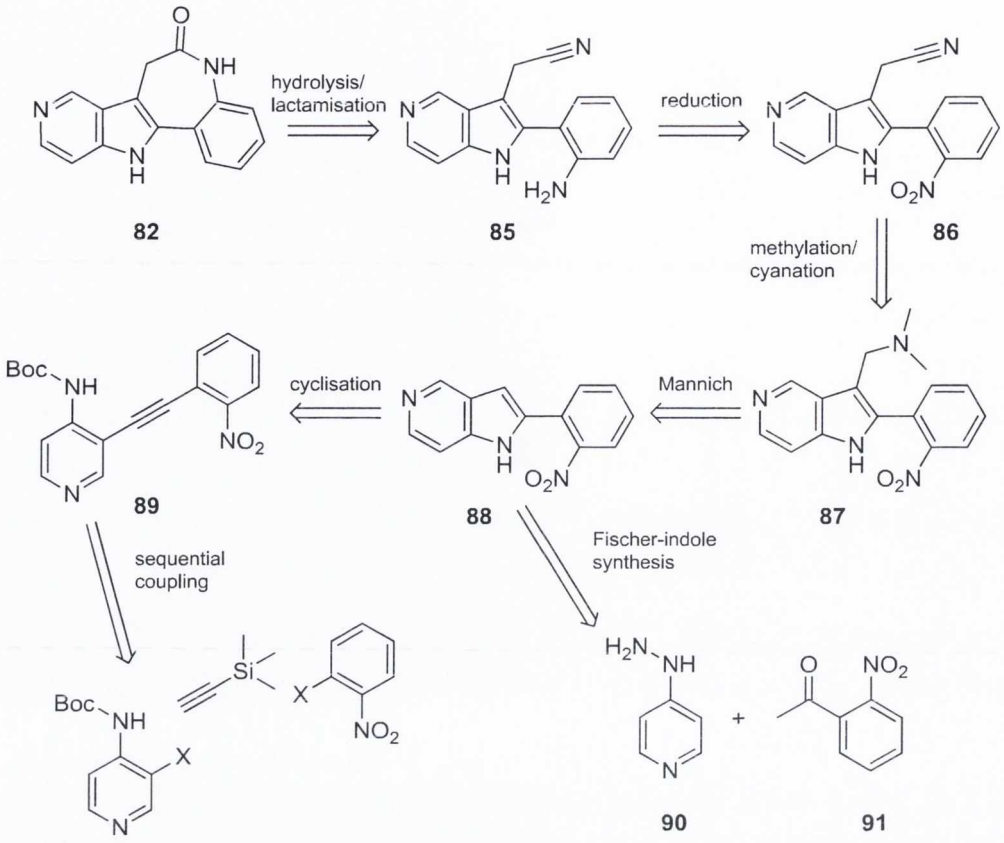

Scheme 2.1: Initial retrosynthetic analysis for azapaullone **82**.

In Scheme 2.1, two methods are proposed for the synthesis of azaindole **88**, the sequential palladium-catalysed coupling strategy and subsequent base-mediated cyclisation of **89** was chosen over the Fischer indole synthesis between hydrazine **90** and nitroacetophenone **91**. Some uncertainty existed with this method however: which is the best order to do the coupling to form alkyne **89,** i.e. should the pyridine or the nitrobenzene incorporate the alkyne first?

Scheme 2.2 has much more in common with 'method C' (Section 1.4.8.3), than the previous outlined route. It includes a boration that is unknown for 5-azaindoles, whereas the method for synthesising azaindoles in Scheme 2.1 is well known in the literature.[104]

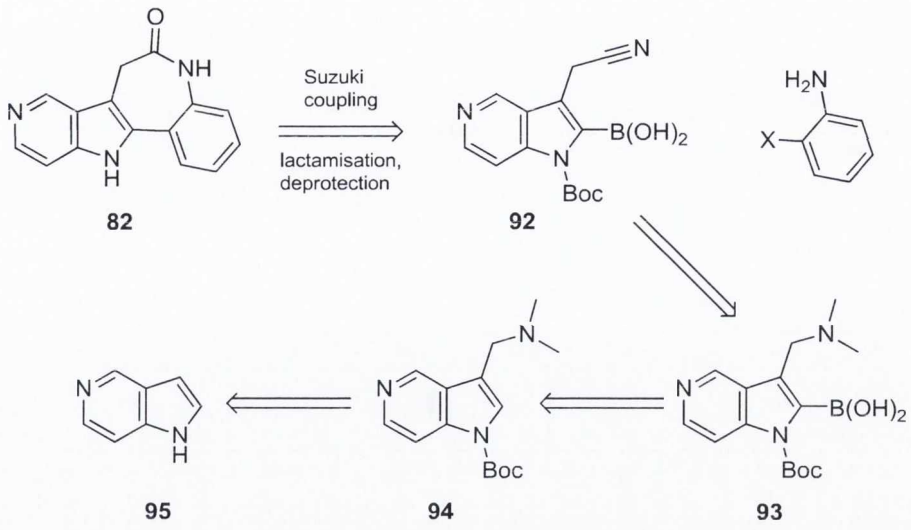

Scheme 2.2: An alternative retrosynthetic analysis.

2.1 Synthetic strategies to azaindole 88

Having defined azaindole **88** as a key intermediate, it was necessary to find an efficient route to this molecule so that sufficient quantities could be obtained, and the 9-azapaullone synthesis completed, with enough material in hand to test and derivatise.

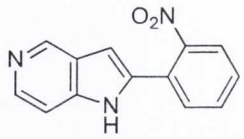

88

Figure 2.1: Initial target azaindole **88**.

2.2 Preparation of 3-halogenated 4-aminopyridines

The halogenation of 4-aminopyridine (**96**) was found to be a difficult reaction to achieve regioselectively. The amino group is strongly electron donating and thus makes the molecule much more receptive to electrophilic aromatic substitution (EAS) than pyridine itself, and it is rapidly halogenated at both the 3- and 5- positions. Also **96** is similar in structure to the nucleophilic catalyst DMAP and can be expected to behave in an analogous manner (Figure 2.2).

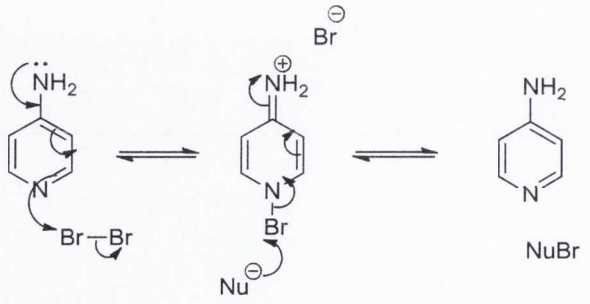

Figure 2.2: Catalytic ability of 4-aminopyridine.

Two different procedures were used to either brominate or iodinate **96**, and both gave moderate isolated yields of 25-35 % of the desired mono-halogenated products, these yields varied slightly with scale, multi-gram reactions were typically at the lower end of the range.

Bromination was achieved in a mixture of dichloromethane and acetonitrile (2:1), this solvent mixture had been determined to be optimal in previous unpublished research work within the group (Scheme 2.3). Bromine (1.2 equiv.) was added neat and dropwise. Solid sodium carbonate was added after 3.5 h which caused an observable decolourisation; sodium bicarbonate was found not to be as effective in this case. It was ascertained that an aqueous work-up has to be avoided for this method; by treating a small portion of one reaction with an aqueous work-up and the remainder with solid sodium carbonate and then examining the ratio of **97** to **98** remaining in each, it was clear that there was loss of **97** when an aqueous work-up was employed, likely due to the water solubility of this compound.

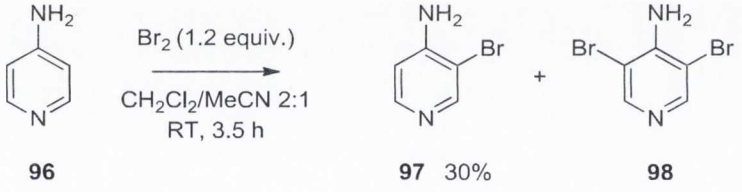

96 **97** 30% **98**

Scheme 2.3: Bromination of **96**.

Some simple modifications were tested in this reaction, for example adjusting the rate of addition of bromine, the temperature during the addition and the time the base was added (Table 2.1). In attempting to slow down the rate of reaction, by diluting the bromine and adding it at a slow rate to the reaction, this led to a good ratio in favour of the desired product (entry 1). By either including an excess of sodium carbonate in the reaction before the addition of bromine or introducing the bromine quickly into the reaction mixture leads to an excess of **98** (entries 2 and 3). When a reaction was performed at 0 °C, the result was to slow the rate of reaction but at the same time not improve the selectivity between **97** and **98** (entry 6).

Table 2.1: Bromination of 4-aminopyridine (**96**)

Entry	Dilution of Bromine[a]	Base	T (°C)	Time (h)	Rate of addition[b]	Ratio[c] (**96**:**97**:**98**)
1	1:25	-	RT	4	slow	0.6:1:0.3
2	neat	-	RT	4	fast	0:1:1
3	neat	Na_2CO_3	RT	4	fast	0:1:1.8
4	neat	-	RT	2	slow	0.4:1:0.6
5	neat	-	RT	2	fast	0.6:1:0.8
6	1:25	-	0	4	slow	1:1:0.5

[a] Dilution is expressed in terms of *v/v* of bromine in dichloromethane. [b] Rate of addition: 'fast' indicates less than 30 mins, 'slow' is a duration up to 3 h. [c] Ratio is determined by ^{1}H NMR spectroscopy.

The iodination procedure that was employed was based on a published method (Scheme 2.4).[105] In contrast to the previous methodology, base (sodium bicarbonate) was added to the reaction mixture at the start, less than one equivalent was used, this means that the starting material should be protonated preferentially as the reaction proceeds as it is the most basic of the pyridines. This may seem undesirable, but as these reactions were difficult to drive to completion without resulting in **100** as the dominant product, any remaining starting material could be protonated and removed by aqueous work-up, leaving a two component mixture that was considerably easier to separate by column chromatography; while this may not have led to optimal conversion, in practical terms it allowed rapid access to sufficient amounts of product. Although an aqueous work-up was included in the isolation of **99**, the yields were comparable between this and the preceding bromination procedures. Little additional experimentation was done with this method as it already produced similar if not slightly better results to the improved bromination conditions.

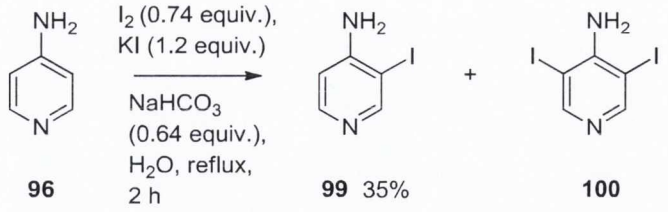

Scheme 2.4: Iodination of **96**.

While the yields from either reaction were only moderate, these methods were more straight-forward to perform and avoided the use of butyllithium and low temperatures, and were considered acceptable for the present work.

The halogenated 4-aminopyridines (**97**, **99**) were readily protected with a Boc group, using Boc anhydride without the addition of any catalyst (Scheme 2.5). The reaction is self catalysed and proceeds rapidly with the possible formation of a doubly protected compound when more than 1.0 equivalent was used. Initially, it was thought that rotamers were being observed in the ^{1}H NMR spectrum of the crude reaction mixture, but the pattern was not consistent (Figure 2.3). By integration of ^{1}H NMR spectra it was possible to tell that one of the compounds had a broad singlet at 7.23 ppm, while the second compound did not, this peak was attributed as the carbamate proton. In addition the second compound also had two peaks that integrated to nine protons each, suggesting it had two Boc protecting groups. This is also backed up by experimentation, adding additional equivalents of Boc anhydride led to more of the doubly protected compound. Conversely, washing the crude mixture with dilute acid resulted solely in the isolation of the desired singly protected product.

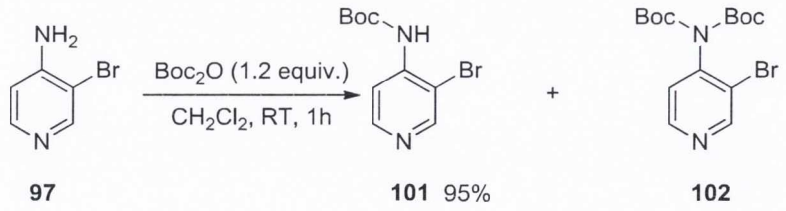

Scheme 2.5: Boc protection of **97**.

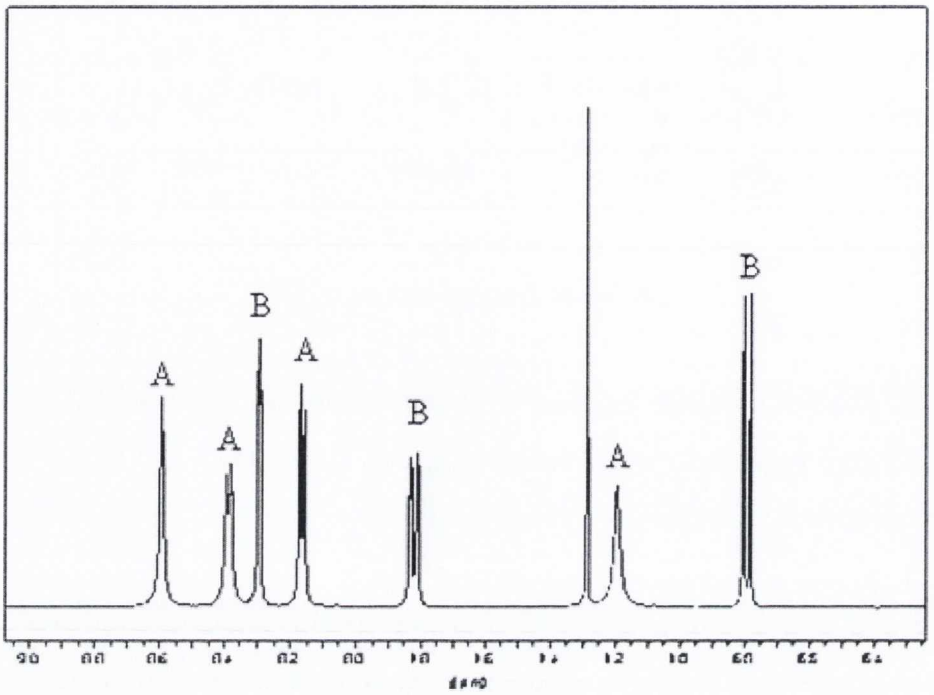

Figure 2.3: ^{1}H NMR spectrum of the two products from the Boc protection reaction (A = **101** and B = **102**).

At times it was necessary to add additional quantities to achieve full conversion on a multi-gram scale, and in such cases any superfluous Boc groups could be removed with a dilute acid wash, either an aqueous work-up with 0.1 M HCl or adding 0.1 mol % TFA to the reaction mixture after it had judged to be gone to completion.

As obtaining doubly protected **102** was an unexpected result an attempt was made to utilise it in subsequent reactions. However, it was not advantageous to do so, as it was observed that the extra protecting group is very labile, for example when partial deprotection of the second Boc-group occurred in a subsequent Sonogashira reaction. It was thought that either a mild Lewis acid such as CuI or general base catalysis was sufficient to cleave it.

2.3 Sonogashira couplings

The synthesis requires two sequential Sonogashira couplings, and thus there are two possible routes to make acetylene **89**, the two disconnections are outlined in Scheme

2.6. Disconnection A was favoured because it was thought that alkyne **104** may be prone to premature cyclisation before the second Sonogashira reaction could be completed.

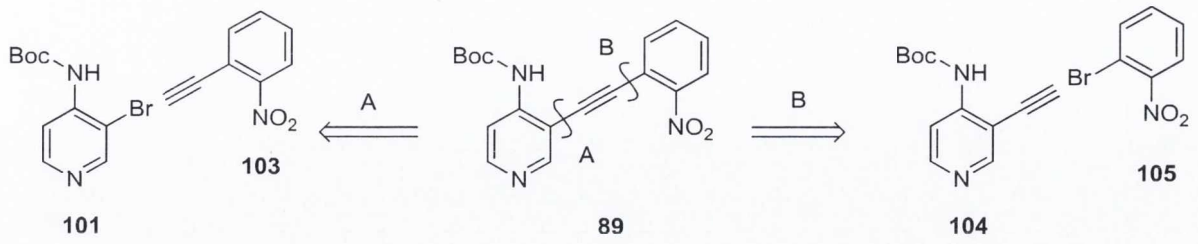

Scheme 2.6: Outline of the two disconnections to synthesise acetylene **89**.

All Sonogashira couplings mentioned in following sections are performed under identical conditions. Triethylamine is both the solvent and base. $PdCl_2(PPh_3)_2$ (0.02 equiv.) is the catalyst with copper(I) iodide (0.06 equiv.) as co-catalyst and triphenylphosphine (0.08 equiv.) as reductant. The reaction is heated at 55 °C, and is conducted under an atmosphere of argon.

2.3.1 Disconnection A

Having decided that this seemed the more promising of the two disconnections, it was attempted first. The initial operation was the synthesis of alkyne **103** *via* a Sonogashira reaction between 1-bromo-2-nitrobenzene (**105**) and a protected acetylene, followed by deprotection. Two alkynes were investigated: 2-methyl-3-butyn-2-ol (**106**) and TMS-acetylene (**107**). Butynol **106** was found to be the less suitable substrate of the two alkynes, it gave a yield of 36%, consistent with that reported by the literature.[106] Secondly, it could not be deprotected to give terminal alkyne **103** (Scheme 2.7). The deprotection was envisaged to occur by deprotonation of the alcohol, elimination of the alkynyl anion and formation of acetone as a by-product.[107] In practice this reaction was attempted with sodium hydride in toluene (under reflux) with any acetone distilled from the reaction mixture as formed, however no product was observed in an intractable mixture by ^{1}H NMR spectroscopy.

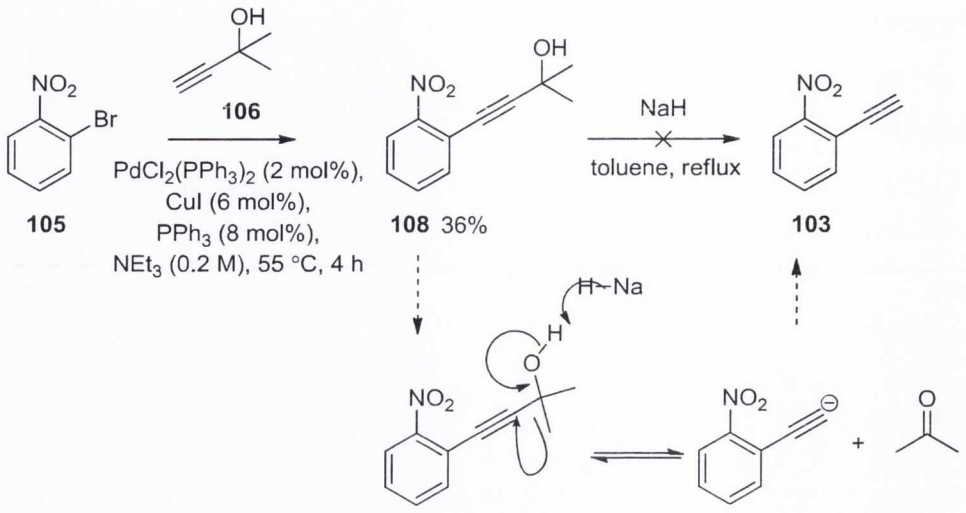

Scheme 2.7: Attempted deprotection of alkynol **108**.

Conversely, when alkyne **107** was used instead of **106** it was found both to be a much better substrate in the Sonogashira coupling and the silyl protecting group could be more easily removed by treatment with a tetrabutylammonium fluoride (TBAF) solution (Scheme 2.8).

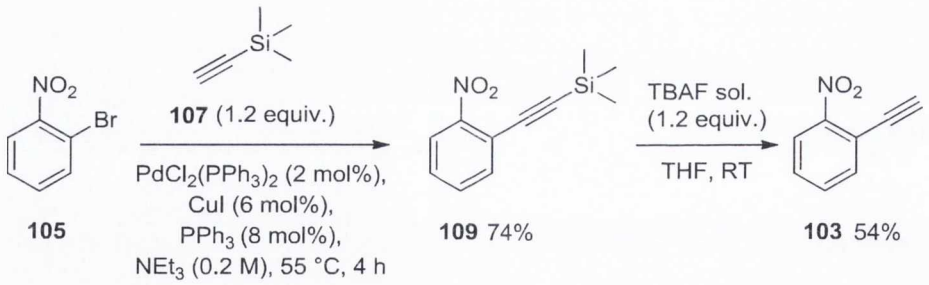

Scheme 2.8: Synthesis of alkyne **103**.

Unfortunately having prepared alkyne **103**, the subsequent Sonogashira reaction failed to occur, no trace of product was obtained and both starting materials were recovered unchanged (Scheme 2.9). It was not investigated beyond this point because these same conditions were successful in completion of the corresponding Sonogashira couplings associated with disconnection B.

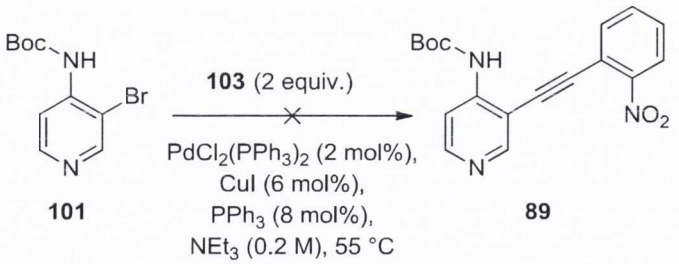

Scheme 2.9: Failure of disconnection A.

2.3.2 Disconnection B

Attention then turned to disconnection B. The first coupling and deprotection sequence was completed without encountering any difficulties, with high yields obtained for both steps. For the first coupling both the bromide and iodide were tested, with both giving near identical yields, yields for the bromide **101** given in Scheme 2.10. As before the silyl protecting group could be removed easily with TBAF solution to provide alkyne **104** in 89% yield.

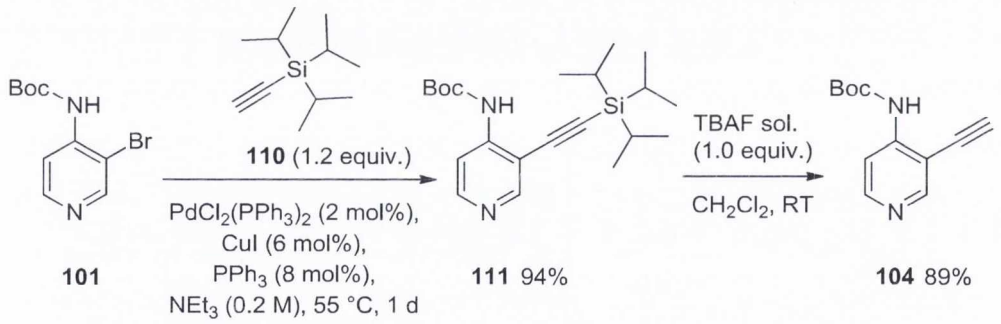

Scheme 2.10: Synthesis of alkyne **104**.

Alkyne **104** was found to be difficult to handle, it was observed to cyclise on occasion such as during chromatographic separation and also heating above 30 °C led to obvious discolouration particularly when solvent was removed at reduced pressure; in addition only moderate yields in the subsequent coupling reaction were obtained. However, if this compound was dried and stored carefully at low temperatures and it could be kept in good condition for months and retain its appearance as a white, crystalline solid.

The subsequent coupling was more difficult to improve upon, until this point all Sonogashira couplings were carried out at 55 °C, which was seen as deleterious for this particular alkyne. Attempts at a one-pot procedure gave moderate but variable yields. Lowering the temperature of the reaction failed to give any product when using bromide **105**; even when increasing the amount of palladium catalyst to 5 mol% and heating for several days only to observe no appearance of a product and no change in the ratio of both starting materials. Fortunately, when the coupling partner was changed to the iodide, not only did this facilitate a lower required temperature but it also gave very good, consistent yields even on a multigram scale (Scheme 2.11). It was necessary to synthesise iodide **112**, while commercially available it was expensive considering the quantities needed, and large quantities could be acquired easily *via* diazotisation and substitution with iodide of an aniline (**113**; Scheme 2.12).

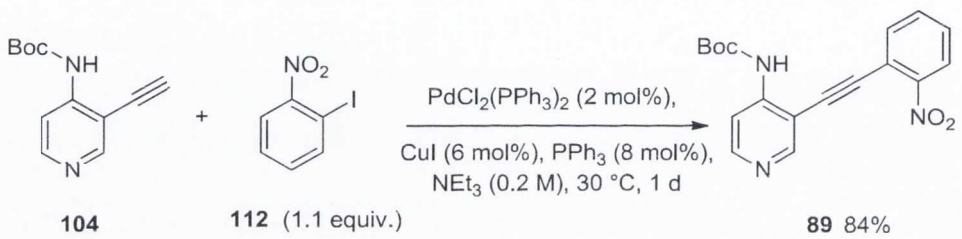

104 **112** (1.1 equiv.) **89** 84%

Scheme 2.11: Success of disconnection B.

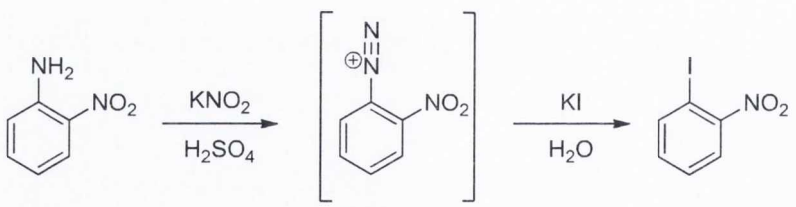

113 **114** **112** 72%

Scheme 2.12: Synthesis of 1-iodo-2-nitrobenzene (**112**).

2.4 Base-catalysed 5-*endo-dig* cyclisation

Having synthesised **89** in high yield, the next step required a base catalysed ring-closure. This is a well known reaction in the literature, and has been successfully applied to numerous, diverse examples relevant to the current work, and encompassing each of the isomeric azaindoles.[104,108]

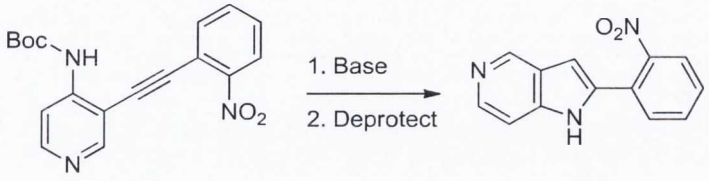

89 **88**

Scheme 2.13: Overview for Section 2.1.3.

The success of this cyclisation is predicted by Baldwin's rules. These are empirical guidelines based on the outcomes of various cyclisation reactions. A notable example of these rules occurs with 5-*endo-trig* cyclisations that seems at first glance a likely reaction, these even appear to be more likely than the 5-*endo-dig* reaction in which we are interested, but they are found not to occur. The reason for the success of a 5-*endo-dig* is the availability of a π^* orbital in the same plane as the anion, and thus overlap can occur between the two orbitals; in contrast the single π^* orbital in a 5-*endo-trig* reaction is orthogonal to the anion and any motion in the intervening bonds will only serve to swing the anion further away (Figure 2.4).

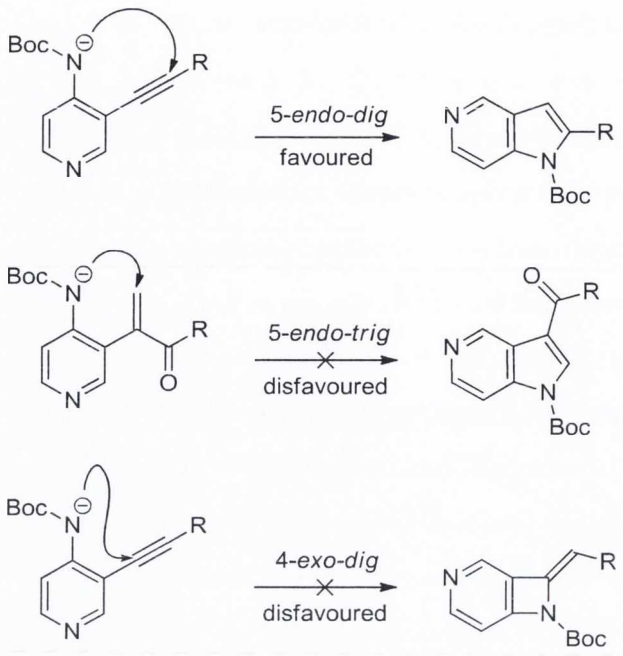

Figure 2.4: Selected examples of applying Baldwin's rules.

Initial attempts to achieve the cyclisation used either sodium hydride or DBU as the base, in solvents THF or DMF (Table 2.2). In these reactions a temperature of 80 °C was required to achieve conversion and hence DMF was the more suitable choice of solvent. For reactions involving sodium hydride (entry 3), it was observed that a partial loss of the Boc protecting group occurred, and thus before the product was isolated the remainder of the protecting group was removed to obtain indole **88**. In the case of DBU as base, no such loss of the protecting group occurred, and indole **115** could be isolated in good yield (entry 4).

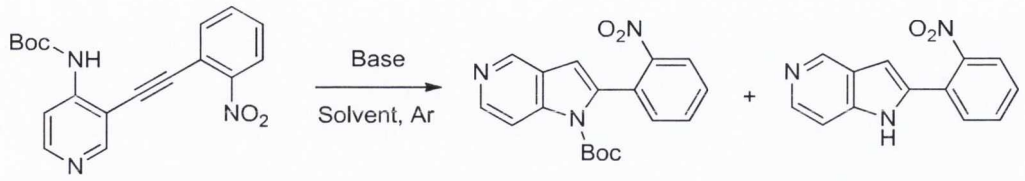

89 **115** **88**

Table 2.2: Base-mediated cyclisation of alkyne **89**.

Entry	Base	Equiv.	Solvent	T (°C)	Yield (%)[a] (indole isolated)
1	NaH	1.2	THF	50	-
2	NaH	1.2	THF	65	-
3	NaH	1.2	DMF	80	70 (**88**)
4	DBU	1.1	DMF	80	79 (**115**)

[a] Isolated yields

While the initial results were quite encouraging, milder conditions and optimised yields were desirable. While DBU may have given only a slightly improved yield than NaH in preliminary tests, a more valuable factor was keeping the protecting group in place. This would mean a less polar compound and be beneficial in the aqueous work-up necessary to remove DMF and also in the subsequent chromatography. Hence choosing DBU for further experimentation was the obvious choice for both of these reasons. Quite quickly it was found that catalytic amounts of both copper iodide and DBU could effect the transformation at a lower temperature of 50 °C. Neither of these on their own could complete the cyclisation efficiently at this temperature. Ultimately on multi-gram scale, the reaction afforded **115** in 82% yield, and it was achieved consistently (Scheme 2.14).

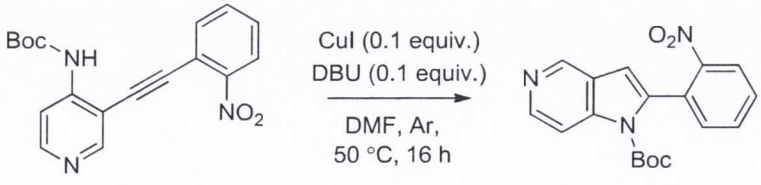

89 **115** 82%

Scheme 2.14: Improved conditions identified for the cyclisation of **89**.

Another method that we envisaged may improve yields was to perform a one-pot coupling and cyclisation strategy.[105] The coupling between alkyne **104** and bromide **105** was performed as before, however when it was judged as being complete by TLC analysis, DBU (2 equiv.) was added to the reaction. Unlike the previous Sonogashira reactions, this reaction was carried out in DMF. This strategy proved efficacious, and the yield of product was moderate (Scheme 2.15), however over the course of several experiments it was found not to be as reliable as isolating alkyne **89**, purifying this material and then performing the cyclisation in a separate reaction vessel.

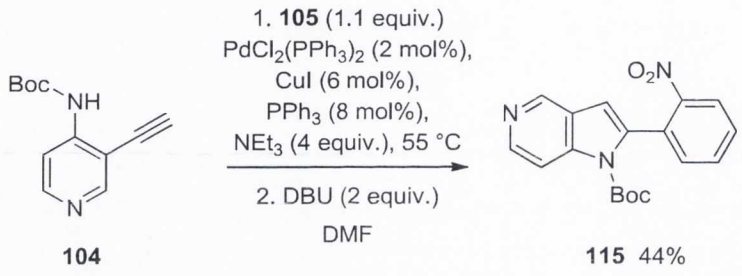

104 **115** 44%

Scheme 2.15: One-pot Sonogashira coupling and 5-*endo-dig* cyclisation.

Finally, to remove the Boc protecting group, the standard protocol involving the use of excess trifluoroacetic acid in dichloromethane was utilised (Scheme 2.16). While it may have been desirable to keep the protecting group, none of the succeeding reactions could be expected to proceed with it in place.

115 **88** 88%

Scheme 2.16: Removal of Boc protecting group from **115**.

2.5 Synthesis of azaindoles *via n*-Buli cyclisation

As an alternative route to access azaindoles, work was carried out within the research group to test the feasibility of the transformation shown in Scheme 2.17. It was based on a published methodology for the synthesis of 4- and 6-azaindoles.[109]

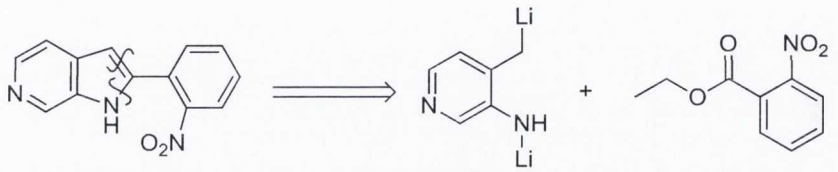

116 117 118

Scheme 2.17: Synthesis of 6-azaindole **116**.

While the procedure could be successfully replicated by another within the research group when ethyl benzoate was employed, it failed for nitrobenzoate **118**; also this benzoate had not been demonstrated in the original literature. This result ended endeavours to make aminopicolines **119** and **120** (Figure 2.5), the latter *via* 3-nitro-2-picoline (**121**). In addition, because several steps were needed in preface to the condensation reaction, it was deemed to not garner any particular advantage over the chemistry already employed in the preceding sections.

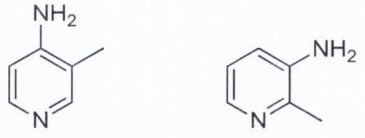

119 120

Figure 2.5: Amino-picolines.

2.6 Synthesis of 5-azaindoles *via* Fischer indole synthesis

The original synthesis developed by Kunick depended on a Fischer indole synthesis in the final step (see Section 1.4.7.1). At first it was thought unlikely that a similar

procedure could be applied to **82,** especially if acidic conditions were used and protonation of the pyridine results in a less nucleophilic hydrazine, hence other strategies were given priority. As evidence for utilising this strategy, 11-azapaullone (**122**; Scheme 2.18) had been made *via* a Fischer indole reaction; it was thermally induced in refluxing diphenyl ether to give a yield of 70%.[78] Against such a strategy was the apparent lack of literature precedent for the corresponding transformation when employing a 4-pyridylhydrazone (Scheme 2.18), searches only turned up one account of it,[110] and the reaction was reported to be low to moderate yielding.

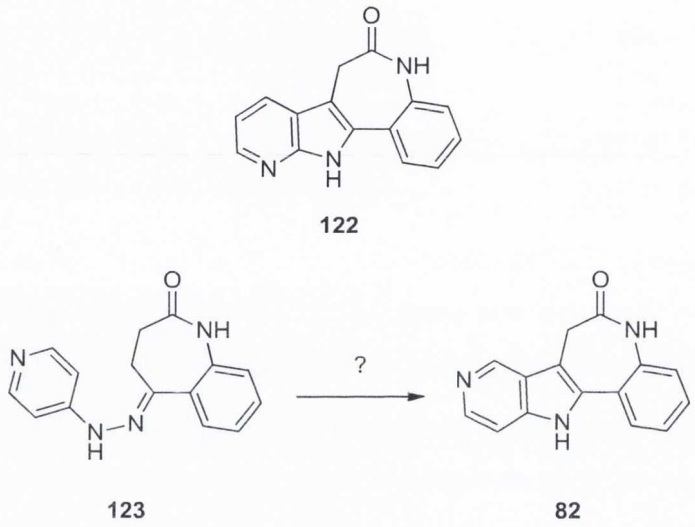

Scheme 2.18: A Fischer indole synthesis of 9-azapaullone.

The reported reactions, carried out in refluxing ethylene glycol,[110] required temperatures in excess of 200 °C, for a nitrophenyl hydrazone this was expected to be potentially destructive. In addition, the hydrazones used by Crooks and Robinson are invariably very reactive, such as hydrazones made from aliphatic aldehydes (**124**; Scheme 2.19).

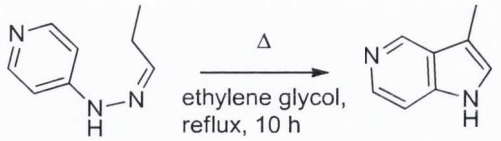

124 **125** 35%

Scheme 2.19: Reported synthesis of 2-methyl-5-azaindole (**125**).[110]

In an endeavour to make paullone (**25**) as a model for the synthesis of 9-azapaullone (**82**), 2-(2'-nitrophenyl)indole (**126**) was synthesised. In contrast to the corresponding 5-azaindole (**88**), it could be quite simply made in a two-step procedure, by gently heating phenylhydrazine and 2'-nitroacetophenone (**91**) together, collecting the resulting hydrazone (**127**) by filtration and then heating this solid for a short duration in polyphosphoric acid (PPA), Scheme 2.20.

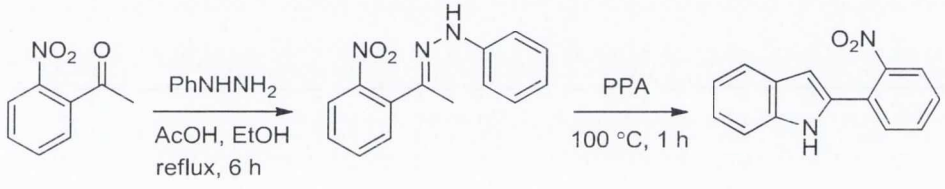

91 **127** **126** 35%

Scheme 2.20: Synthesis of **126**.

It was attempted to use a similar strategy for the formation of the corresponding azaindole. Firstly, 4-pyridylhydrazine (**90**) was synthesised as it was not commercially available. Two methods for preparing **90** were investigated (i) *via* the formation of a diazonium salt (**128**) and subsequent reduction or (ii) *via* nucleophilic substitution of 4-chloropyridine (**129**) by hydrazine (Scheme 2.21).

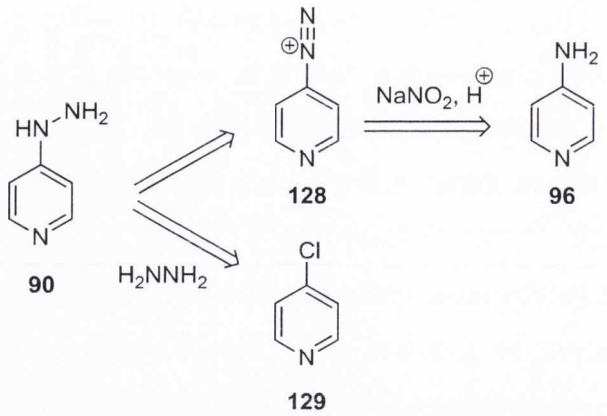

Scheme 2.21: Two alternative routes for the synthesis of **90**.

Formation of the diazonium salt **128** proved to be difficult, it was observed to decompose very rapidly despite cooling on an ice/salt bath, careful additions and monitoring of the temperature of solution. It is probable that nucleophilic attack of H_2O occurs even before the loss of nitrogen gas. Attempts were made to add the reductant immediately to the diazotization mixture, but to no avail. Reducing agents employed were either tin (II) chloride or sodium bisulfite.

Nucleophilic substitution of **129·HCl** with hydrazine hydrate is a known reaction[111] and was found to occur quite readily, it did prove difficult to isolate and purify. Success was achieved by forming **90·2HCl** and recrystallising this salt from acidic solutions, this material was then reacted with nitroacetophenone **91** to generate hydrazone **130** in good yield (Scheme 2.22).

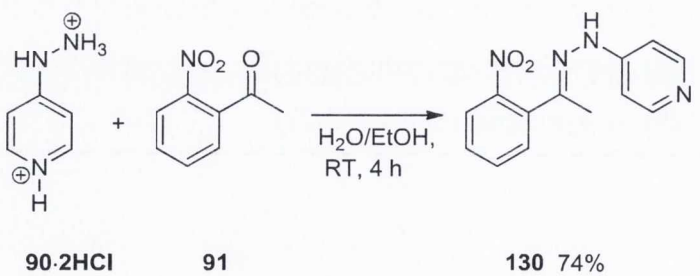

Scheme 2.22: Synthesis of hydrazone **130**.

Somewhat surprisingly the resulting material did not have the characteristic intense red colour of a hydrazone, accordingly a more intensive investigation of the structure was performed by NMR spectral analysis. This analysis was complicated by the two halves of the molecule being connected by a chain of hetero-atoms and quaternary carbons, thus long-range and correlation NMR techniques were necessary, especially useful were HMBC and selective 1D-TOCSY techniques. The two pairs of pyridine signals were easily identified, with the furthest downfield assigned as the pair closest to the pyridine nitrogen. For assignment of the nitrophenyl protons, selective 1D-TOCSY experiments were employed as shown in Figure 2.6. One experiment (A) shows all the protons in the spin system. The second experiment (B) shows the nearest neighbours to the proton ortho to the nitro group, with the furthest upfield triplet being the most prominent and this was assigned as the proton adjacent to the ortho proton, this aligns with the expected chemical shifts of these protons. The remaining two protons overlap. A HMBC spectrum of this molecule is shown in Figure 2.7 and the through bond interactions for the hydrazone proton are highlighted. This indicates its proximity to a pyridine proton and two quaternaries, namely the hydrazone and pyridine quaternaries as suggested by the ^{13}C-^{1}H correlations. Also highlighted in the same figure is the correlations for the remaining two quaternaries and the assignment of these can be made with certainty because each has a distinct set of interactions.

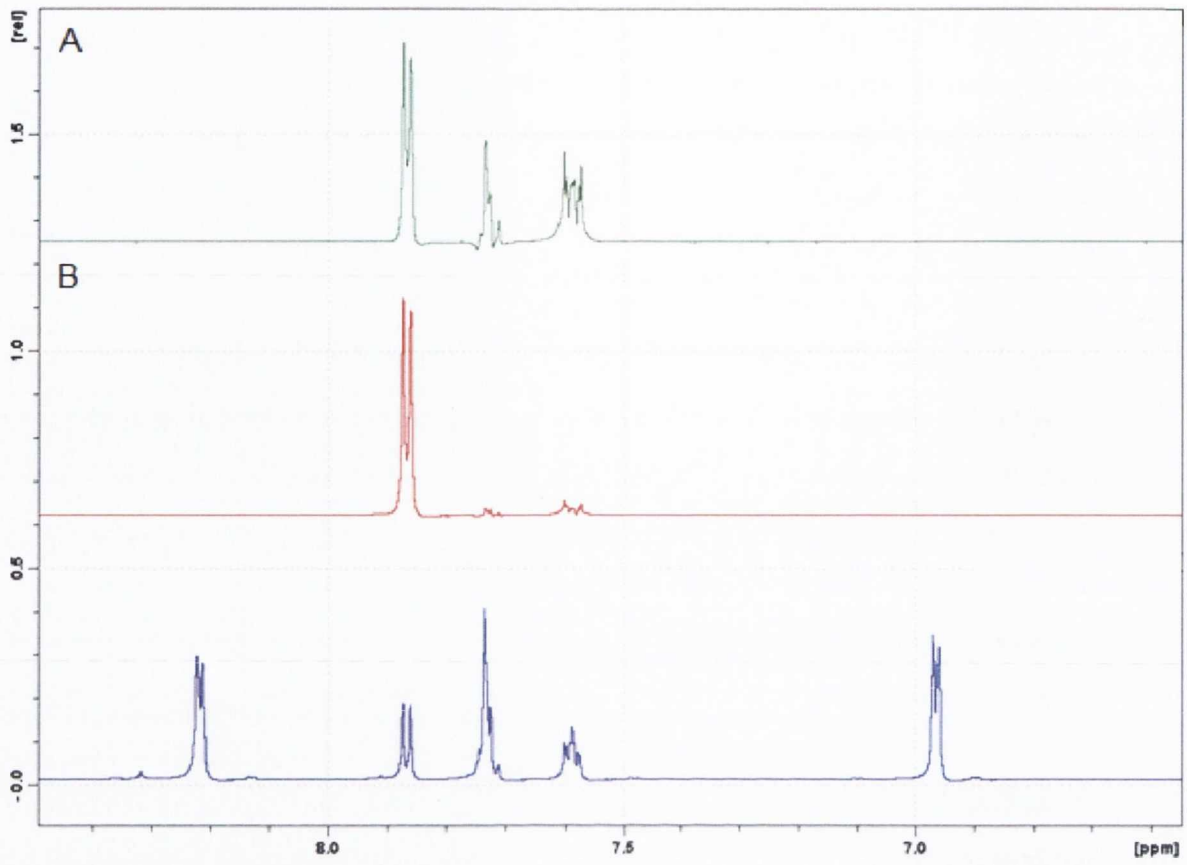

Figure 2.6: Selective 1-D TOCSYs for hydrazone **130**, showing all interactions in same spin system (A) and nearest interactions (B).

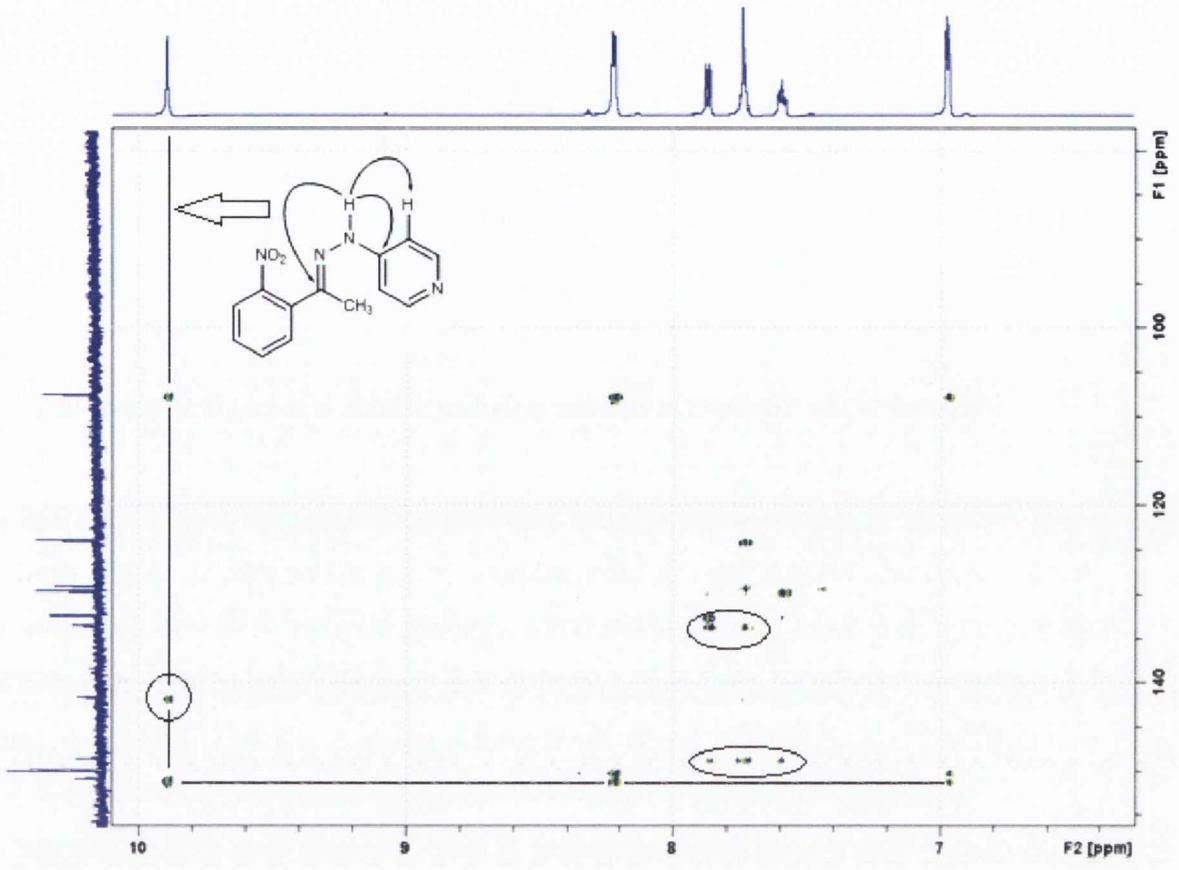

Figure 2.7: A HMBC spectrum of hydrazone **130**, with the interactions for the hydrazone proton and the four quaternary carbons highlighted.

No acid catalysed (either Bronsted or Lewis) Fischer indole synthesis was known for hydrazones derived from 4-pyridyl hydrazines, however as thermal conditions were known to be effective for the formation of **122** and 5-azaindoles, it was these conditions primarily that were tested. However, the desired reaction was not observed and hydrazone **130** decomposed when heating up to 300 °C in diphenyl ether. An alternative method using microwave heating was evaluated, with the expectation that the reaction could proceed on a shorter timescale, however this was also unsuccessful.

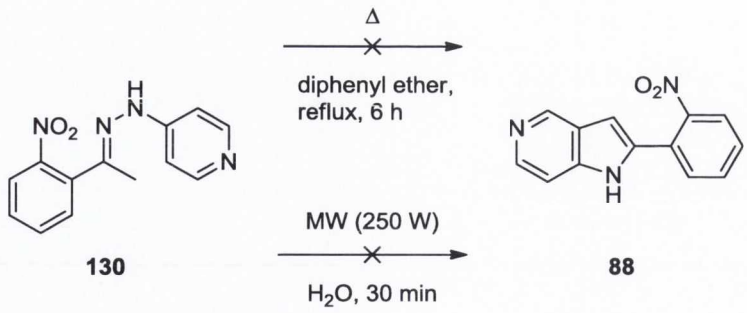

Scheme 2.23: Attempts at Fischer indole synthesis using hydrazone **130**.

There remains a question about whether more success would have been achieved with the ketone which Kunick uses in his syntheses. It is a cyclic ketone, which would be expected to more reactive and robust. Thus a question arises of why this reaction was not attempted by Kunick previously as while the 4-pyridyl hydrazine is commercially unavailable it is quite simply made, for Kunick's group to not have attempted making such an interesting paullone previously is unlikely. An alternative that was considered was to replace the Fischer indole synthesis in Kunick's route with a Heck-like reaction as outlined (Scheme 2.24).

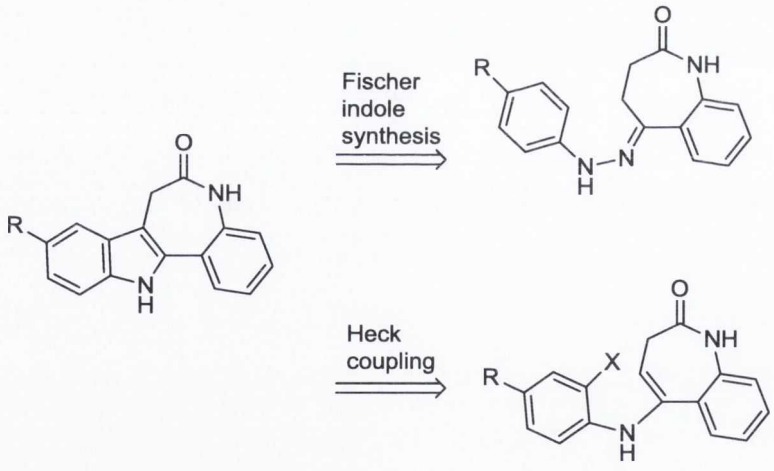

Scheme 2.24: A proposed alternative route to paullones *via* a Heck reaction.

Unfortunately, there were no reports of imine formation with 4-aminopyridine, and using standard methods of a Dean-Stark apparatus and PTSA as catalyst failed to give any product when using pyridine **99** and cyclohexanone (**131**; Scheme 2.25); this reaction was also attempted with 4 Å molecular sieves or triethyl orthoformate. This is

disappointing as it also rules out another potential paullone synthesis (method B; Section 1.4.7.2) which depended on a Strecker reaction.

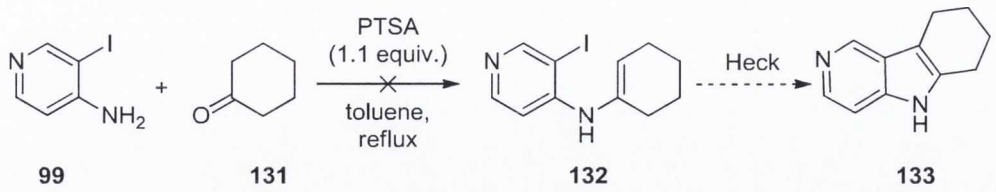

Scheme 2.25: Attempted imine formation with pyridine **99**.

2.7 Conclusion

The only workable method developed to make azaindole **88** has been described (Scheme 2.26); with the advantage that it could be adapted to make the other isomeric azaindoles if required as has been widely demonstrated in literature. While initially it was an unwieldy route to such a simple structure, however with practice and modification it was made much more workable and high yielding, necessary to complete the synthesis (Section 3.0) and make derivatives (Section 4.0).

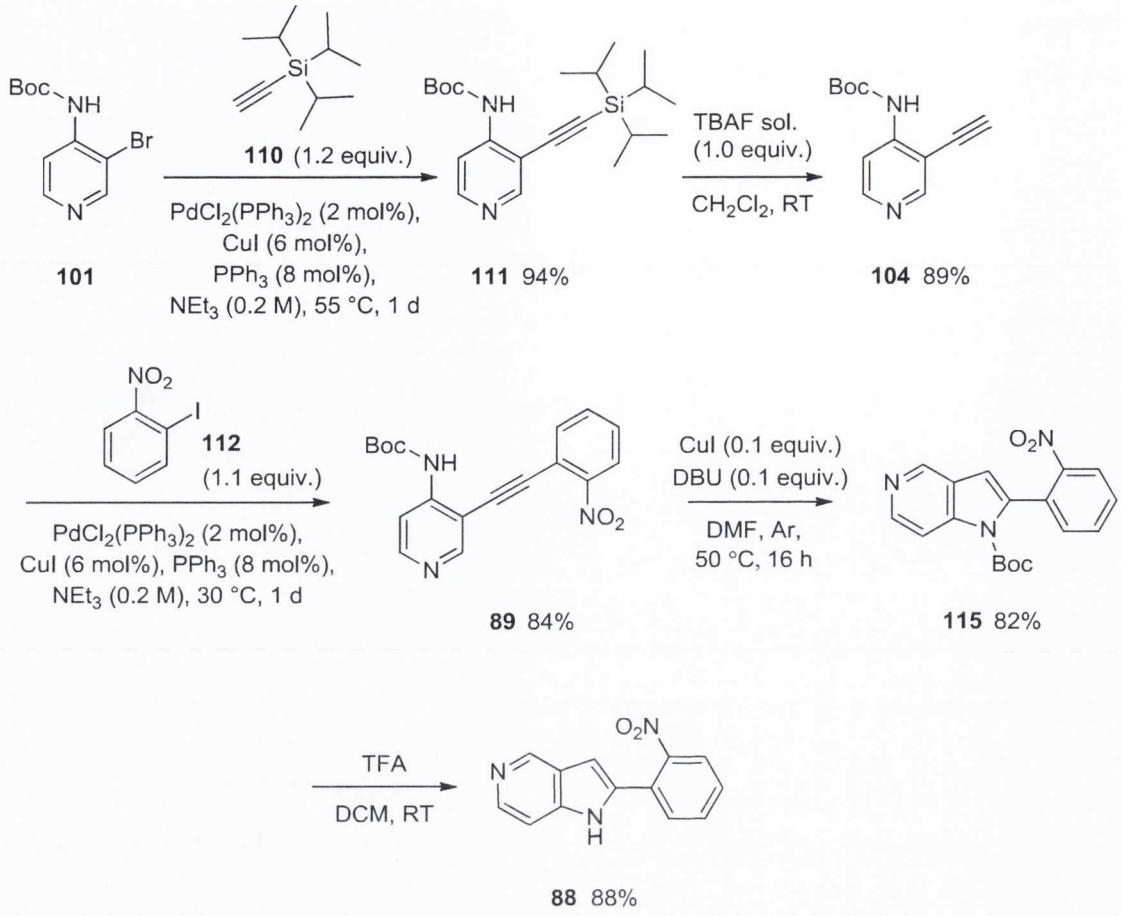

Scheme 2.26: Completed synthetic route to azaindole **88**.

3.0 Completion of 9-Azapaullone Synthesis

Having sufficient quantities of the previously synthesised azaindole **88** in hand, it was attempted to complete the synthesis and obtain 9-azapaullone. The early strategies focused on synthesising nitrile **85**, which could be hydrolysed and lactamised *in situ* as shown in Scheme 3.1.

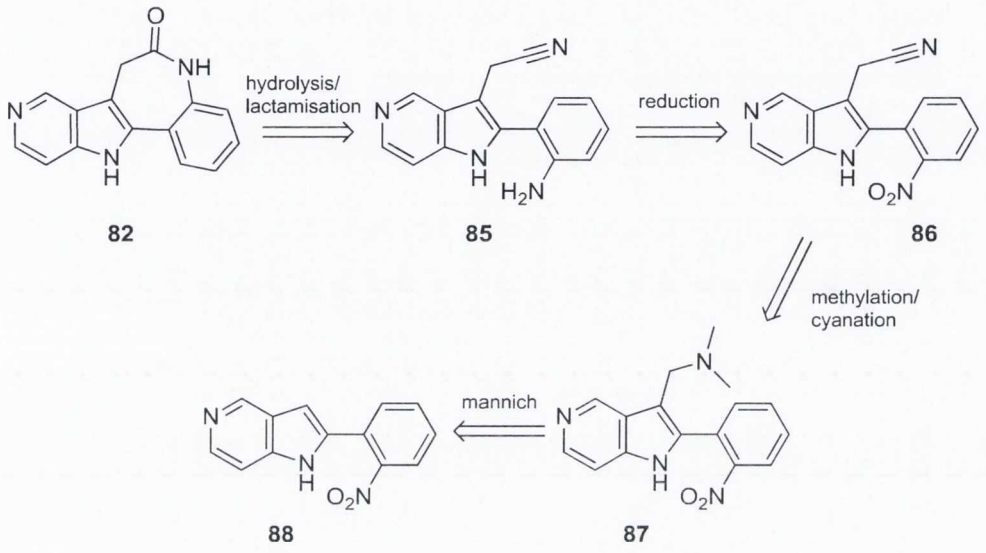

Scheme 3.1: Outline of proposed strategy to synthesise 9-azapaullone.

3.1 Mannich reaction, quaternisation and cyanation of 88

The synthesis was continued by synthesising gramine **87** using Eschenmoser's salt, and subsequently attempting to alkylate and substitute the resulting methiodide with cyanide Scheme 3.2).

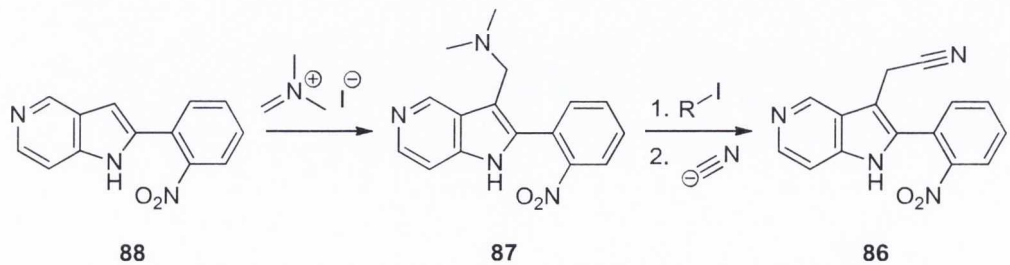

Scheme 3.2: Synthesis of nitrile **86**, *via* gramine **87**.

3.1.1 Mannich reactions

Traditionally Mannich reactions are performed with aqueous solutions of dimethylamine and formaldehyde (formalin), under acidic conditions. The imine salt intermediate is stable enough to be isolated, and the iodide is a commercially available as 'Eschenmoser's salt'. It is this reagent that was chosen to carry out the transformation to **87**, due to ease of use and its solubility in common organic solvents. Thus, **88** and Eschenmoser's salt were heated under reflux in acetonitrile for 16 h, and **87** was obtained in good yield (Scheme 3.3).

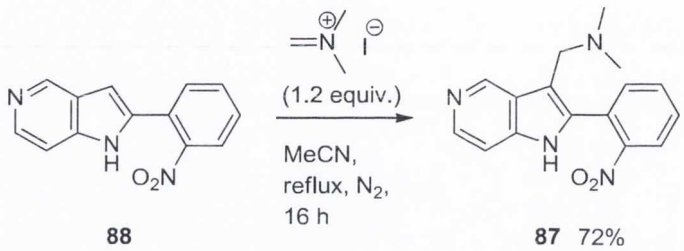

Scheme 3.3: Formation of gramine **87**.

Attempts at carrying out the same transformation with the protecting group still in place failed, which was not unexpected. It remained a desirable target because in subsequent reactions the isolation of the desired products proved difficult, as these were salts and their isolation could not be effected by conventional means. A tandem reaction sequence was proposed, whereby the intermediate anion from the 5-*endo-dig* cyclisation may be trapped by the iminium electrophile. To this extent **89** was treated with sodium hydride in DMF at 80 °C, with Eschenmoser's salt already *in situ*. No reaction occurred and the starting material was recovered with the loss of the Boc protecting group (Scheme 3.4).

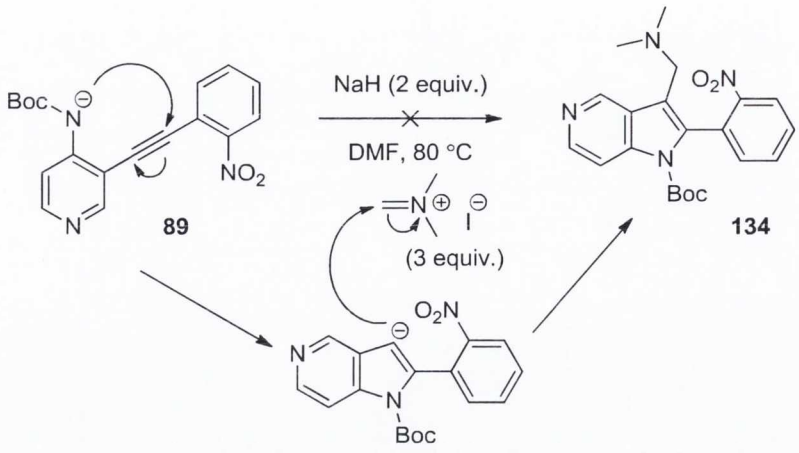

Scheme 3.4: Attempted one-pot reaction to form **134**.

3.1.2 Methylations

Initially, to identify conditions for the efficient quaternisation of **87**, we investigated the alkylation of 5-nitroindole gramine base (**135**). Indole **135** was chosen because its mono- (**136**) and bis- indolyl methiodide (**137**) products were well characterised[112] and determination of the product ratio in the crude reaction mixture could be easily made by ^{1}H NMR spectroscopic analysis. The ratio of **136** to **137** formed is dependent on the concentration of alkylating agent present. Initially, a better ratio is obtained in solutions of ethanol than in neat methyl iodide (Table 3.1), presumably because of better mixing between substrate and reagent. In addition, when the reactions were performed with the same amounts of methyl iodide but different concentrations, 0.2 M was found to be optimal (entry 3), with more dilute reactions (0.05 M, entry 4) resulting in a poorer ratio. This result is contrary to what we had expected; a more dilute reaction should diminish the rate of interaction. The actual result is possibly tied to how quickly the methylation occurs, and this reaction proceeding to completion before any undesired elimination can occur (Scheme 3.5). It was desirable to only use 1.1 equivalent of alkylating agent (entry 2), but this was found to result in the poorest ratio of **136** to **137**.

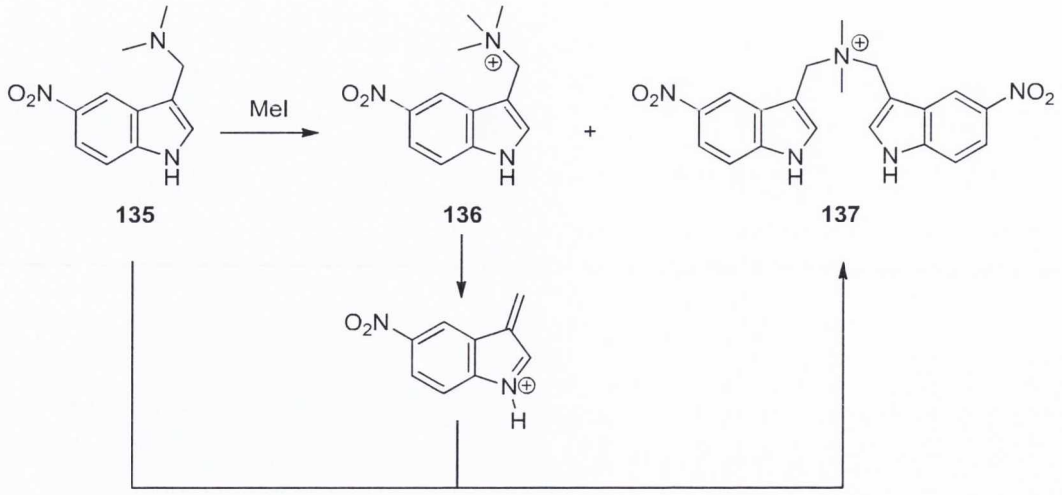

Scheme 3.5: Rationale for the formation of bisindolyl methiodide product (**137**).

Table 3.1: Improving the ratio of **136** to **137**.

Entry	Solvent	Conc.	MeI (equiv.)	Product Ratio[a] **136**:**137**
1	-	Neat	-	3:1
2	EtOH	0.2M	1.1	3:1
3	EtOH	0.2 M	4	10:1
4	EtOH	0.05 M	4	2:1

[a] Ratio is determined by ^{1}H NMR spectroscopy

When the optimised conditions were applied to azaindole **87**, an indecipherable mixture was observed. A number of solutions were proposed to solve this issue and strive for a cleaner alkylation, most simply was to use 1.0 equivalent of methyl iodide, this gave no improvement on the intractable mixtures already observed. Attempts to take these mixtures and continue on with the next step of substitution by cyanide, in the hope that at least this product could be expected to be less polar and resolvable by chromatography, proved a futile endeavour. Another possibility involved leaving out the methylating agent, in favour of the substitution promoted by heat alone

.

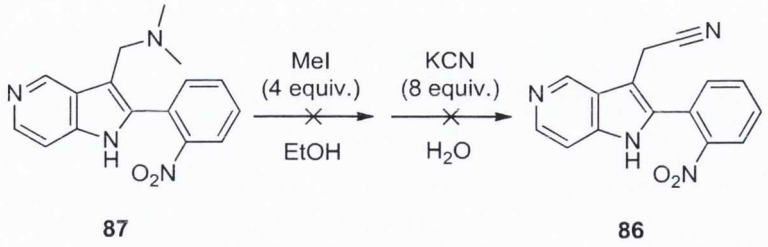

87 86

Scheme 3.6: One-pot procedure for methylation and cyanation of **87**.

Attempts to carry out the methylation and substitution in the one-pot failed to yield any product (Scheme 3.6). This strategy succeeded for indole **135** whereby the methylation was carried out in ethanol, then water and excess potassium iodide could be added to obtain good yields of the corresponding nitrile **138** (Scheme 3.7).

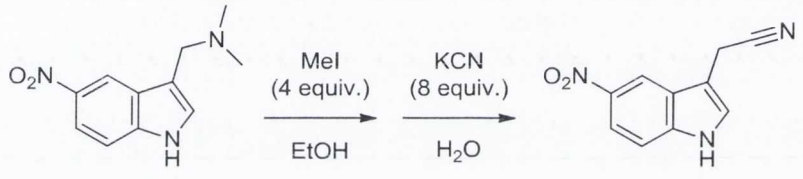

135 **138** 69%

Scheme 3.7: One-pot procedure for methylation and cyanation of **135**.

The reactions involving heating were carried out in either *i*-propanol, methanol or dioxane together with water in a 1:1 ratio, with up 8 equiv. of potassium cyanide, and heated under reflux (Scheme 3.8). After several days heating, only poor conversions were achieved in all cases. These reactions were tested first on **135**, but when **87** was tried only traces of possible product were observed.

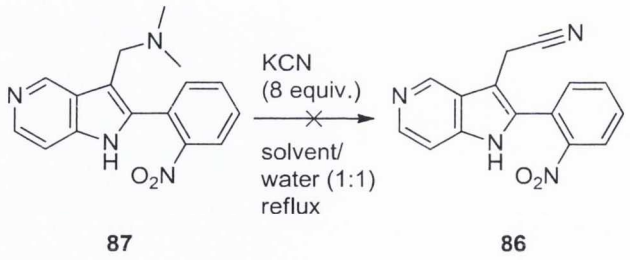

Solvent: IPA, MeOH, Dioxane.

Scheme 3.8: Prolonged heating of **87** in presence of cyanide.

3.2 Acetylation and cyanation of azaindole gramine 87

This strategy started with gramine **87**, which is then acetylated and substituted by acetate to give bis-acetate **139**, this compound is substituted with cyanide to give the desired nitrile (Scheme 3.9). It was hoped that the reversibility of acetylation would avoid problems that hindered the preceding work with alkylations. These acetates are desirable intermediates as they allow access to both nitrile and ethers.

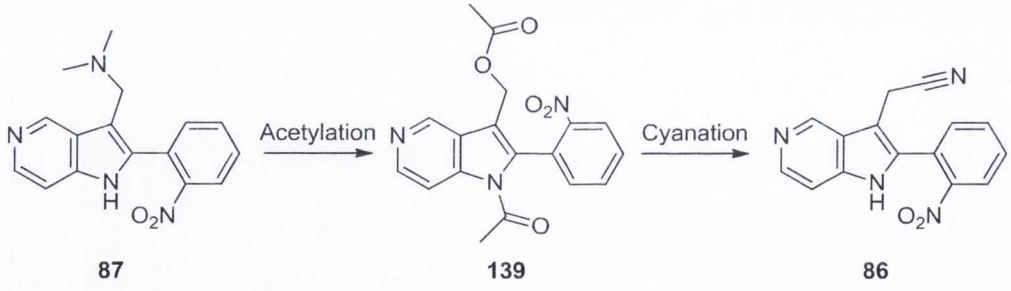

Scheme 3.9: Sequence for the synthesis of nitrile **86** *via* acetate **139**.

The acetylation was carried out neat in acetic anhydride, in the presence of sodium acetate, heated under reflux. These are vigorous conditions, but despite this were found to be very effective for the model indole substrate, **135**, giving excellent yields and producing a very stable, crystalline solid (Scheme 3.10). It is based on a literature procedure for 6-azaindole,[113] however it did not give good results for **87**. The problem centres on isolation, because the reaction did not afford clean product, the crude

mixture was very difficult to purify either by recrystallisation due to poor solubility in common solvents, or by column chromatography due again to solubility and also an observed loss of product on silica; the published procedure was able to avoid a purification step. It is suspected that the nitro-phenyl ring is the differing factor, it likely hinders the substitution by acetate, leading to an incomplete reaction, which is surprising since there is essentially only one end-point to the reaction and it would be expected to reach it eventually.

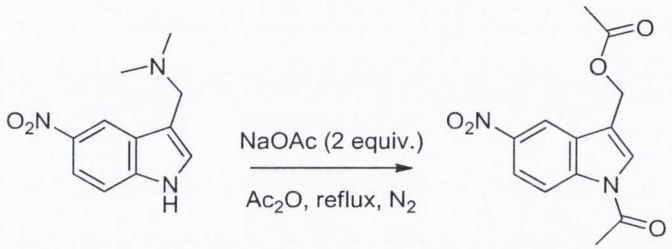

135 **140** 84%

Scheme 3.10: Successful acetylation reaction of **135**.

Several modifications were proposed and tested: to lower the temperature and/or to carry out the reaction in a solvent in addition to the acetic anhydride, also to include DMAP as catalyst. Lowering the temperature to 80 °C did produce product, although at the expense of a much slower reaction that did not achieve completion. Including both THF and DMAP in the reaction, did not lead to the formation of the desired product.

A more successful strategy than the preceding modifications was including both potassium cyanide and acetic anhydride in the same reaction. A good solvent mixture for this reaction was acetonitrile and *tert*-butanol (1:1), better conversions were observed in this mixture than in either solvent alone (Scheme 3.11). Using 1.5 equivalent of acetic anhydride and 4 equivalent of potassium cyanide while heating under reflux, conversions of up to 71% were obtained with indole **135**. Employing similar conditions using **87** was much less successful, some product was observed but no more than 10%, which was unfeasible for synthesising enough of the final product.

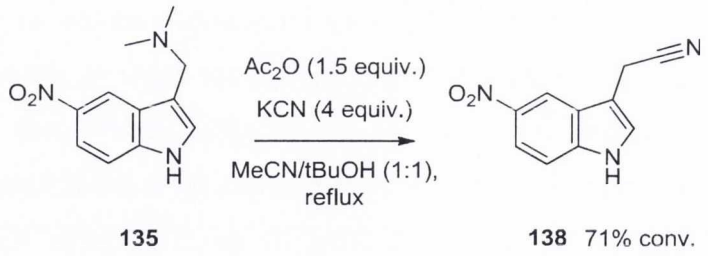

Scheme 3.11: One-pot acetylation/cyanation of **135**.

While initially both alkylation and acetylation seemed to be the most promising strategies, they failed to produce any significant results. These reactions proceeded as expected for indoles but not in the case of azaindole **87.** There is perhaps some potential to return to one-pot acetylation/cyanation reactions for further development, but at the time it did not meet expectations. Thus attention was turned to a different strategy involving the synthesis of an aldehyde and reduction to an alcohol in the next section.

3.3 Strategies involving the formylation at C-3 of 88

Having failed to make progress in synthesising the nitrile with other methods, it was thought that a more reliable nucleophilic substitution could be found by employing the alcohol (**142**), which could then be either tosylated or mesylated (Scheme 3.12), followed by a subsequent substitution with cyanide. To access the alcohol, aldehyde **141** was required. The Vilsmeier reaction seemed the most likely methodology to prepare this key intermediate.

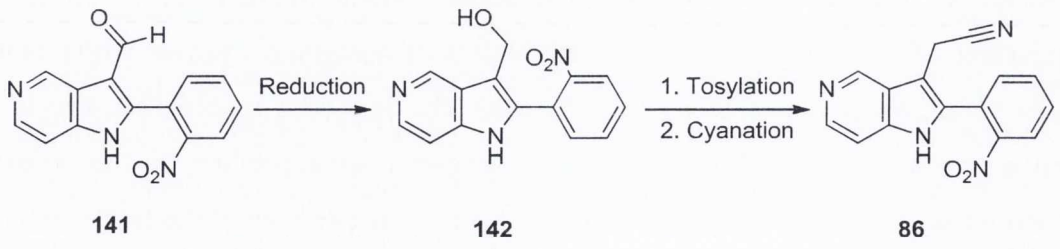

Scheme 3.12: An alternative route to nitrile **86**.

The Vilsmeier reaction generates the aldehyde *via* an iminium chloride intermediate as shown in Scheme 3.13. The reagents are phosphorous oxychloride or oxalyl chloride with DMF that together form the reactive species, which reacts at C-3 of indole, with an aqueous work-up releasing the aldehyde.

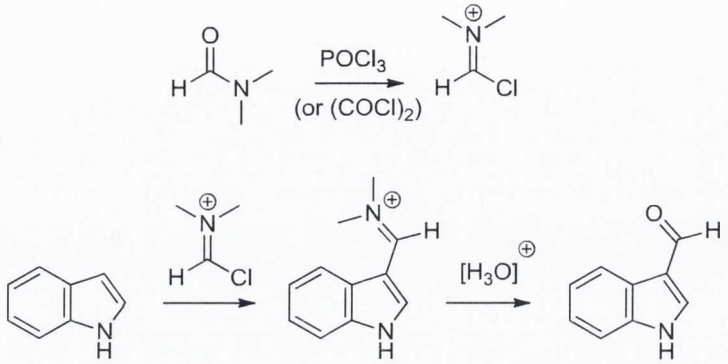

Scheme 3.13: Outline of the Vilsmeier reaction.

Two protocols were used, either formation the iminium chloride intermediate *in situ*[114] or pre-forming and collecting the solid to be used intermediately in a separate reaction vessel.[115] The first reaction was performed in DMF as solvent and phosphorous oxychloride was added and allowed to react before the substrate was introduced. For the latter, DMF and oxalyl chloride were mixed in dichloromethane, the solvents were removed, and the resulting solid added to a separate flask containing THF and then the substrate was added to this solution. Neither of the methods gave any product that could be extracted and identified as the desired aldehyde.

An alternative that made use of remaining gramine from previous endeavours was using hexamethyltetraamine (HMTA) in acetic acid under reflux (Scheme 3.14).[116] This reaction proceeded adequately in the case of **143** but not when using **87** and was wasteful of both the remaining indole and azaindole. Interestingly, HMTA can also be used to prepare the aldehyde from the unsubstituted indole (the Duff reaction, a reaction that has been shown to be effective for 7-azaindole[117]) or even an indole with a 3-chloromethyl group (Sommelet reaction) not just gramines, though these were not investigated.

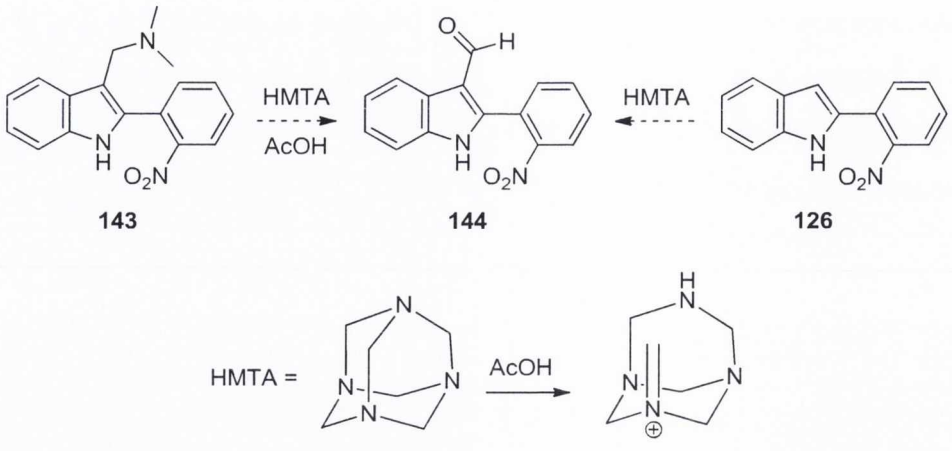

Scheme 3.14: HMTA and reaction with gramines and indoles.

This work was stopped when Friedel-Crafts reactions with oxalyl chlorides was found to be a more promising strategy.

3.4 Friedel-Crafts acylation

The target was changed from nitrile **85** to ester **146**, and the strategy was altered to involve an oxalyl ester (**145**) which we envisaged could be reduced to afford target **146** as shown in Scheme 3.15.

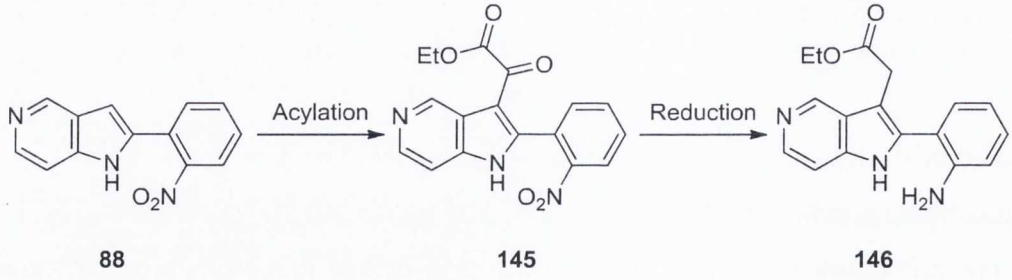

Scheme 3.15: Acylation of azaindole with an oxalyl chloride.

Using an indole substrate this transformation is most simply performed by adding oxalyl chloride to the substrate without the need for catalysis (Scheme 3.16).[118] In the case of azaindoles, an excess of an oxalyl chloride and a catalyst was found to be

necessary, thus highlighting the difference in electrophilicity at the C-3 position in both compounds.

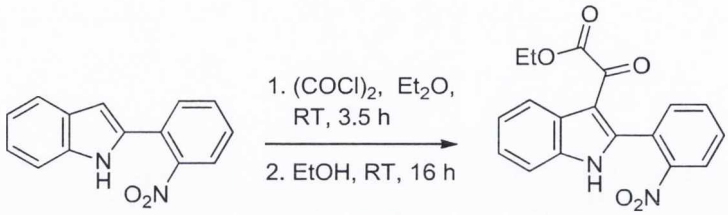

126 **147** 85%

Scheme 3.16: Acylation of indole **126** with oxalyl chloride.

The method that was developed was based on a procedure published by Wang *et al.*[119] It was not without problems, as a more recent paper from the same research centre highlighted,[120] most notably the unreliability of the original procedure when working on multi-gram scale. This was a problem that had been recognised and steps were taken to remedy it.

Initially, using dichloromethane as solvent was not particularly effective, it had been demonstrated for an unsubstituted azaindole with high dilution, however the azaindole we employed did not dissolve easily and later when the aluminium chloride was added a sticky deposit was observed on the sides of the reaction vessel. A variety of other solvents were considered: nitrobenzene was used on its own but it was a difficult solvent to remove, carbon disulphide and nitromethane were discounted as either hazardous or difficult to remove especially in large volume, as the original publication had done when promoting the use of dichloromethane. Since dichloromethane had been successful, it was used as the major solvent when testing a variety of solvent mixtures. Thus it was found that a 9:1 (*v/v*) mixture of dichloromethane and nitromethane produced a perfectly clear solution, even when adding excessive amounts of aluminium chloride and the reaction proceeded successfully (Scheme 3.17).

Striving for complete conversion was another challenge, remedied simply by adding additional portions of both ethyl chloro(oxo)acetate (**148**) and aluminium chloride at intervals over a few hours. Adding all the reagents in a single portion at the start led to

an incomplete reaction. In addition, it was necessary to add the aluminium chloride and azaindole together and to allow the resulting solution to stir for 1 h before adding **148**.

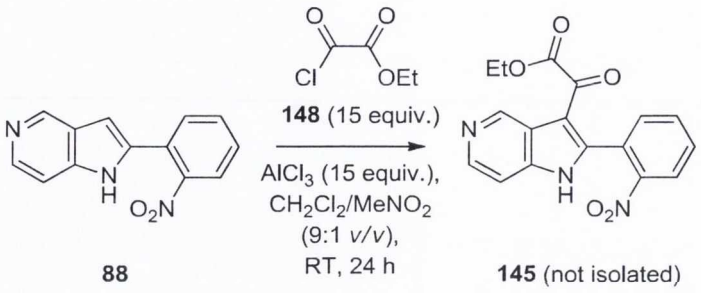

Scheme 3.17: Acylation of **88** with choride **148**.

The most difficult part was the isolation, in the original published research the authors quenched the completed reaction with alcohol and passed the crude material down a chromatography column, however in our hands this technique was a complete failure, the product could not be eluted even when excessively polar mobile phase was used. Adding ethanol and heating to reflux gave a mixture of ketal and the desired ketone. This mixture could not be pushed to uniformity, and was not easy to resolve by chromatography. Finally, to resolve these issues, a typical aqueous work-up for these azaindoles was employed: effecting the separation with mixtures of dichloromethane and ethanol; this gave good yields despite fears of losing material to the aqueous layer and hydrolysis.

As an alternative strategy, it was considered that it may be possible to effect the transformation shown in Scheme 3.18, whereby it was expected that acylation of the aniline would occur rapidly and this would position the electrophile close to the C-3 position of the azaindole and facilitate an intramolecular reaction to furnish **150**. Various attempts failed to produce the desired product, acylation of the aniline was trivial however substitution at C-3 was never observed, as evidenced in ^{1}H NMR spectra of the crude reaction mixtures where the appearance of a conspicuous broad singlet and no alteration to the H-3 proton were observed. From examining the literature and previous work undertaken in the research group, acylation at C-3 of 5-azaindoles is difficult, so it was fortuitous to have at least one method that proved effective.

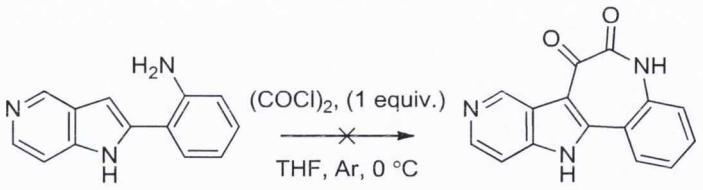

149 150

Scheme 3.18: Outline of desired intramolecular acylations.

3.5 Synthesis of dithiolane 151

For expedience the crude product **145**, from the acylation reaction of **88**, was treated with 1,2-ethanedithiol to form a dithiolane ring, which proved effective and the product was found to be a much more straightforward material to isolate and purify by recrystallisation. To form the dithiolane ring several different procedures were evaluated (Table 3.2). Initially ethanol saturated with gaseous hydrochloric acid, was efficacious if somewhat unreliable for indole substrates but not for the corresponding transformation of azaindole **145**. To modify the conditions to make them suitable for use with azaindoles, the reaction was carried out neat in trifluoroacetic acid and heated at 60 °C for 1 d (Scheme 3.19). The ketal that was formed during the work-up of the Friedel-Crafts reaction is much more readily transformed to the thioketal than the ketone so a small quantity of ethanol was added to the reaction. The reaction also proceeds using dichloromethane as solvent with lesser amounts of trifluroacetic acid.

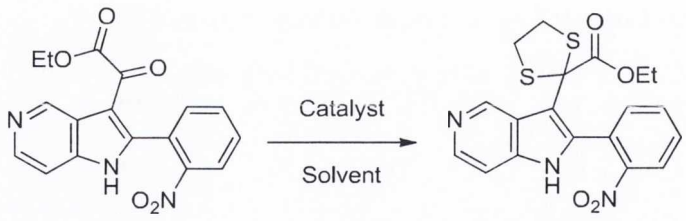

145 **151**

Table 3.2: Various catalysts used in the formation of dithiolane **151**.

Entry	Catalyst	Solvent	Equiv.	Conversion (%)
1	HCl(g)	EtOH	N/A	0
2	H_2SO_4(c)	EtOH	1.1	0
3	*p*TSA	EtOH	0.1	0
4	TFA	neat	N/A	100
5	$AlCl_3$	CH_2Cl_2	2.0	100
6	I_2	CH_2Cl_2	0.1	0

For entries 1-5, reactions were stirred at RT, then if no product was observed the reactions were heated under reflux, except for entry 6, which was done according to a published procedure.[121]

Scheme 3.19: Formation of dithiolane **151**.

Synthesising ditholane **151** was the only option that was found to achieve the desired outcome, because using a reducing agent at the oxalyl ester stage, particularly one that (partly) reduces nitro groups would produce a ring closed product, but not the desired one (**152**; Scheme 3.20). One method that was trialled was to reduce the ketone with

Pd/C as catalyst and sodium hypophosphite as hydrogen source,[122] however no product was obtained with these reducing reagents.

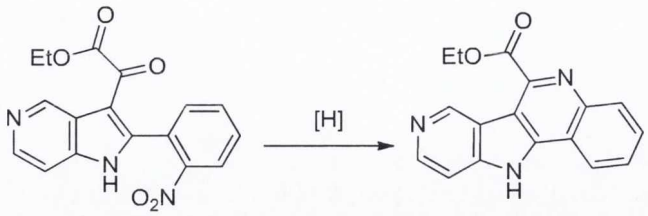

145 152

Scheme 3.20: Undesired pyridine ring formation.

To facilitate ring closure to form the lactam we expected that having the dithiolane ring present would increase the rate of this transformation due to the Thorpe-Ingold effect. One difficulty was that once the lactam was formed with the dithiolane ring remaining in place this compound was particularly insoluble and difficult to isolate. Thus, the decision was made to remove the dithiolane before lactam formation, it was suspected that the molecules were already quite rigid without making use of the Thorpe-Ingold effect bestowed by the additional ring.

3.6 Reduction of dithiolane 151 and lactam formation

To remove the dithiolane ring there was one reducing agent considered above all others: Raney Nickel. However, good success was obtained with iron powder in acetic acid, which had the advantage of being able to reduce the nitro group and ring close to the lactam quickly and effectively giving good conversion, except it had one drawback, it was only successful for **25** and not **82**; as separating the products from the iron at the end of the reactions was not so straightforward.

Initially the reductions involving Raney nickel were performed in ethanol. However, with poor solubility of the starting material and the resulting lactam, it was necessary to exchange this solvent for dioxane. Although, as the reaction proceeded there was still some precipitation observed. Thus it was necessary to ensure all materials were

redissolved before removing RaNi by filtration, and to wash the filter cake with DMSO. The crude aniline was not isolated and the synthesis was completed by heating it in dioxane with acetic acid (2 equiv.). This is similar to the conditions employed by Ferenc and Opatz to complete their synthesis of paullone (Section 1.4.8.2). The final results were less than satisfactory (Scheme 3.21). It was necessary to purify the materials by MPLC, however the return from the material loaded was quite poor and it is this fact that is attributed to low isolated yields for **82·TFA**. The purification of 9-azapaullone is detailed in the Section 3.7.

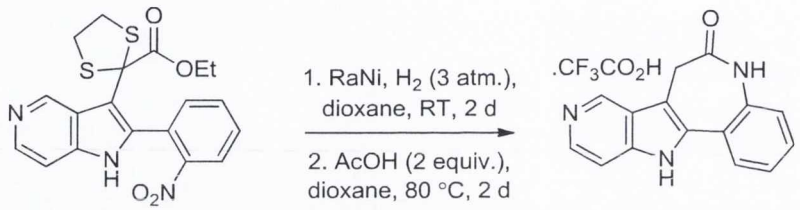

151 **82·TFA** 17%

Scheme 3.21: Final conditions and isolated yield for the synthesis of **82·TFA**.

3.7 Purification of azapaullones

While we were initially reluctant to protonate azapaullone **82**, it was found to greatly help solubilise the material, and allowed some precipitation methods to clean up the crude material *i.e.* dissolving in hot mixtures of water and polar solvents (methanol, acetonitrile or dioxane were all tested), and allowing precipitation to occur; it was not considered a proper recrystallisation as the solid precipitated too quickly and the materials could not be fully purified by these methods. To further effect the purification of the material, reverse phase MPLC techniques were used.

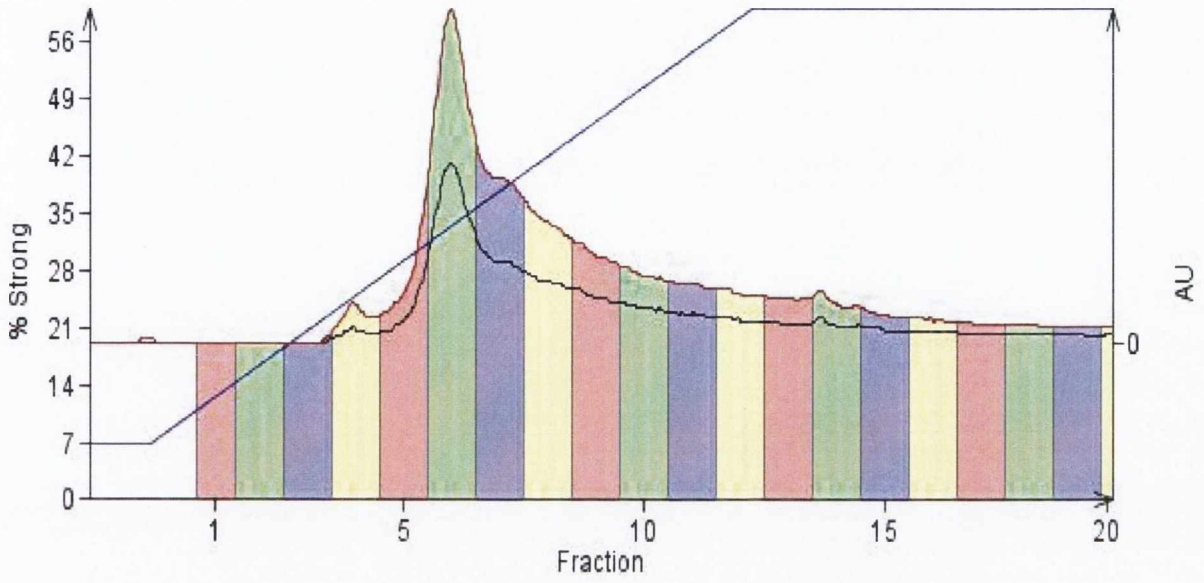

Figure 3.1: Chromatogram for the purification of **82·TFA**.

In Figure 3.1 is shown a typical chromatogram for these compounds, the individual fractions are marked, and the gradient of the mobile phase is represented as a graph (blue line) against the left scale; from 7-60% of acetonitrile (strong solvent) and water is designated the weak solvent. The amount of **82** loaded is minimal compared to the volume of stationary phase used, also DMSO was required to dissolve the material and load it on the column. The stationary phase used was in the form of pre-packed C-18 silica cartridges.

It was found to be difficult to obtain a clean separation; the DMSO that was necessary created problems in running the column. Removing the DMSO by flushing the column with water first after loading was effective, however this disrupted the stationary phase to some extent, producing cavities and cracks over time. It was necessary to use a high proportion of water as a water/acetonitrile (9:1) mobile phase was sufficient to move the product from the baseline before the desired time. Conversely, the compound does not seem to be completely soluble, judging by the shoulder and long tail observed in Figure 3.1. The difficulty was in finding a balance between removing the DMSO, not having the product run off too quickly or remain unmoving on the stationary phase.

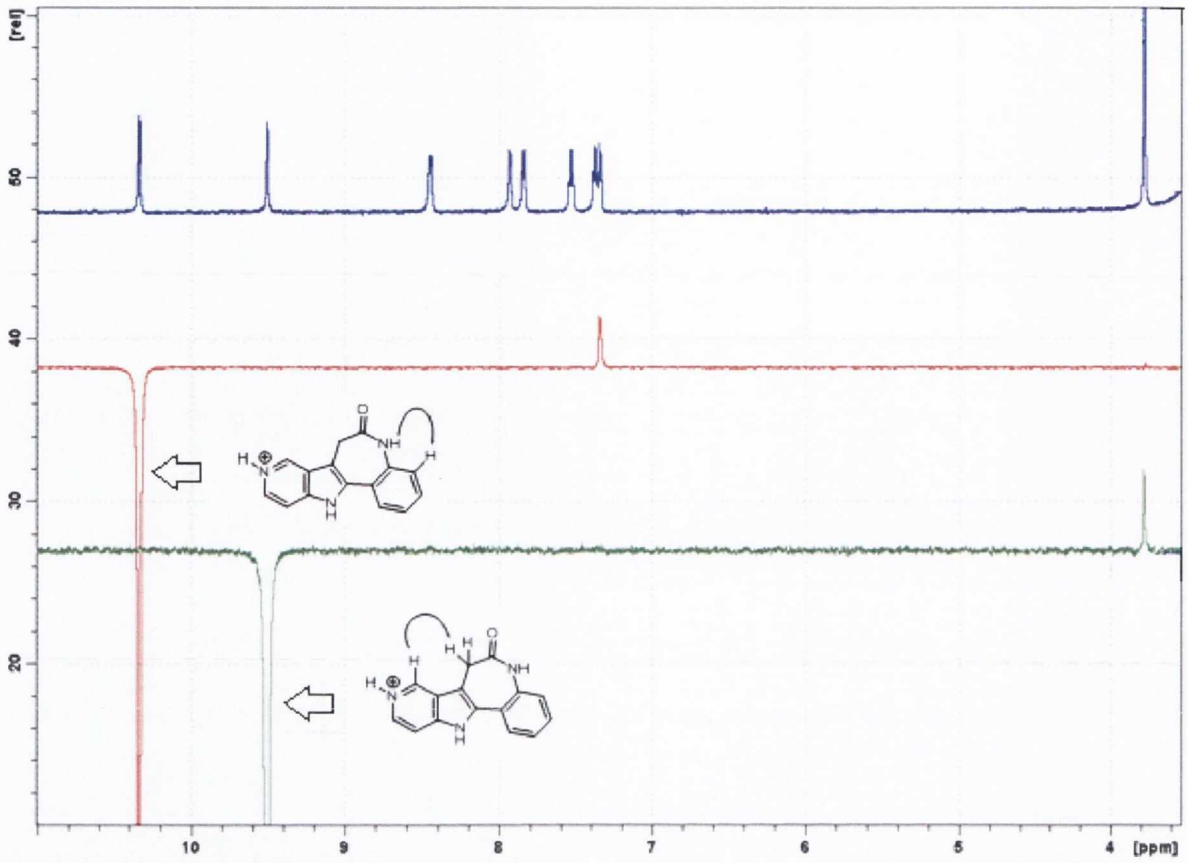

Figure 3.2: NOE interactions observed for 9-azapaullone.TFA.

When characterising azapaullone **82·TFA**, a very helpful technique in NMR spectroscopy was studying through space (NOE) interactions. Since this is a very rigid molecule, the experiments were especially effective. For example it allowed for the observation of the interaction between the lactam proton and the proton ortho to this group (Figure 3.2), this was useful to begin assigning the protons of the phenyl ring. To assign the remaining protons of the 'A' ring, selective 1D-TOCSYs were used (Figure 3.3), which showed all the protons of the phenyl ring (A) and displayed the nearest neighbours in the spin system to the irradiated proton (B).

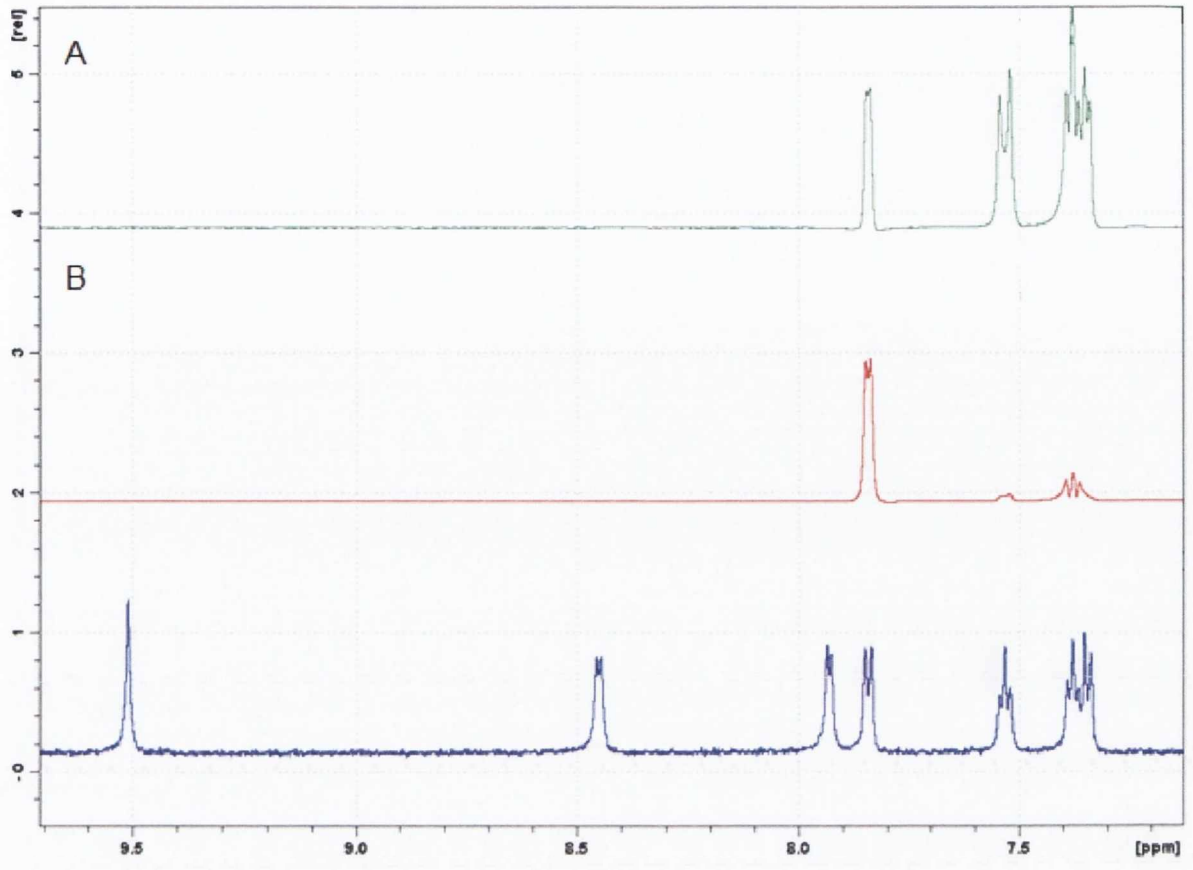

Figure 3.3: Selective 1D-TOCSYs for 9-azapaullone.TFA

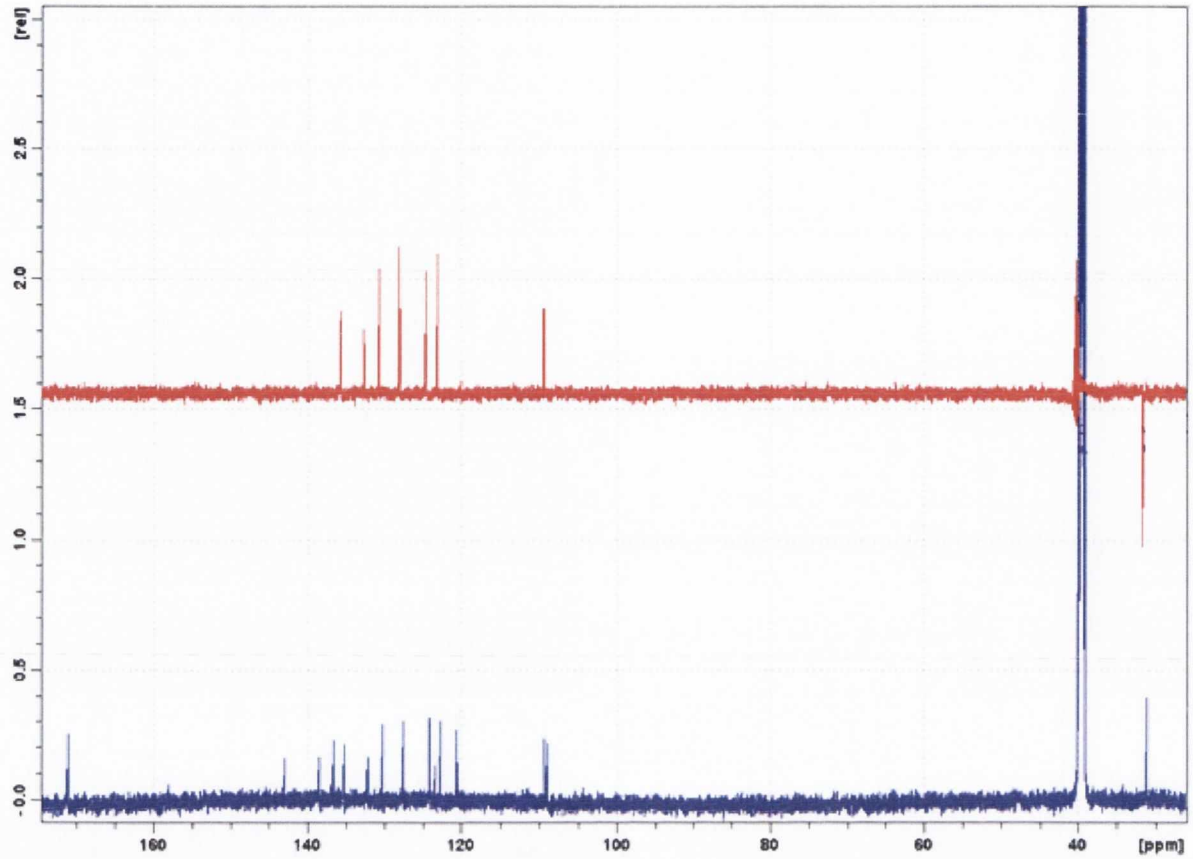

Figure 3.4: ^{13}C NMR spectrum and DEPT 135 experiment for 9-azapaullone.TFA.

3.8 Comparison with later stages of paullone synthesis

In contrast to the difficulty experienced in synthesising **82·TFA**, by using a similar method for the synthesis of paullone **25** it was found to be much easier sequence to complete, with very respectable yields as shown in Scheme 3.22. Firstly, gaseous hydrochloric acid was a suitable catalyst for the formation of dithiolane **153**, and subsequently the dithiolane group could be reduced, the compound cyclised and the product isolated much more readily. The resulting material could be separated by column chromatography, however various attempts at recrystallisation failed and could not be used to further the purification, though trituation and filtration was deemed sufficient in this case.

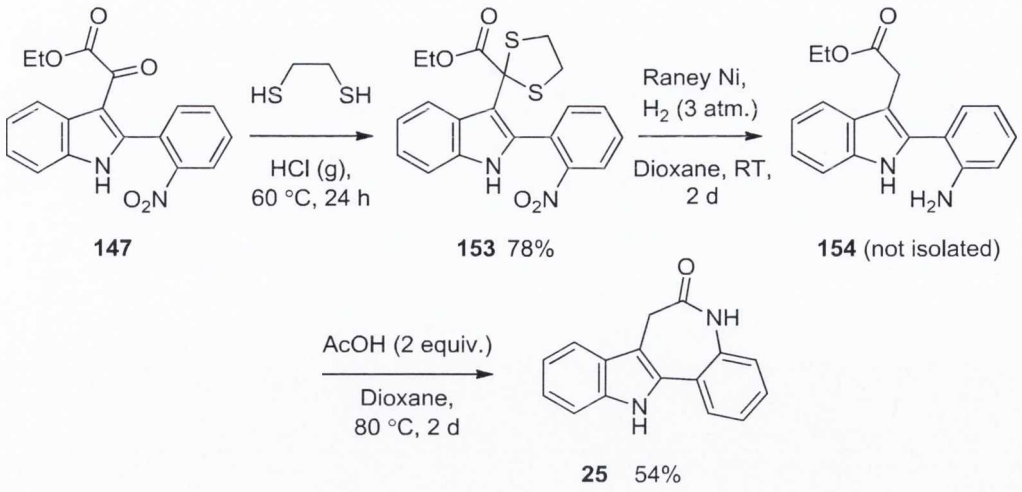

Scheme 3.22: Completed synthesis of paullone **25**.

3.9 Conclusion

While initial work in this section involved reactions that were proven for indole substrates, this was found to be an unyielding endeavour when attempting to adapt them for azaindoles. It was only when the literature was re-examined solely for methods that worked for azaindoles, and although the literature in this area is very scarce, a method was found that had potential to work as we desired. Consequently, Friedel-Crafts acylation of azaindole **88** with chloride **148**, subsequent synthesis of a dithiolane and its reduction is the sole working method demonstrated by this research to produce 5-azaindole-3-acetates, for which synthetic methodologies are practically unknown in the literature. More importantly we successfully completed the synthesis and obtained the highly desired product 9-azapaullone (Scheme 3.23).

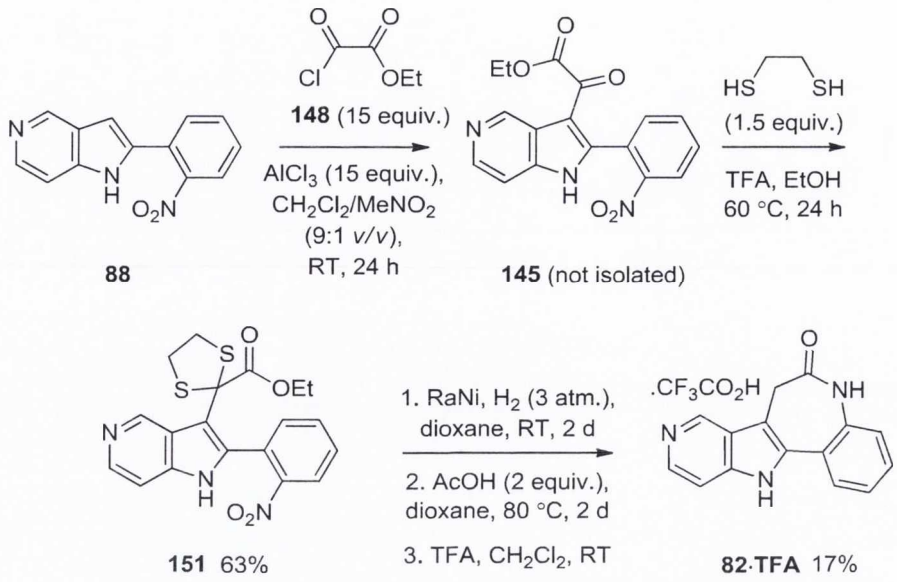

Scheme 3.23: Completed synthesis of 9-azapaullone from azaindole **88.**

4.0 Synthesis and Biological Activity of 9-Azapaullone Derivatives

Once sufficient quantities of the azapaullone were obtained and purified, attention was turned to synthesising derivatives, namely the *N*-oxide (**83**) and *N*-benzyl (**84**) (Scheme 4.1). *N*-oxide **83** was considered for its expected similarity to the nitro- group of Alsterpaullone (**27**) in its hydrogen bond accepting capability, though there being one bond length difference, and the effect of the inductive withdrawing capability of the ring nitrogen atom with a positive charge. For **84**, benzyl was chosen as the alkyl group because of bulk but more expectantly for the possibility of positive interaction with a hydrophobic region nearby.

83 **82·TFA** **84**

Scheme 4.1: Outline of derivatisation of azapaullone **82·TFA**.

We started from **82·TFA**, as it was this species that could be purified and dissolved in a greater number of solvents more readily than the free base. In addition, as it was extrapolated that the pKa_H of the azapaullone nitrogen would be only slightly less basic than DMAP and that it is the most basic of the azaindoles it was necessary to find protocols that included more strongly basic conditions than typically applied.

4.1 Oxidation of 9-Azapaullone

Typically pyridines are oxidised with peroxy acids at or near neutral conditions, or in the case of less basic pyridines in acetic acid. Since we required a pH of at least 9, methods using more than 1 equivalent of carbonate or hydroxide were investigated. Also the necessity to use mixtures of water and polar solvents to dissolve the substrate made avoiding premature hydrolysis of the oxidising agent a particular concern.

4.1.1 Use of Oxone®

Oxone® (is the trade name for a mixture of salts with the formula $2KSO_5H.KSO_4H.K_2SO_4$, also called Caro's acid) was chosen as the first agent to investigate; it is a stable, inexpensive and easy to handle crystalline solid, and also typically employed under aqueous basic conditions in which we were interested.

In preliminary experiments to evaluate the suitability of the reaction conditions, DMAP and 5-azaindole (**95**) were used as model substrates. In both cases the oxidation proceeded as expected. All reactions were carried out in water at room temperature, sodium carbonate was found to be the best base for reactions involving **95·TFA** but aqueous potassium hydroxide was required for good conversions of DMAP due to its higher pKa_H. Sodium carbonate was favoured where it could be used as it yielded a cleaner reaction. Despite obtaining full conversions in these oxidations, we failed to observe any oxidation occurring with **82·TFA** as substrate. Attempts were made at modifying the original conditions (Scheme 4.2) by adding methanol to help solubilise the material, heating the reaction, or adding an additional 4 equivalents of Oxone in portions over the course of the reaction.

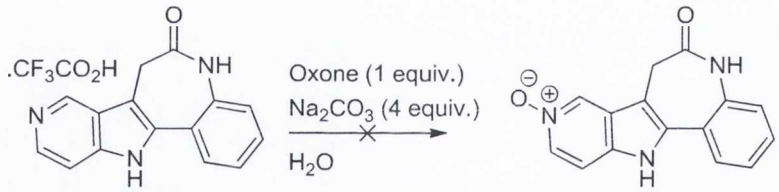

82·TFA **83**

Scheme 4.2: Initial conditions for oxidation by oxone of **82·TFA**.

4.1.2 Utilising Payne conditions

According to Payne *et al.*,[123] a mixture of benzonitrile and hydrogen peroxide generates perbenzimidic acid under alkaline conditions which can oxidise pyridines with the formation of a neutral by-product (benzamide) (Scheme 4.3). It is based on the

Radziszewski reaction, which is the hydrolysis of an organic nitrile by alkaline hydrogen peroxide.

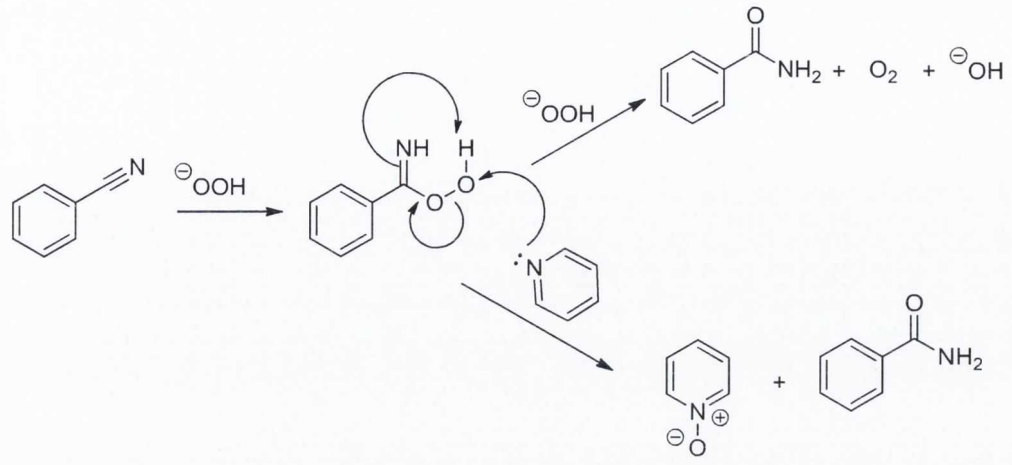

Scheme 4.3: Outline of the Payne reaction condtions.

From an examination of Scheme 4.3 it becomes clear the main drawback for these conditions is that if the pyridine does not react fast enough then the perbenzimidic intermediate is decomposed to benzamide as shown. When testing the reaction it was successful in obtaining full conversion DMAP but no sign of product was observed for **95·TFA**, suggesting it is not nucleophilic enough (Scheme 4.4).

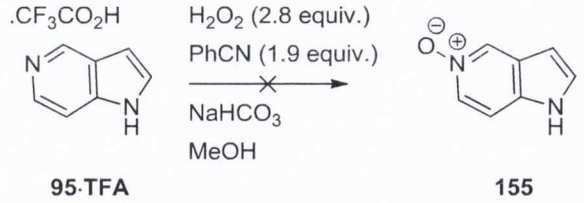

Scheme 4.4: Failure of oxidation by Payne conditions of **95·TFA**.

Also it was found to be very difficult to isolated the DMAP-*N*-oxide from the benzamide formed; the method used was to dissolve the crude product in water and filter, which needed to be repeated several times, this would be an unworkable procedure for use with **82** as material would be expected to be lost with each filtration. Acetonitrile was considered as a replacement for benzonitrile; the by-product in that case would have been acetamide that could have been removed by distillation at

reduced pressure, however it was noted by the authors of the original research[122] as being much less active than benzonitrile and hence its use was not attempted.

4.1.3 Use of *m*-chloroperbenzoic acid (*m*CPBA)

m-Chloroperbenzoic acid is a commonly used peroxyacetic acid which is soluble in most organic solvents. It is purchased as a mixture of the active agent, the corresponding benzoic acid and water and a material of high purity can be achieved by washing with a pH 8 phosphate buffer.

Typically *m*CPBA is used in a chlorinated solvent, however these were not a suitable choice for use with **82·TFA**, thus it was desirable to test *m*CPBA's activity in mixtures of water and polar solvents in which some solubility could be expected. Again testing with DMAP and **95·TFA**, using a mixture of acetonitrile and aqueous potassium hydroxide solution as solvent, the reaction was found to be very slow with moderate conversions. Adding additional quantities of oxidising agent at intervals of several hours did improve the conversion to acceptable levels, but no better than 70%. However, using such conditions for **82·TFA** failed to yield any product. Replacing acetonitrile with dioxane did allow the reaction to proceed successfully; through conversion appeared complete the isolated yield was only 19% (Scheme 4.5), which was attributed to the poor solubility when purifying the material by reverse phase chromatography.

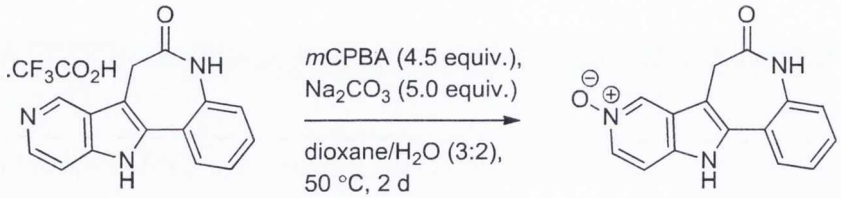

82·TFA **83** 19%

Scheme 4.5: Oxidation of **82·TFA**.

4.2 Alkylation of 9-Azapaullone

In 9-azapaullone.TFA there are three possible sites of alkylation, it was necessary to selectively deprotonate and then alkylate just one of these (Scheme 4.6).

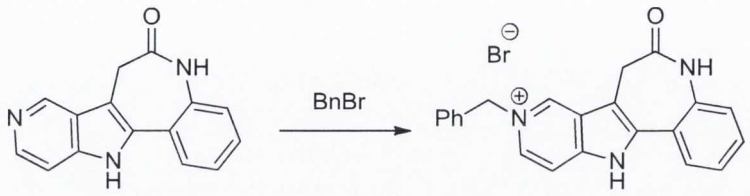

82 **84**

Scheme 4.6: Desired mono-benzylation of azapaullone **82**.

The early strategy revolved about deprotonating the salt in solution, allowing the free base to precipitate and removing the solvent and base (KOH) by filtration, and then performing the alkylation in a separate reaction vessel. The filtration was not as efficacious as expected, with poor return of material, this was likely due to the small scale that this process was performed on and an efficient process was deemed unobtainable under such circumstances.

As an alternative it was thought a better method might be to complete both the deprotonation and alkylation in one-pot. Thus the starting material was suspended in a solvent in which it had limited solubility (acetonitrile), a soluble base (tetrabutylammonium hydroxide) was then added. This method has the advantage of affording a more controllable reaction; the alkylation reaction only occurred when it was heated under reflux (Scheme 4.7). When the reaction was completed the product could be readily isolated by filtration, though additional purification was required.

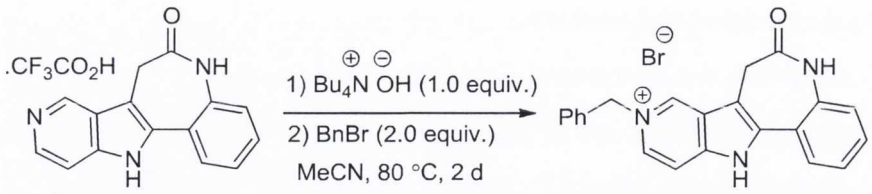

82·TFA **84** 25%

Scheme 4.7: Benzylation of **82·TFA**.

Neither **83** nor **84** could be purified by conventional methods, so reverse phase MPLC was again employed to obtain the final materials for biological testing. Also since the material was quite scarce at this time, a full characterisation was difficult however techniques such as assigning carbon spectra using heteronuclei correlation experiments helped in overcoming this difficulty.

4.3 Biological activity of azapaullones 82·TFA, 83 and 84

Each of the newly synthesised compounds was tested against a panel of several relevant kinases including CDKs. This testing was performed by members of the research group of Laurent Meijer at Station Biologique, Roscoff. The IC_{50} values were determined from dose-response curves and given in Table 4.1. Paullone (**25**) and kenpaullone (**26**) are included for comparison. In addition, Table 4.2 shows a comparison between **82·TFA**, and the previously published data of 11-azapaullone (**122**) and alsterpaullone (**27**).

Table 4.1: Biological activity of tested compounds.

Entry	Kinase	IC_{50} [a]				
		25	**26**	**82·TFA**	**83**	**84**
1	CDK1/cyclin B	3.0	0.5	2.1	5.7	>10
2	CDK2/cyclin A	2.7	0.78	2.1	6.2	>10
3	CDK5/p25	4.2	1.0	3.0	7.3	>10
4	CDK9/cyclin T	0.81	0.064	0.22	0.24	7.4
5	CK1	>10	>10	>10	>10	>10
6	CLK1	>10	>10	>10	>10	>10
7	DYRK1A	>10	>10	>10	>10	>10
8	GSK-3	1.1	0.078	0.81	3.4	>10
9	PfGSK-3	>10	>10	>10	>10	>10

[a] IC_{50} values are determined from dose-response curves and reported in μM.

Derivative **82·TFA** had moderate activity, but was 2-3 times less active than **26**, with its best activity against CDK9/cyclin T with an IC_{50} of 0.22 μM. *N*-oxide **83** possessed a similar activity against this complex, but was less active against the other CDKs. This apparent selectivity for the CDK9/cyclin T complex, which is 3 times greater than that of **26**, is of great interest and has potential for further development.

One difference between the two compounds was in their activities towards GSK-3, with **83** having poorer activity than **82·TFA**. For the paullone class, which are usually quite active against these kinases, this is particularly noteworthy finding, for example **27** inhibits most CDKs and GSK-3 in the low nanomolar range. While more selective GSK-3 inhibitory paullones have been synthesised, the inverse *i.e.* attempting to synthesise paullones highly selective for CDKs and devoid of GSK-3 activity has not been developed to date.

N-benzyl **84** can be discounted as having no significant activity against the CDKs tested. Most probable is that steric bulk is not tolerated in this area and this is seen quite clearly in CoMSIA studies (Section 1.4.5), and series of paullones containing an ester or amide and increasingly bulky alkyl groups;[77] also it casts doubt on the existence of a possible positive interaction with a phenylalanine in the binding pocket, which had been deduced from examining a homology model of CDK2.

Table 4.2: Comparison between two azapaullones **82·TFA** and **122**.

Entry	Kinase	pIC_{50} (M)		
		82·TFA	**122**	**27**
1	CDK1/cyclin B	5.68	5.66	7.46
2	CDK5/p25	5.68	5.48	7.39
3	GSK-3	6.09	5.26	8.39

There were two forms of GSK-3 used in the assay: one designated GSK-3 is derived from porcine brain (entry 8); the second designated PfGSK-3 is derived from *Plasmodium falciparum* (entry 9), this parasite causes the majority of malaria and especially lethal. Typically paullones follow the trend of high selectivity for CDK9/cyclin T, inhibiting GSK-3 less effectively and the remaining CDKs less selectively still, and the new compounds tested follow this trend as well. Another existing trend is that paullones are more active for human/mammalian form of GSK than the protozoan form,[124] PfGSK-3, however none of the present compounds tested had any significant activity against it.

Other targets included in the panel beside CDKs and GSK-3 includes: CK1, Casein Kinase 1, an important and ubiquitous kinase in signal transduction; CLK1, CDC-Like Kinase 1 is involved in mRNA splicing; DYRK1A, Dual-specific Tyrosine-phosphorylation Regulated Kinase 1A, a kinase involved in cell proliferation and brain development. These kinases were included based on the selectivity profile of (*R*)-

roscovitine and its derivatives. It is not an extensive selection, but none of the compounds tested had any noticeable activity for these kinases.

4.4 Conclusion

Of the compounds tested *N*-oxide **83** had the most interesting activity profile; it is most selective for CDK9/cyclin T and less selective for GSK-3, although in absolute terms it did not exhibit inhibitory activity against either as well as alsterpaullone or even kenpaullone. From this study it is the most likely compound to be selected for further development. The most desired piece of information that should be obtained is *in vitro* data from cancer cell-line cultures, this is essential to determine at the earliest opportunity what the increased selectivity for CDK9 means in terms of anti-proliferative ability and for the paullone class as a whole.

Experimental

5.1 General

Proton nuclear magnetic resonance spectra were recorded on a Bruker Avance 400 or 600 MHz spectrometer in $CDCl_3$ or d_6-DMSO, and referenced relative to residual $CHCl_3$ (δ = 7.26 ppm) or residual DMSO (δ = 2.50 ppm) respectively. Chemical shifts were measured in ppm, and coupling constants, J given in Hz. Carbon-13 nuclear magnetic resonance spectra were recorded on the same instruments (100 or 150 MHz) with total proton spin-decoupling. Flash chromatography was carried out on silica gel 60 (Fluka), particle size 0.04-0.063 mm. MPLC was performed on a Biotage SP4 system. TLC analysis was performed on pre-coated silica gel 60 F_{254} (Merck), with visualisation by UV irradiation or $KMnO_4$ staining. Melting points were taken on a Stuart SMP1 apparatus and are uncorrected. Infrared spectra were obtained with a Perkin Elmer Spectrum One NTS spectrometer, with an ATR sampling accessory. Mass spectra were obtained on a MALDI Q-TOF Premier MS system. Solvents were distilled as required: Et_2O and THF were distilled from sodium/benzophenone; toluene, dichloromethane, TEA and acetonitrile were distilled from calcium hydride. Unless otherwise stated, all chemicals were obtained from commercial sources and used as received.

4-Amino-3-bromopyridine (97)

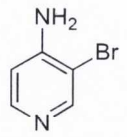

In a 1 L round bottom flask, fitted with a stirring bar, 4-aminopyridine (4.69 g, 49.8 mmol) was dissolved in a mixture of CH_2Cl_2 (300 mL) and MeCN (150 mL). The solution was cooled to 0 °C, and bromine solution (3.0 mL, 60 mmol of bromine in CH_2Cl_2 (80 mL)) was added dropwise with stirring over 20 min. Once the addition was complete the bright orange solution was allowed warm to RT and left to stir for 4 h. Solid sodium carbonate was added and allowed to stir for a further 1 h until the solution had decolourised. It was then filtered and the solvent removed *in vacuo* to give a solid residue, consisting of two products (**97**, **98** = dibromo product) as shown by TLC. The crude mixture was separated by column chromatography (hexane/EtOAc, 2:1) to obtain **97**, which had the lower R_f, as an oil that crystallised on standing (2.58 g 30%).

m.p. 65-66 °C, (lit.,[125] 65-66 °C)

δ_H (400 MHz, $CDCl_3$): 4.66 (br s, 2H, NH_2), 6.63 (d, 1H, J 5.5, H-5), 8.13 (d, 1H, J 5.5, H-6), 8.42 (s, 1H, H-2).

3-Bromo-4-(*N*-boc)aminopyridine (101)

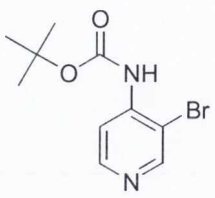

In a 250 mL round bottom flask, fitted with a stirring bar, **97** (6.78 g, 39.2 mmol) was dissolved in CH_2Cl_2 (80 mL), boc-anhydride solution (10.26 g, 47.0 mmol in CH_2Cl_2 (80 mL)) was adding dropwise over 30 min with stirring at 0 °C. The resulting solution was stirred for 3 h at RT. TFA (0.4 mL, 4 mmol) was added and the solution left stirring overnight, then it was examined by ^1H NMR to determine if any of the doubly

protected compound remained. Solid sodium carbonate was added and the solution stirred for 1 h, it was filtered and the solvent removed *in vacuo* to give a solid residue. The crude was passed through a plug of silica (CH_2Cl_2) to obtain the product, after the solvent was removed *in vacuo,* as an oil that crystallized on cooling (10.18 g, 95%). ^1H NMR spectral data was consistent with previously published data.[126]

m.p: 96-97 °C (dec.)

δ_H (400 MHz, $CDCl_3$): 1.57 (s, 9H, *t*-butyl), 7.23 (br s, 1H, carbamate NH), 8.20 (d, 1H, J 5.5, H-5), 8.39 (d, 1H, J 5.5, H-6), 8.60 (s, 1H, H-2) ppm.

3-Iodo-4-(*N*-boc)aminopyridine

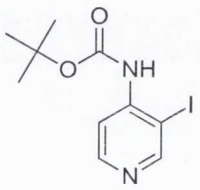

In a 500 mL RBF, fitted with a stirring bar, 4-aminopyridine (5.02 g, 53.3 mmol) and sodium carbonate (3.61 g, 34.0 mmol) were dissolved in water (20 mL), the resulting solution was heated to reflux. To this refluxing solution was added dropwise a solution of iodine (10.00 g, 64.0 mmol) and potassium iodide (10.63 g, 64.0 mmol) in water (50 mL). Upon completion the mixture was heated for a further 2 h under reflux, then cooled and extracted with EtOAc (150 mL). The organic layer was washed with saturated sodium thiosulfate solution (3 x 100 mL), and then dried over $MgSO_4$, filtered and solvent removed under reduced pressure. This crude solid was found to also contain both 4-aminopyrdine and diiodo pyridine **100**, and was purified by column chromatography (hexane/EtOAc, 3:1 to 1:1) to obtain 3.66 g of **99** as an orange oil, that solidified on standing at ambient temperature. This material was protected in an identical manner to bromide **97**. ^1H NMR spectral data was consistent with previously published data.[105]

m.p: 85-86 °C.

δ_H (400 MHz, $CDCl_3$): 1.56 (s, 9H, *t*-butyl), 7.07 (br s, 1H, carbamate NH), 8.12 (d, 1H, J 5.6, H-5), 8.36 (d, 1H, J 5.6, H-6), 8.77 (s, 1H, H-2) ppm.

2-Methyl-4-(2'-nitrophenyl)-but-3-yn-2-ol (108)

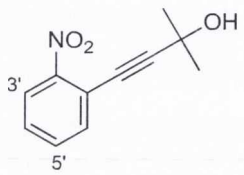

In a 25 mL two-necked round bottom flask, fitted with stirring bar and condenser, under an atmosphere of N_2, 2-bromonitrobenzene **(105)** (1.02 g, 5.05 mmol) was dissolved in freshly distilled TEA (10 mL). To this solution copper (I) iodide (0.070 g, 0.37 mmol), triphenylphosphine (0.107 g, 0.40 mmol) and $PdCl_2(PPh_3)_2$ (0.076 g, 0.11 mmol) were added, followed by 2-methyl-but-3-yn-2-ol (0.40 mL, 5.6 mmol) *via* syringe. The resulting mixture was heated under reflux for 4 h. Solvent was removed *in vacuo*, the residue was dissolved in CH_2Cl_2 (50 mL) and washed with saturated NaCl solution, water (3 x 10 mL). The organic extract was dried ($MgSO_4$), filtered and the solvent removed *in vacuo*. The product was purified by column chromatography (hexane/EtOAc, 6:4) and obtained as a pale brown solid (0.36 g, 36%).

m.p: 62-63 °C.

δ_H (400 MHz, $CDCl_3$): 1.67 (s, 6H, CH_3), 7.49 (dt, 1H, J 1.7, 7.8, H-4'), 7.61 (m, 2H, H-5'/H-6'), 8.06 (d, 1H, J 8.0, H-3') ppm.

δ_C (100 MHz, $CDCl_3$): 30.6, 65.3 (q), 77.1 (q), 101.2 (q), 117.7 (q), 124.1, 128.3, 132.3, 134.1, 149.4 (q) ppm.

HRMS (ESI): $[C_{11}H_{11}NO_3 + Na]^+$ requires 228.0637, found 228.0630.

IR (ν_{max}): 3275, 2978, 2238 (weak), 1608, 1568, 1518, 1336, 1262, 1151, 957, 855, 738.91 cm^{-1}.

Attempted preparation of 1-Ethynyl-2-nitrobenzene (103)

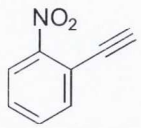

In a 25 mL round bottom flask, fitted with stirring bar and micro-distillation apparatus, the alkynol **108** (0.360 g, 1.75 mmol) was dissolved in dry toluene (10 mL), to this was added sodium hydride (0.051 g, 60% dispersion in oil) and the solution was heated gradually to 110 °C and maintained at this temperature until approximately half the volume of toluene had been distilled. No trace of the desired product was found and no starting material remained in the indecipherable mixture.

1-(TMS-ethynyl)-2-nitrobenzene (109)

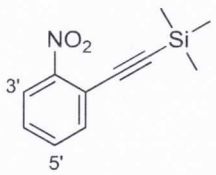

In a 100 mL two-necked round bottom flask, fitted with stirring bar and condenser, under an atmosphere of N_2, 2-nitrobromobenzene (**105**) (4.16 g, 20.6 mmol) was dissolved in freshly distilled TEA (80 mL). To this solution copper (I) iodide (0.247 g, 1.30 mmol), triphenylphosphine (0.439 g, 1.67 mmol) and $PdCl_2(PPh_3)_2$ (0.290 g, 0.41 mmol) were added, followed by TMS-acetylene (3.5 mL, 25 mmol) *via* syringe. The resulting mixture was heated at 55 °C for 4 h. Solvent was removed *in vacuo*, the residue was dissolved in CH_2Cl_2 (50 mL) and washed with saturated NaCl solution, then water (3 x 10 mL), organic extract was dried ($MgSO_4$), filtered and the solvent

removed *in vacuo*. The resulting oil was purified by column chromatography (hexane/EtOAc, 10:1) to obtain the title compound as a yellow oil (3.34 g, 74%). ^{1}H NMR spectral data was consistent with previously published data.[127]

δ_H (400 MHz, $CDCl_3$): 1.17 (s, 21H, *i*-propyl), 7.46 (t, 1H, J 8.0, H-4'), 7.58 (t, 1H, J 7.7, H-5'), 7.68 (d, 1H, J 7.5, H-6'), 8.04 (d, 1H, J 8.4, H-3')

1-Ethynyl-2-nitrobenzene (103)

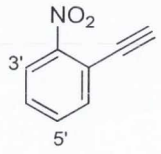

In a 250 mL round bottom flask, fitted with a stirring bar, TMS-protected alkyne **109** (4.60 g, 15.2 mmol) was dissolved in THF (45 mL), to this solution at 0 °C was added TBAF solution (18 mL, 18 mmol) *via* syringe. The solution was allowed to stir at 0 °C for 40 min. The solvent was removed at reduced pressure. Saturated ammonium chloride solution (50 mL) was added and the product extracted with EtOAc (3 x 50 mL), dried ($MgSO_4$) and the solvent removed *in vacuo*. The product was purified by passing it through a plug of silica (hexane/EtOAc, 5:1) and after the solvent was removed a dark residue was obtained, which was recrystallised twice from hexane to give a pink solid (1.25 g, 54%).

m.p: 83-85 °C (dec.) (lit.,[128] 79.5-81 °C).

δ_H (400 MHz, $CDCl_3$): 3.54 (s, 1H, alkyne), 7.53 (m, 1H, H-4'), 7.62 (m, 1H, H-5'), 7.72 (dd, 1H, J 1.5, 8.0, H-6'), 8.07 (dd, 1H, J 1.0, 8.0, H-3')

4-(*N*-boc)amino-3-(TIPS-ethynyl)pyridine (111)

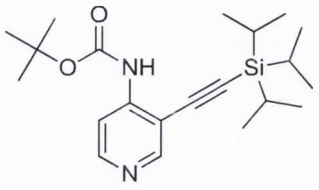

In a 250 mL three-necked round bottom flask, fitted with a stirring bar and condenser, bromide **101** (4.05 g, 14.9 mmol) was dissolved in freshly distilled TEA (60 mL) and argon was bubbled through the resulting mixture. To this solution copper (I) iodide (0.179 g, 0.89 mmol), triphenylphosphine (0.314 g, 1.19 mmol) and $PdCl_2(PPh_3)_2$ (0.213 g, 0.30 mmol) were added under a gentle stream of argon, followed by (triisopropylsilyl)acetylene (4.0 mL, 18 mmol) *via* syringe. The resulting mixture was heated at 55 °C for 1 d. Solvent was removed *in vacuo*, the residue was trituated in hexane and filtered through a plug of celite, the filtrate was collected and the solvent removed under reduced pressure. The resulting oil was purified by column chromatography (hexane/EtOAc, 95:5) to obtain the desired product as a white solid (5.23, 94%).

m.p. >110 °C (dec.)

δ_H (400 MHz, $CDCl_3$): 1.18 (m, 21H, *i*-propyl), 1.55 (s, 9H, *t*-butyl), 7.68 (s, 1H, carbamate NH), 8.18 (d, 1H, J 5.7, H-5), 8.41 (d, 1H, J 5.8, H-6), 8.57 (s, 1H, H-2) ppm.

δ_c (100 MHz, $CDCl_3$): 11.1 (CH), 18.7 (CH_3), 28.1 (CH_3), 81.9 (q), 98.7 (q), 102.3 (q), 110.7, 146.8 (q), 149.7, 151.5 (q), 151.7 ppm.*

HRMS (ESI): $[C_{21}H_3N_2O_2Si + H]^+$ requires 375.2468, found 375.2485.

IR (ν_{max}): 3387, 2939, 2834, 2152 (weak), 1741, 1567, 1501, 1368, 1243, 1224, 1146, 984, 882, 841 cm^{-1}.

* For alkynes **111**, **104** and **89**, despite numerous scans a single quaternary carbon in each case could not be found.

4-(*N*-Boc)amino-3-ethynylpyridine (104)

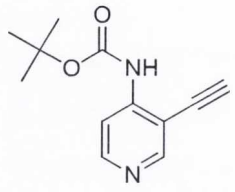

In a 250 mL round bottom flask, fitted with a stirring bar, alkyne **111** (8.06 g, 21.5 mmol) was dissolved in CH_2Cl_2 (108 mL), to this solution at 0 °C was added dropwise TBAF solution (21.6 mL, 21.6 mmol). The solution was stirred at RT for 1 h. Saturated ammonium chloride solution (100 mL) was added and the layers separated, the organic layer was dried over magnesium sulfate and the solvent removed *in vacuo*.* The product was purified by column chromatography (hexane/EtOAc, 70:30) and after the solvent was removed*, a white solid was obtained (4.20g, 89%).

m.p: 110-112 °C

δ_H (400 MHz, $CDCl_3$): 1.57 (s, 9H, t-butyl), 3.64 (s, 1H, alkyne), 7.37 (s, 1H, carbamate NH), 8.14 (d, 1H, J 5.5 Hz, H-5), 8.45 (d, 1H, J 5.5, H-6), 8.59 (s, H, H-2) ppm.

δ_c (100 MHz, $CDCl_3$): 27.7 (CH_3), 75.7 (q), 81.8 (q), 86.7 (CH), 110.5, 146.4 (q), 149.7, 151.0 (q), 152.2 ppm.

HRMS (ESI): $[C_{12}H_{14}N_2O_2 + H]^+$ requires 219.1134, found 219.1164, also 163.0361 (loss of *t*-butyl 163.0508).

IR (ν_{max}): 3400, 3167, 2094 (weak), 1739, 1574, 1512, 1458, 1366, 1247, 1222, 1144, 1056, 838 cm^{-1}.

* On both occasions when the solvent was removed at reduced pressure, it was ensured that the temperature of the water bath was kept below 30 °C.

1-Iodo-2-nitrobenzene (112)

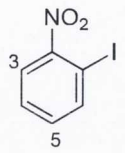

In a 250 mL round bottom flask, fitted with a stirring bar, finely ground 2-nitroaniline (10.05 g, 72.8 mmol) was suspended in water (30 mL), containing concentrated sulphuric acid (8.4 mL), the suspension was stirred for 1 h before cooling to 0 °C. A solution of potassium nitrite (5.0 g in water (16 mL)) was added slowly while the temperature of solution was maintained below 5 °C. The cold mixture was filtered, and the filtrate was collected and added slowly to a solution of potassium iodide (20.0 g in water (30 mL)). The yellow precipitate was collected and passed through a plug of silica (hexane) and the solvent was removed, a yellow solid was obtained (13.0 g, 72%).

m.p: 51-53 °C (lit.,[129] 52-54 °C).

δ_H (400 MHz, $CDCl_3$): 7.30 (dt, 1H, J 1.4, 7.7, H-4), 7.52 (dt, 1H, J 1.3, 7.8, H-5), 7.89 (dd, 1H, J 1.4, 7.9, H-6), 8.07 (dd, 1H, J 1.3, 8.1, H-3) ppm.

Attempted synthesis of 4-(*N*-boc)amino-3-((2'-nitrophenyl)ethynyl)pyridine (89) *via* disconnection A

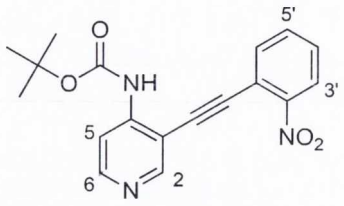

In a 50 mL RBF, fitted with stirring bar and condenser, alkyne **103** (0.145 g, 0.48 mmol) was dissolved in freshly distilled TEA (4 mL) and placed under an atmosphere of N_2. To this solution copper (I) iodide (0.006 g, 0.024 mmol), triphenylphosphine (0.008 g, 0.32 mmol) and $PdCl_2(PPh_3)_2$ (0.007 g, 0.008 mmol) were added, followed by bromide **101** (0.150 g, 0.40 mmol). The resulting mixture was heated at 55 °C overnight. Solvent was removed *in vacuo*, the residue was dissolved in EtOAc (20 mL) and washed with saturated ammonium chloride solution, followed by water, the organic extract was dried ($MgSO_4$) and the solvent removed *in vacuo*. The crude residue was examined by ^1H NMR spectroscopy, both starting materials remained, with some loss of the alkyne and no new product observed.

4-(*N*-Boc)amino-3-((2'-nitrophenyl)ethynyl)pyridine (89)

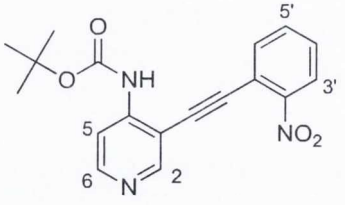

In a 250 mL three-necked RBF, fitted with stirring bar and condenser, alkyne **104** (3.96 g, 18.1 mmol) was dissolved in freshly distilled TEA (90 mL) and argon was bubbled through the resulting mixture. To this solution copper (I) iodide (0.206 g, 1.08 mmol), triphenylphosphine (0.380 g, 1.45 mmol) and $PdCl_2(PPh_3)_2$ (0.252 g, 0.36 mmol) were added, followed by iodide **112** (4.96 g, 19.9 mmol) under a gentle flow of argon. The resulting mixture was heated at 30 °C for 2 d. Solvent was removed *in vacuo*, the residue was dissolved in EtOAc (100 mL) and washed with saturated ammonium

chloride solution, followed by water, the organic extract was dried ($MgSO_4$) and the solvent removed *in vacuo*. The resulting residue was purified by column chromatography (hexane/EtOAc, 60:40) to obtain the title compound as an orange solid (5.16 g, 84%).

m.p: >110 °C (dec.).

δ_H (400 MHz, $CDCl_3$): 1.60 (s, 9H, *t*-butyl), 7.56 (t, 1H, J 7.5, H-4'), 7.70 (t, 1H J 7.5, H-5'), 7.79 (d, 1H, J 7.0, H-6'), 8.05 (s, 1H, carbamate NH), 8.20 (d, 1H, J 5.5, H-5), 8.23 (d, 1H, J 8.0, H-3'), 8.47 (d, 1H, J 6.0, H-6), 8.86 (s, 1H, H-2)

δ_c (100 MHz, $CDCl_3$): 27.7, 81.5 (q), 89.2 (q), 93.9 (q), 110.7, 117.5 (q), 124.8, 128.9, 133.0, 134.0, 146.9 (q), 148.3 (q), 150.5, 151.5 (q), 152.2 ppm.

HRMS (ESI): $[C_{18}H_{17}N_3O_4 + H]^+$ requires 340.1297, found 284.0673 (loss of *t*-butyl, 284.0671).

IR (ν_{max}): 3363, 2979, 2213 (weak), 1730, 1567, 1511, 1367, 1338, 1241, 1148, 838, 742 cm^{-1}.

_N_-Boc-2-(2'-nitrophenyl)-5-azaindole (115)

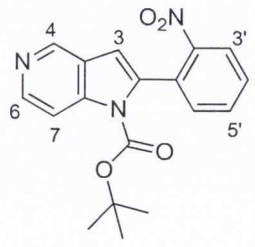

Via base catalysed cyclisation of **89**:

In a 50 mL two-necked round bottom flask, fitted with stirring bar and condenser, under an atmosphere of N_2, alkyne **89** (0.376 g, 1.11 mmol) was dissolved in anhydrous DMF (20 mL). To this solution DBU (0.17 mL, 1.11 mmol) was added *via* syringe and allowed to stir for 2 h at 80 °C. When the reaction was complete (TLC), the solution was cooled to RT, and Et_2O (50 mL) added, this was washed with water (5 x 20 mL), dried ($MgSO_4$) and the solvent removed *in vacuo*. The residue was purified by column chromatography (CH_2Cl_2/EtOAc, 9:1) to give an orange solid (0.30 g, 79%).

Via sequential coupling and one-pot cyclisation from **104**:

Alkyne **104** (0.678 g, 3.11) was added to a 100 mL two-necked round bottom flask, fitted with stirring bar and condenser, under an atmosphere of argon, already containing bromide **105** (0.692 g, 3.42 mmol) dissolved in anhydrous DMF (15.6 mL). To this solution copper (I) iodide (0.044 g, 0.19 mmol), triphenylphosphine (0.076 g, 0.25 mmol), TEA (1.73 mL, 12.44mmol) and $PdCl_2(PPh_3)_2$ (0.048 g, 0.06 mmol) were added. The resulting mixture was heated at 55 °C for 4 h. When the reaction was complete (TLC), DBU (0.93 mL, 6.22 mmol) was added *via* syringe and the mixture allowed to stir for 1 h at 55 °C. When the reaction was complete (TLC), solution was cooled to room temperature, and Et_2O (100 mL) added, this was washed with water (5 x 100 mL), dried ($MgSO_4$) and the solvent removed *in vacuo*. The residue was purified by column chromatography (hexane/EtOAc, 1:1) to give an orange solid (0.46 g, 44%).

Utilising catalytic copper iodide and DBU:

In a 100 mL two-necked round bottom flask, fitted with stirring bar and condenser, under an atmosphere of argon, alkyne **89** (5.16 g, 15.2 mmol) was dissolved in anhydrous DMF (75 mL). To this solution copper (I) iodide (0.289 g, 1.52 mmol) and DBU (0.23 mL, 1.52 mmol) were added and the solution allowed to stir overnight at 50 °C. When the reaction was complete (TLC), solution was cooled to room temperature, and diluted with EtOAc (300 mL), this was washed with water (5 x 100 ml), dried over magnesium sulfate and the solvent removed *in vacuo*. The residue was purified by column chromatography (hexane/EtOAc, 1:1) to give an orange solid (4.22g, 82%).

m.p: 108 °C (dec.).

δ_H (400 MHz, $CDCl_3$): 1.36 (s, 9H, *t*-butyl), 6.68 (s, 1H, H-3), 7.56 (d, 1H, J 7.0, H-6'), 7.66 (t, 1H, J 7.7, H-4'), 7.76 (t, 1H, J 7.2, H-5'), 8.19 (d, 1H, J 5.4, H-7), 8.26 (d, 1H, J 8.0, H-3'), 8.56 (d, 1H, J 5.4, H-6), 8.96 (s, 1H, H-4)

δ_c (100 MHz, $CDCl_3$): 27.5, 85.1 (q), 108.3, 110.8, 124.6, 125.5 (q), 129.7, 129.7 (q), 132.5, 133.4, 136.8 (q), 141.1 (q), 143.4, 144.4, 148.0 (q), 149.1 (q) ppm.

HRMS (ESI): $[C_{18}H_{17}N_3O_4 + H]^+$ requires 340.1297, found 340.1299, also 284.0618 (loss of *t*-butyl, 284.0671) and 240.0768 (loss of carbamate, 240.0773).

IR (ν_{max}): 3374, 2984, 1736, 1523, 1356, 1345, 1318, 1227, 1125, 925, 851, 824, 744 cm^{-1}.

2-(2'-Nitrophenyl)-5-azaindole (88)

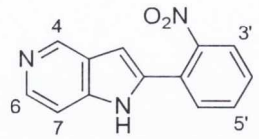

Via base catalysed cyclisation with sodium hydride:

In a 50 mL two-necked round bottom flask, fitted with stirring bar and condenser, under an atmosphere of N_2, alkyne **89** (0.510 g, 1.50 mmol) was dissolved in anhydrous DMF (20 mL). To this solution NaH (0.067 g, 2.79 mmol) was added and the mixture allowed to stir for 1 h at 80 °C. When the reaction was complete (TLC), the solution was cooled to room temperature, and EtOAc (50 mL) added, this was washed with water (5 x 50 mL), dried ($MgSO_4$) and the solvent removed *in vacuo*. The residue was purified by column chromatography (CH_2Cl_2) to give an orange solid (0.252 g, 70%).

Via deprotection of boc group with trifluoroacetic acid:

In a 100 mL round bottom flask, fitted with a stirring bar, azaindole **115** (4.22 g, 12.4 mmol) was dissolved in CH_2Cl_2 (50 mL), to this solution was added dropwise TFA (12 mL). The solution was stirred at RT overnight. The solution was diluted with EtOAc (200 mL) and was washed with saturated sodium carbonate solution (100 mL) and the layers separated. The aqueous layer was extracted twice more with EtOAc (2 x 50 mL). The combined organic extracts were dried over magnesium sulfate and the solvent removed *in vacuo*. The product was purified by column chromatography (EtOAc, 1% TEA) and after the solvent was removed, an orange solid was obtained (2.87 g, 96%).

m.p:	228-229 °C.
δ_H (400 MHz, DMSO):	6.70 (s, 1H, H-3), 7.39 (d, 1 H, J 5.5, H-7), 7.70 (m, 1H, H-4'), 7.76 (m, 2H, H-5'/H-6'), 8.08 (d, 1H, J 8.5, H-3'), 8.22 (d, 1H, J 5.5, H-6), 8.87 (s, 1H, H-4), 11.98 (s, 1H, H-1) ppm.
δ_c (100 MHz, $CDCl_3$):	100.7, 106.8, 124.3, 125.1 (q), 125.9 (q), 129.8, 131.8, 133.0, 134.1 (q), 140.1 (q), 140.8, 143.5, 148.4 (q) ppm.
HRMS (ESI):	$[C_{13}H_{10}N_3O_2 + H]^+$ requires 240.0773, found 240.0777.
IR (ν_{max}):	2668, 1611, 1524, 1364, 1283, 1029, 928, 854, 804, 776, 744 cm^{-1}.

3-Nitro-2-picoline (121)

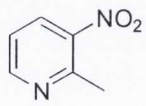

In a 250 mL 3-necked round bottom flask, fitted with a stirring bar and dropping funnel, under an atmosphere of N_2, NaH (3.81 g, 159 mmol) was added to anhydrous DMF (30 mL) at 0 °C. To the resulting mixture was added diethyl malonate (23.8 mL, 139 mmol) dropwise at 0 °C. 2-Chloro-3-nitropyridine (10.02 g, 63.2 mmol) was dissolved in anhydrous DMF (20 mL) and the solution added to the dropping funnel *via* syringe, and added dropwise to the reaction mixture with stirring at 0 °C over 20 min. When the addition was complete, the mixture was left stirring for 3 h at RT. Water (40 mL) was added slowly to the reaction mixture and extracted with CH_2Cl_2 (3 x 100 mL). The solvent was removed *in vacuo* and the residue was dissolved in HCl solution (6 M, 210 mL). The resulting light brown solution was added to a 500 mL round bottom flask fitted with a reflux condenser and heated under reflux for 8 h. When the reaction was complete (TLC), the solution was cooled to RT and carefully neutralised with solid NaOH, and the product extracted with CH_2Cl_2 (3 x 100 mL), the organic extracts were combined and dried ($MgSO_4$) and the solvent removed *in vacuo*. The residue was purified by column chromatography (hexane/EtOAc, 3:1) to give a yellow, crystalline solid (4.36 g, 50%). ^{1}H NMR spectral analysis consistent with previously published spectroscopic data.[130]

m.p: 35-36 °C.

δ_H (400 MHz, $CDCl_3$): 2.89 (s, 3H, CH_3), 7.38 (dd, 1H, J 8.0, 4.8, H-5), 8.30 (dd, 1H, J 8.0, 1.5, H-4), 8.74 (dd, 1H, J 4.8, 1.5, H-6) ppm.

2-(2'-Nitrophenyl)indole (126)

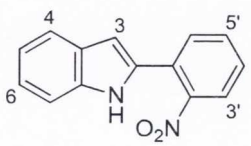

In a 50 mL RBF nitroacetophenone **91** (8.43 g, 51.1 mmol) was dissolved in EtOH (16 mL), and phenylhydrazine (7.0 mL, 71 mmol) and acetic acid (1.0 mL) were added, this solution was heated under reflux for 6 h. The resulting dark red solution was cooled

overnight in the freezer, a brown-red solid is expected to have crystallized, if not the solution was poured into ice-water and stirred until the red oil solidified, the solid hydrazone (**127**) was then collected by filtration and washed with diethyl ether, it was used without further purification in the next step.

Hydrazone **127** (5.16 g, 20.2 mmol) was ground to a fine powder and suspended in polyphosphoric acid (50 g) warmed to 80 °C with stirring. The temperature was increased gradually to 100 °C, while the temperature of the suspension was monitored. The mixture was allowed to stir at this temperature for 1 h. Water (200 mL) was added to the still warm mixture and stirred for a further 1 h. The warm suspension was filtered, and the collected black solid was extracted with hot chloroform (3 x 100 mL). The extracts were combined, washed with saturated sodium carbonate solution, dried over magnesium sulfate and solvent removed under reduced pressure. The residue was recrystallized from EtOH to obtain a red-brown crystalline solid (1.68 g, 35 %).

m.p: 140-142 °C (lit.,[131] 140-141 °C).

δ_H (400 MHz, $CDCl_3$): 6.75 (s, 1H, H-3), 7.18 (t, 1H, J 7.5, H-5), 7.28 (t, 1H, J 7.3, H-6), 7.44 (d, 1H, J 8.1, H-7), 7.52 (d, 1H, J 7.7, H-6'), 7.66-7.72 (m, 3H, H-4/4'/5'), 7.84 (d, 1H, J 8.1, H-3'), 8.52 (s, 1H, H-1) ppm.

_N_-(4-Pyridyl)-2-nitrophenyl hydrazone (130)

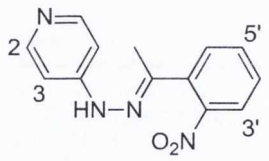

In a 10 mL round bottom flask, **90·2HCl** (0.74 g, 4.06 mmol) was dissolved in a mixture of water (2 mL) and EtOH (1 mL), to this solution was added nitroacetophenone **91** (0.68 g, 4.11). The resulting suspension was stirred at RT for 4 h.

The reaction was neutralised with 1 M NaOH solution, and then extracted with 9:1 CH_2Cl_2/MeOH (4 x 20 mL), the organic extracts were combined and dried ($MgSO_4$) and the solvent removed *in vacuo*. The residue was purified by column chromatography (95:5 EtOAc/MeOH, 1% TEA), to give a bright yellow solid (0.77 g, 74%).

m.p:	152-154 °C.
δ_H (400 MHz, DMSO):	2.29 (s, 3H, CH_3), 6.96 (d, 2 H, J 4.8, H-3), 7.58 (m, 1H, H-4'), 7.72 (m, 2H, H-5'/H-6'), 7.87 (d, 1H, J 7.8, H-3'), 8.22 (d, 2 H, J 4.8, H-2) ppm.
δ_c (100 MHz, $CDCl_3$):	16.1, 107.9, 124.3, 129.5, 129.9, 132.8, 133.8 (q), 141.9 (q), 148.9 (q), 150.4, 151.3 (q) ppm.
HRMS (ESI):	$[C_{13}H_{12}N_4O_2 + H]^+$ requires 257.1039, found 257.1031.
IR (ν_{max}):	2889, 1589, 1522, 1357, 1209, 1134, 1089, 992, 816, 748 cm^{-1}.

Attempted synthesis of 2-(2'-Nitrophenyl)-5-azaindole (88), *via* a thermally induced Fischer indole synthesis

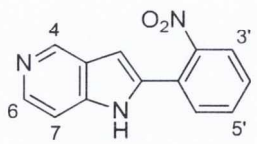

Hydrazone **130** (0.102 g, 0.40 mmol) was dissolved in diphenylether (1.0 mL), and under an atmosphere of argon the resulting solution was heated under reflux using a Kugelrohr apparatus (T = 300 °C). The reaction mixture was examined after 2 h by ^1H NMR spectroscopy, and when mostly starting material was observed the heating was continued for an additional 4 h. After this time the diphenylether was removed at reduced pressure, the starting material was consumed but the desired product could not be identified in the black residue remaining.

Attempted synthesis of 4-(Cyclohexylimino)-3-iodopyridine (132)

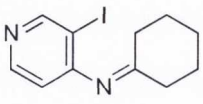

4-Amino-3-iodopyridine (**99**) (1.00g, 4.55 mmol) was dissolved in freshly distilled toluene (9.2 mL), molecular sieves (4 Å) were added. To this solution was added PTSA (0.951 g, 5.00 mmol), followed by cyclohexanone (0.95 mL, 9.10 mmol). The resulting suspension was heated under reflux overnight. The reaction mixture was examined by ^{1}H NMR spectroscopy, but no reaction was found to have occurred and both starting materials remained.

2-(2'-Nitrophenyl)-5-azaindole gramine (87)

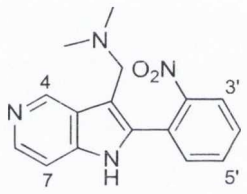

In a 10 mL two-necked round bottom flask, fitted with stirring bar and condenser, under an atmosphere of N_2, azaindole **88** (0.051 g, 0.21 mmol) was dissolved in freshly distilled MeCN (1.0 mL). To this solution Eschenmoser's salt (0.047 g, 0.26 mmol) was added, it was heated under reflux overnight. The solution was cooled to room temperature, and was then partitioned between CH_2Cl_2/EtOH (9:1, 10 mL) and saturated sodium carbonate solution. The layers were separated and the aqueous layer was extracted with CH_2Cl_2/EtOH (9:1, 3 x 10 mL). The organic extracts were combined and dried ($MgSO_4$) and the solvent removed *in vacuo*. The resulting yellow residue was recrystallised from chloroform to give a yellow solid (0.045 g, 72%).

m.p: 148-150 °C.

δ_H (400 MHz, DMSO): 2.06 (s, 6H, CH_3), 3.47 (s, 2H, CH_2), 7.34 (d, 1H, J 5.5, H-7), 7.76 (m, 2H, H-4'/H-6'), 7.87 (dt, 1H, J 1.1, 7.4, H-

5'), 8.20 (m, 2 H, H-6/H-3'), 8.99 (s, 1H, H-4), 11.79 (s, 1H, H-1) ppm.

δ_c (100 MHz, $CDCl_3$): 45.2 (CH_3), 53.6 (CH_2), 106.9, 110.7 (q), 125.2, 126.9 (q), 130.7, 133.4 (q), 133.8, 134.0, 139.8 (q), 141.1, 143.3, 149.3 (q) ppm.

HRMS (ESI): $[C_{16}H_{16}N_4O_2 + H]^+$ requires 297.1352, found 297.1356.

IR (ν_{max}): 2856, 2814, 2765, 1611, 1524, 1457, 1343, 1169, 1094, 1026, 854, 784, 748 cm^{-1}.

Attempted synthesis of *N*-boc-2-(2'-nitrophenyl)-5-azaindole gramine (134)

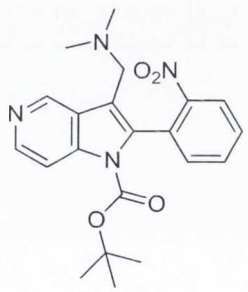

In a 10 mL oven-dried RBF, fitted with a stirring bar and condenser, alkyne **89** (0.095 g, 0.28 mmol) was dissolved in anhydrous DMF (3.0 mL), and placed under an atmosphere of N_2. To this solution was added sodium hydride (0.010 g, 0.42 mmol), followed by Eschenmoser's salt (0.160 g, 0.86 mmol). The reaction was heated at 80 °C and the progress was monitored by TLC, but no change was observed. In addition, the reaction mixture was examined by ^1H NMR spectroscopy, no reaction occurred with the starting material recovered having lost some of the protecting group.

5-Nitroindole gramine (135)

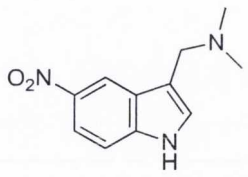

In a 50 mL RBF, fitted with stirring bar, 5-nitroindole (0.503 g, 3.10 mmol) was dissolved in freshly distilled MeCN (10 mL), Eschenmoser's salt (0.692 g, 3.74 mmol) was added. The resulting mixture was heated under reflux for 16 h under an atmosphere of argon. Solvent was removed *in vacuo*, the residue was dissolved in CH_2Cl_2/EtOH (60 mL, 9:1) and washed with saturated sodium carbonate solution, the layers were separated and the aqueous layer extracted twice more, the combined organic extracts was dried ($MgSO_4$), filtered and the solvent removed *in vacuo*. The resulting residue was purified by column chromatography (CH_2Cl_2/MeOH, 9:1) to obtain a yellow powder (0.62 g, 91%).

m.p: 165-166 °C (lit.[132] 169-170 °C).

δ_H (400 MHz, $CDCl_3$): 2.32 (s, 6H, CH_3), 3.67 (s, 2H, CH_2), 7.31 (s, 1H, H-2), 7.41 (d, 1H, J 8.9, H-7), 8.14 (dd, 1H, J 2.0, 8.9, H-6), 8.61 (br s, 1H, H-1), 8.72 (d, 1H, J 2.0, H-4) ppm.

5-Nitroindole-3-acetonitrile (138)

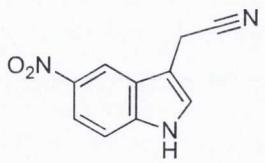

In a 10 mL RBF, fitted with stirring bar, **135** (0.202 g, 0.92 mmol) was dissolved in EtOH (5.0 mL), iodomethane (0.23 mL, 3.66 mmol) was added. The resulting solution was stirred at RT for 4 h. Water (5 mL) was added followed by potassium cyanide (0.478 g, 7.37 mmol) and the suspension heated at 40 °C overnight. The mixture was

extracted with CH_2Cl_2 (50 mL), which was washed with dilute sodium thiosulfate solution then water. The organic extract was dried ($MgSO_4$), filtered and the solvent removed *in vacuo*. The resulting residue was purified by column chromatography (EtOAc) to obtain a yellow powder (0.12 g, 69%).

m.p: 184-186 °C (lit.,[133] 180-182 °C).

δ_H (400 MHz, DMSO): 4.21 (s, 2H, CH_2), 7.59 (d, 1H, J 8.9, H-7), 7.65 (s, 1H, H-2), 8.05 (dd, 1H, J 2.1, 8.9, H-6), 8.67 (d, 1H, J 2.1, H-4), 11.88 (s, 1H, H-1) ppm.

_N_-Acetyl-5-nitroindole-3-methylacetate (140)

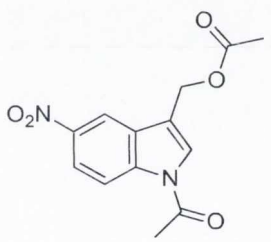

In a 50 mL RBF, fitted with stirring bar, **135** (1.54 g, 7.02 mmol) and sodium acetate (1.18 g, 14.5 mmol) were dissolved in freshly distilled acetic anhydride (14 mL). The resulting suspension was heated under reflux and an atmosphere of argon for 4 h. The cooled reaction was poured into saturated sodium bicarbonate solution (50 mL) which was extracted with CH_2Cl_2 (3 x 50 mL). The organic extracts were dried ($MgSO_4$), filtered and the solvent removed *in vacuo*. The resulting residue was purified by recrystallisation (chloroform) to obtain a white crystalline solid (1.62, 84%).

m.p: 177-179 °C

δ_H (400 MHz, $CDCl_3$): 2.14 (s, 3H, CH_3), 2.72 (s, 3H, CH_3), 5.32 (s, 2H, CH_2), 7.68 (s, 1H, H-2), 8.30 (dd, 1H, J 2.3, 9.1, H-6), 8.58 (d, 1H, J 2.3, H-4), 8.61 (d, 1H, J 9.1, H-7) ppm.

δ_c (100 MHz, $CDCl_3$):	20.5 (CH_3), 23.5 (CH_3), 56.7 (CH_2), 115.1, 116.6, 117.5 (q), 120.5, 127.4, 128.8 (q), 138.4 (q), 143.9 (q), 168.1 (q), 170.4 (q) ppm.
HRMS (ESI+):	$[C_{13}H_{12}N_2O_5 + Na]^+$ requires 299.0644, found 299.0635.
IR (ν_{max}):	3097, 1736, 1712, 1514, 1451, 1385, 1330, 1214, 1113, 1003, 912, 829, 740 cm^{-1}.

Attempted synthesis of 2-(2'-Nitrophenyl)-5-azaindole aldehyde (141)

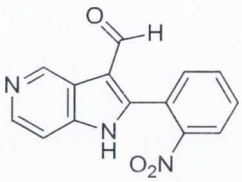

In a 5 mL RBF, fitted with a stirring bar and condenser, azaindole gramine **87** (0.057 g, 0.19 mmol) was dissolved in AcOH (0.38 mL), the solution was then heated to reflux. HMTA (0.029 g, 0.19 mmol) was then added, and the resulting suspension heated under reflux for 10 min. After this time an additional equivalent of HMTA was added and continued heating for another 10 min. The reaction mixture was then cooled, and neutralized with saturated sodium carbonate solution, and extracted with CH_2Cl_2/EtOH (9:1, 2 x 10 mL). The organic extracts were combined and dried ($MgSO_4$) and the solvent removed *in vacuo*. The yellow oil thus obtained was not identified as product.

Attempted synthesis of 5-azaindolo[3,2-d][1]benzazepine-6,7-dione (150)

In a 5 mL oven-dried RBF, fitted with a stirring bar, azaindole **149** (0.050 g, 0.24 mmol) was dissolved in freshly distilled THF (1.0 mL), and placed under an atmosphere of argon. To this solution was added oxalyl chloride (0.020 mL, 0.24 mmol) dropwise and the reaction allowed to stir at RT overnight. The reaction mixture was poured onto an ice and saturated sodium carbonate mixture, the resulting grey solid was collected by filtration and dried. The solid was examined by ^{1}H NMR spectroscopy but no sign of acylation of C-3 was observed.

Ethyl-2-(2-(2'-nitrophenyl)-5-azaindol-3-yl)-2-(1,3-dithiolan-2-yl)acetate (151)

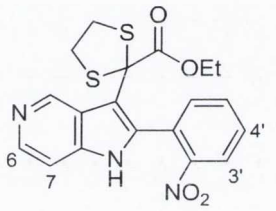

In a 100 mL RBF with a drying tube ($CaCl_2$) attached, aluminium chloride (1.39 g, 10.45 mmol) was dissolved in CH_2Cl_2 (22.5 mL) and $MeNO_2$ (2.5 mL). To this solution was added azaindole **88** (0.505 g, 2.09 mmol) and the dark-red solution was allowed to stir for 1 h. Ethyl chloro(oxo)acetate **148** (0.47 mL, 4.2 mmol) was added dropwise *via* syringe. After 2 h stirring 5 equiv. each of $AlCl_3$ and **148** were added, these additions were repeated after a further 2 h. When the reaction had stirred for 2 h after the final additions, the reaction was quenched with EtOH (20 mL) and allowed to stir overnight. The reaction mixture was diluted with CH_2Cl_2 (150 mL), and water (150 mL) was added, saturated sodium bicarbonate was added gradually until neutralisation was complete. The layers were separated and the aqueous layer was extracted with CH_2Cl_2 (2 x 150 mL). The combined organic extracts were dried ($MgSO_4$), filtered and solvent removed at reduced pressure. This crude residue was found to be a mixture of ketal and desired ketone, and it was transformed directly into dithiolane **151**. The crude residue was dissolved in TFA (0.25 M), 1,2-ethanedithiol (1.5 equiv.) and EtOH (1 mL) were added. The reaction was heated at 60 °C for 1 d. The solvents were removed *in vacuo* and the residue taken up in CH_2Cl_2, which was then washed with saturated sodium carbonate solution. The layers were separated and the organic layer was dried ($MgSO_4$), filtered and solvent removed at reduced pressure. The crude solid was recrystallised

from EtOH to give a yellow solid. The combined isolated yield from several identical reactions totalling 2.66 g of starting material (11.12 mmol) was 2.91 g of product (63%).

m.p: 150 °C (dec.).

δ_H (400 MHz, $CDCl_3$): 1.11 (t, 3H, J 8.0, CH_3), 3.40 (m, 4H, CH_2), 3.88 (m, 2H, CH_2), 7.32 (d, 1H, J 5.7, H-7), 7.61-7.71 (m, 3H, H-4'/H-5'/H-6'), 8.13 (d, 1H, J 7.8, H-3'), 9.23 (s, 1H, H-4), 10.45 (br s, 1H, H-1) ppm.

δ_c (100 MHz, $CDCl_3$): 13.6 (CH_3), 40.6 (CH_2), 62.7 (CH_2), 67.3 (q), 106.7, 111.7 (q), 123.9 (q), 124.6, 127.2 (q), 130.6, 132.6 (q), 132.7, 134.0, 140.1, 140.2 (q), 143.3, 149.1 (q), 170.2 (q) ppm.

HRMS (ESI): $[C_{19}H_{17}N_3O_4S_2 + H]^+$ requires 416.0739, found 416.0741.

IR (ν_{max}): 2976, 2736, 1732, 1613, 1529, 1464, 1346, 1202, 1049, 1027, 807, 793 cm^{-1}.

Attempted synthesis of ethyl-2-(2-(2'-nitrophenyl)-5-azaindol-3-yl)acetate (146)

In a 5 mL RBF, fitted with a stirring bar, oxalylate ester **145** (0.102 g, 0.30 mmol) was dissolved in freshly distilled dioxane (0.78 mL). To this suspension was added Pd/C (0.022 g, 10% w/w), followed by $NaH_2PO_2.xH_2O$ solution (0.136 g in water (0.2 mL), 1.56 mmol) and the reaction mixture was heated under reflux for 4 h. An additional identical quantity of $NaH_2PO_2.xH_2O$ solution was added and heating was continued for a further 2 h. The solvents were removed *in vacuo* and the residue taken up in

CH_2Cl_2/EtOH (9:1, 20 mL), which was then washed with saturated sodium bicarbonate solution. The layers were separated and the organic layer was dried ($MgSO_4$), filtered and solvent removed at reduced pressure. The crude residue was examined by ^1H NMR spectroscopy, but an intractable mixture was observed.

Attempted reduction of dithiolane 151 *via* iron in acetic acid

In a 5 mL RBF, fitted with a stirring bar and condenser, dithiolane **151** (0.053 g, 0.13 mmol) was dissolved in acetic acid (1.30 mL), to this solution was added iron powder (0.036 g, 0.64 mmol). The suspension was then heated overnight at 40 °C. A dark coloured suspension was observed, the reaction mixture was poured onto ice and saturated sodium carbonate solution, at which point a dark green solution was obtained. The product could not be isolated by filtration in a similar manner to the corresponding indole. This reaction was abandoned in favour of reduction by RaNi, which didn't have the same isolation problems.

9-Azapaullone·TFA (82·TFA)

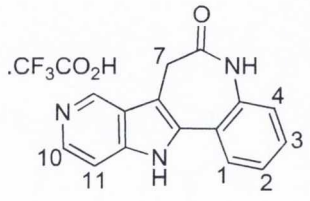

Dithiolane **151** (0.598 g, 1.44 mmol) was dissolved in dioxane (60 mL) and Raney nickel (1 tsp, wet) was added. This suspension was shaken on a Parr hydrogenator under an atmosphere of hydrogen (3 atm.) for 2 d. The reaction was then filtered through celite to remove the nickel, and the solvent was concentrated to approximately a third of its volume. To this solution was added AcOH (0.17 mL), and was then heated at 80 °C for 2 d. The solvent was removed at reduced pressure. Saturated sodium

carbonate was added to the residue and the resulting white precipitate was collected by filtration and dried. The crude solid was protonated with dilute TFA and purified by reverse-phase MPLC (gradient of MeCN, 7 to 60% in water). A combined isolated yield from several identical reactions totalling 2.91 g (6.99 mmol) was 0.43 g (17%).

m.p: >280 °C.

δ_H (400 MHz, DMSO): 3.78 (s, 2H, CH_2), 7.36 (m, 2H, H-4/H-2), 7.53 (t, 1H, J 7.6, H-3), 7.84 (d, 1H, J 7.4, H-1), 7.93 (d, 1H, J 6.0, H-11), 8.45 (d, 1H, J 6.0, H-10), 9.51 (s, 1H, H-8), 10.34 (s, 1H, H-5) 13.37 (s, 1H, H-12) ppm.

δ_c (100 MHz, $CDCl_3$): 31.1 (CH_2), 108.9, 109.2 (q), 120.5 (q), 122.6, 123.3 (q), 123.9, 127.5, 130.1, 132.1, 135.2, 136.5 (q), 138.5 (q), 142.8 (q), 171.1 (q) ppm.

HRMS (ESI): $[C_{15}H_{12}N_3O]^+$ requires 259.0980, found 250.0973.

IR (ν_{max}): 3078, 2785, 2086, 1664, 1485, 1421, 1204, 1183, 1124, 841, 815, 771 cm^{-1}.

Ethyl-2-(2-(2'-nitrophenyl)indolyl)-2-(1,3-dithiolane)acetate (153)

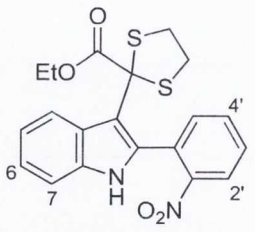

In a 3-necked RBF, oxalyl chloride (1.28 mL, 15.1 mmol) was added to dry Et_2O (16 mL) under an atmosphere of argon, the solution was cooled to 0 °C and indole **126** (1.64 g, 5.87 mmol) was added. The resulting suspension was stirred at RT for 3.5 h. The solid was collected by filtration, and suspended in EtOH and allowed to stir

overnight at RT. The resulting solid was removed by filtration, washed with a mixture of EtOH and Et_2O yielding 1.89 g of crude ethyl oxalate, **147** which was used without further purification.

The ethyl oxalate was suspended in EtOH (85 mL), which was then saturated with HCl gas and 1,2-ethanedithiol (0.59 mL, 7.04 mmol) was added. The solution was heated overnight at 60 °C and under an argon atmosphere. The orange solid was filtered off and used without further purification (1.84 g, 78 %).

m.p:	228-230 °C.
δ_H (400 MHz, DMSO)	0.98 (t, 3H, J 7.1, CH_3), 3.30 (m, 4H, SCH_2) 3.74 (m, 2H, $C\underline{H_2}CH_3$), 7.06 (t, 1H, J 7.5, H-5), 7.16 (t, 1H, J 7.5, H-6), 7.33 (d, 1H, J 8.0, H-7), 7.57 (d, 1H, J 7.3, H-5′), 7.75 (m, 2H, H-4 and H-3′), 7.82 (t, 1 H, J 7.4, H-4′), 8.21 (d, 1 H, J 8.0, H-2′), 11.51 (s, 1 H, H-1) ppm.
δ_c (100 MHz, DMSO)	13.4 (CH_3), 39.7 (CH_2), 61.6 (CH_2), 67.7 (q), 108.7 (q), 111.3, 118.9, 120.2, 121.3, 124.4, 126.5 (q), 128.2 (q), 130.4, 131.4 (q), 132.9, 133.7, 135.7 (q), 148.5 (q), 170.0 (q) ppm.
HRMS (ESI):	$[C_{20}H_{18}N_2O_4 + Na]^+$ requires 437.0613, found 437.0606.
IR (ν_{max}):	3305, 2929, 1701, 1528, 1455, 1353, 1224, 1012, 785, 743, 697 cm^{-1}.

Paullone (25)

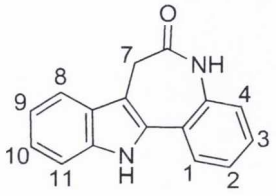

Dithiolane **153** (0.580 g, 1.40 mmol) was dissolved in dioxane (58 mL), Raney nickel was added and the suspension was shaken on a Parr hydrogenator under an atmosphere of hydrogen (3 atm.) for 24 h. until it was observed that both the dithiolane ring and nitro group has been reduced by ^{1}H NMR. The nickel was removed by filtration through celite, the filtrate was concentrated to approximately 10 mL in volume. Acetic acid (1.60 mL, 28.0 mmol) was added and the solution heated at 60 °C for 2 d. The solvent was removed under reduced pressure. The resulting residue was triturated with EtOAc/hexane (1:1) and an off-white solid was collected by filtration (0.189 g, 54%).

m.p: > 300 °C (lit.[95] > 280 °C).

δ_H (400 MHz, DMSO): 3.51 (s, 2H, H-7), 7.08 (t, 1H, J 7.5, H-9), 7.18 (t, 1H, J 7.5, H-10), 7.28 (m, 2H, H-2/H-4), 7.38 (t, 1H, J 7.4, H-3), 7.44 (d, 1H, J 8.4, H-11), 7.66 (d, 1H, J 7.9, H-8), 7.76 (d, 1H, J 7.7, H-1), 10.08 (s, 1H, H-5), 11.57 (s, 1H, H-12) ppm.

δ_c (100 MHz, DMSO): 31.6 (CH_2), 107.5 (q), 111.4, 117.9, 119.1, 122.1, 122.2, 122.8 (q), 123.6, 126.5 (q), 126.8, 127.9, 132.4 (q), 135.4 (q), 137.4 (q), 171.6 (q) ppm.

Oxidations with Oxone

In a RBF, with a stirring bar, DMAP or 5-azaindole (1 equiv.) was dissolved in water (1 M), solid potassium hydroxide (10 equiv.) was added. Oxone (2 equiv.) was added in portions over 30 mins, and the reaction allowed to stir overnight at RT. The water was evaporated at reduced pressure and the solid residue was extracted with hot chloroform, the extracts cooled and dried over magnesium sulphate, and solvent removed at reduced pressure to obtain the crude product.

Oxidations with benzonitrile and hydrogen peroxide

In a RBF, with stirring bar, DMAP (1 equiv.) was dissolved in methanol (0.2 M), to this solution was added benzonitrile (1.5 equiv.), sodium hydrogen carbonate (0.6 equiv.) followed by hydrogen peroxide solution (35%, 1.8 equiv.) drop-wise over 6 h. The reaction was then stirred overnight at RT, and conversion checked by ^{1}H NMR, additional quantities of benzonitrile and hydrogen peroxide were added as necessary. The completed reaction was diluted with water and the concentrated at reduced pressure, it was cooled at 0 °C and the precipitated white solid was removed by filtration. The water was evaporated from the collected filtrate at reduced pressure. The solid residue was extracted with hot chloroform, the extracts cooled and dried over magnesium sulphate, and solvent removed at reduced pressure to obtain the crude product.

9-Azapaullone *N*-oxide (83)

In a 10 mL RBF, fitted with stirring bar, **82·TFA** (0.020 g, 0.06 mmol) was dissolved in DMF (2.0 mL) and water (1.3 mL), followed by solid sodium carbonate (0.029 g, 0.28 mmol) and then mCPBA (0.020 g, 0.12 mmol). The reaction was stirred at RT for 4 h, at which point additional mCPBA (0.020 g) was added and stirring was continued overnight. The precipitated solid was filtered from the reaction mixture, washed with water then MeOH and air dried. The collected solid was purified by reverse phase MPLC (water/MeCN, 90:10) to obtain the desired product as a white solid (3 mg, 19%).

δ_H (400 MHz, DMSO): 3.56 (s, 2H, H-7), 7.29 (m, 2H, H-2/H-4), 7.44 (m, 2H, H-3/H-11), 7.75 (d, 1H, J 6.6, H-1), 7.94 (d, 1H, J 6.9, H-10), 8.81 (s, 1H, H-8), 10.18 (s, 1H, H-5) 12.1 (br s, 1H, H-12) ppm.

δ_c (100 MHz, DMSO): 31.4, 109.3, 122.6, 123.9, 127.4, 129.4, 129.4, 133.4 171.3 (q) ppm.

HRMS (ESI): $[C_{15}H_{12}N_3O_2 + H]^+$ requires 266.0930, found 266.0938.

IR (ν_{max}): 3199, 2979, 1662, 1578, 1423, 1375, 1183, 1109, 986 cm^{-1}.

9-Azapaullone-*N*-benzyl (84)

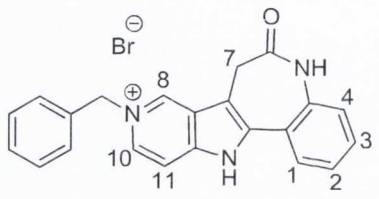

In a 10 mL RBF, fitted with stirring bar, **82·TFA** (0.020 g, 0.06 mmol) was suspended in MeCN (0.5 mL), tetraethylammonium hydroxide solution (25% w/v, 18 μL) was added and the reaction was stirred for 30 mins at RT. Benzyl bromide was added (14 μL, 0.11 mmol), and the reaction mixture heated at 80 °C for 24 h. The solid was filtered from the reaction mixture, washed with MeCN and air dried. The collected solid was purified by reverse phase MPLC (water/MeCN, 90:10) to obtain the desired product as a white solid (5 mg, 26%).

δ_H (400 MHz, DMSO): 3.76 (s, 2H, H-7), 5.83 (s, 2H, CH_2), 7.34-7.54 (m, 8H), 7.84 (d, 1H, H-1), 7.99 (d, 1H, H-11), 8.60 (d, 1H, H-10), 9.84 (s, 1H, H-8), 10.36 (s, 1H, H-5), 13.51 (s, 1H, H-12) ppm.

δ_c (100 MHz, DMSO): 31.7 (CH_2), 62.9 (CH_2), 109.4 (q), 110.4, 122.7 (q), 123.1, 124.5, 128.1, 128.6, 129.4, 129.6, 130.8, 135.3, 135.4 (q), 136.6 (q), 138.3, 139.4 (q), 142.0 (q), 171.3 (q) ppm.

HRMS (ESI): $[C_{22}H_{18}N_3O]^+$ requires 340.1450, found 340.1441.

IR (ν_{max}): 3027, 1661, 1487, 1385, 1159, 1031 cm^{-1}.

References

1 Data is taken from *WHO factsheet on cancer*, 2009, URL: http://www.who.int/mediacentre/factsheets/fs297/en/index.html (accessed 30/8/2010).

2 D. Hanahan and R. A. Weinberg, *Cell*, 2000, **100**, 57-70.

3 Y. Lazebnik, *Nature Rev. Cancer*, 2010, **10**, 232-233.

4 B. Pulverer, *Nature Milestones in Cancer: Milestone 20*, 2006, (editorial and references contained within); URL: http://www.nature.com/milestones/milecancer/full/milecancer20.html (accessed 30/8/2010).

5 G. I. Evan and K. H. Vousden, *Nature*, 2001, **411**, 342-348.

6 Y. P. Chen, S. K. Sharma, T. M. Ramsey, L. Jiang, M. S. Martin, K. Baker, P. D. Adams, K. W. Bair and W. G. Kaelin, Jr., *Proc. Natl. Acad. Sci. USA*, 1999, **96**, 4325-4329.

7 J. Taipale and P. A. Beachy, *Nature*, 2001, **411**, 349-354.

8 M. van de Wetering, E. Sancho, C. Verweij, W. de Lau, I. Oving, A. Hurlstone, K. van der Horn, E. Batlle, D. Coudreuse, A. Haramis, M. Tjon-Pon-Fong, P. Moerer, M. van den Born, G. Soete, S. Pals, M. Eilers, R. Medema, H. Clevers, *Cell*, 2002, **111**, 241–250.

9 Nature Publishing Group, W. C. Hahn and R. A. Weinberg, *A subway map of cancer pathways*, 2002, URL: http://www.nature.com/nrc/posters/subpathways/index.html (accessed 30/8/2010).

10 A. B. Pardee, *Proc. Natl. Acad. Sci. USA,* 1974, **71**, 1286-1290.

11 W. R. Sellers and W. G. Kaelin, *J. Clin. Oncol.*, 1997, **15**, 3301-3312.

12 A. S. Lundberg and R. A. Weinberg, *Mol. Cell. Biol.,* 1998, **18**, 753-761.

13 S. A. Ezhevsky, A. Ho, M. Becker-Hapak, P. K. Davis and S. F. Dowdy, *Mol. Cell. Biol.,* 2001, **21**, 4773-4784.

14 S. Lapenna and A. Giordano, *Nature Rev. Drug Dis.,* 2009, **8**, 547-566.

15 D. W. Meek, *Nature Rev. Cancer*, 2009, **9**, 714-723.

16 R. Boutros, V. Lobjois and B. Ducommun, *Nature Rev. Cancer,* 2007, **7**, 495-507.

17 M. Rouleau, A. Patel, M. J. Hendzel, S. H. Kaufmann and G. G. Poirier, *Nature Rev. Cancer*, 2010, 10, 293-301.

18 L. J. Holt, B. B. Tuch, J. Villén, A. D. Johnson, S. P. Gygi and D. O. Morgan, *Science*, 2009, **325**, 1682-1686.

19 J. M. Enserink and R. D. Kolodner, *Cell Division*, 2010, **5**, 11.

20 D. Santamaría, C. Barrière, A. Cerqueira, S. Hunt, C. Tardy, K. Newton, J. F. Cáceres, P. Dubus, M. Malumbres and M. Barbacid, *Nature*, 2007, **448**, 811-816.

21 E. Queralt and F. Uhlmann, *Curr. Opin. Cell Biol.*, 2008, **20,** 661-668.

22 S. Akoulitchev, S. Chuikov and D. Reinberg, *Nature*, 2000, **407**, 102-106

23 D. Salerno, M. G. Hasham, R. Marshall, J. Garriga, A. Y. Tsygankov and X. Graña, *Gene*, 2007, **405**, 65-78.

24 G. Paglini and A. Caceres, *Eur. J. Biochem.*, 2001, **268**, 1528-1533.

25 R. Dhavan and L.-H. Tsai, *Nature Rev. Mol. Cell Biol.*, 2001, **2**, 749-759.

26 E. Iorns, N. C. Turner, R. Elliott, N. Syed, O. Garrone, M. Gasco, A. N. J. Tutt, T. Crook, C. J. Lord and A. Ashworth, *Cancer Cell,* 2008, **13**, 91-104.

27 A. Chandramouli, J. Shi, Y. Feng, H. Holubec, R. M. Shanas, A. K. Bhattacharyya, W. Zheng and M. A. Nelson, *Carcinogenesis*, 2007, **28**, 2028-2035.

28 J. Massagué, *Nature*, 2004, **432**, 298-306.

29 G. He, Z. H. Siddik, Z. Huang, R. Wang, J. Koomen, R. Kobayashi, A. R. Khokhar and J. Kuang, *Oncogene*, 2005, **24,** 2929–2943.

30 E. A. Nigg, *Curr. Opin. Cell Biol.*, 1996, **8**, 312-317.

31 S. Larochelle, K. A. Merrick, M.-E. Terret, L. Wohlbold, N. M. Barboza, C. Zhang, K. M. Shokat, P. V. Jallepalli and R. P. Fisher, *Mol. Cell,* 2007, 25, 839–850.

32 M. Malumbres and M. Barbacid, *Nature Rev. Cancer*, 2001, **1**, 222-231.

33 S. Aggarwal, *Nature Rev. Cancer*, 2010, **9**, 427-428.

34 P. Cohen, *Nature Rev. Drug Dis.*, 2002, **1**, 309-315.

35 H. Zhang, A. Berezov, Q. Wang, G. Zhang, J. Drebin, R. Murali and M. I. Greene, *J. Clin. Invest.*, 2007, **117**, 2051–2058.

36 G. D. Demetri, M. von Mehren, C. D. Blanke, A. D. Van den Abbeele, B. Eisenberg, P. J. Roberts, M. C. Heinrich, D. A. Tuveson, S. Singer, M. Janicek, J. A. Fletcher, S. G. Silverman, S. L. Silberman, R. Capdeville, B. Kiese, B. Peng, S. Dimitrijevic, B. J. Druker, C. Corless, C. D. M. Fletcher and H. Joensuu, *N. Engl. J. Med.*, 2002, **347**, 472-480.

37 M. Malumbres and M. Barbacid, *Nature Rev. Cancer*, 2009, **9**, 153-166.

38 Q. Yu, Y. Geng and P. Sicinski, *Nature*, 2001, **411**, 1017-1021.

39 M. W. Landis, B. S. Pawlyk, T. Li, P. Sicinski and P. W. Hinds, *Cancer Cell,* 2006, **9**, 13-22.

40 P. L. Miliani de Marval, E. Macias, R. Rounbehler, P. Sicinski, H. Kiyokawa, D. G. Johnson, C. J. Conti and M. L. Rodriguez-Puebla, *Mol. Cell. Biol.*, 2004, **24**, 7538-7547.

41 J. Du, H. R. Widlund, M. A. Horstmann, S. Ramaswamy, K. Ross, W. E. Huber, E. K. Nishimura, T. R. Golub and D. E. Fisher, *Cancer Cell*, 2004, **6**, 565-576.

42 M. Malumbres and M. Barbacid, *Trends Biochem. Sci.,* 2005, **30**, 630-641.

43 A. M. Senderowicz, *Oncogene*, 2003, **22**, 6609–6620.

44 E. A. Sausville, *Curr. Top. Med. Chem.,* 2005, **5**, 1109-1117.

45 C. Benson, S. Kaye, P. Workman, M. Garrett, M. Walton and J. de Bono, *Br. J. Cancer*, 2005, **92**, 7– 12.

46 J. C. Byrd, T. S. Lin, J. T. Dalton, D. Wu, M. A. Phelps, B. Fischer, M. Moran, K. A. Blum, B. Rovin, M. Brooker-McEldowney, S. Broering, L. J. Schaaf, A. J. Johnson, D. M. Lucas, N. A. Heerema, G. Lozanski, D. C. Young, J. Suarez, A. D. Colevas and M. R. Grever, *Blood*, 2007, **109**, 399-404.

47 S. George, B. S. Kasimis, J. Cogswell, P. Schwarzenberger, G. I. Shapiro, P. Fidias and R. M. Bukowski, *Clin. Lung Cancer*, 2008, **9**, 160-165.

48 K. S. Joshi, M. J. Rathos, R. D. Joshi, M. Sivakumar, M. Mascarenhas, S. Kamble, B. Lal and S. Sharma, *Mol. Cancer Ther.*, 2007, **6**, 918–925.

49 K. S. Joshi, M. J. Rathos, P. Mahajan, V. Wagh, S. Shenoy, D. Bhatia, S. Chile, M. Sivakumar, A. Maier, H. Fiebig and S. Sharma, *Mol. Cancer Ther.,* 2007, **6**, 926–934.

50 C. Benson, J. White, J. De Bono, A. O'Donnell, F. Raynaud, C. Cruickshank, H. McGrath, M. Walton, P. Workman, S. Kaye, J. Cassidy, A. Gianella-Borradori, I. Judson, and C. Twelves, *Br. J. Cancer*, 2007, **96**, 29-37.

51 K. Bettayeb, N. Oumata, A. Echalier, Y. Ferandin, J. A. Endicott, H. Galons and L. Meijer, *Oncogene*, 2008, **27**, 5797–5807.

52 T. G. Davies, J. Bentley, C. E. Arris, F. T. Boyle, N. J. Curtin, J. A. Endicott, A. E. Gibson, B. T. Golding, R. J. Griffin, I. R. Hardcastle, P. Jewsbury, L. N. Johnson, V. Mesguiche, D. R. Newell, M. E.M. Noble, J. A. Tucker, L. Wang and H. J. Whitfield, *Nature Struct. Biol.,* 2002, **9**, 745–749.

53 M. Pennati, A. J. Campbell, M. Curto, M. Binda, Y. Cheng, L.Wang, N. Curtin, B. T. Golding, R. J. Griffin, I. R. Hardcastle, A. Henderson, N. Zaffaroni, and D. R. Newell, *Mol. Cancer Ther.,* 2005, **4**, 1328–1337.

54 E. Kodym, R. Kodym, A. E. Reisa, A. A. Habibb, M. D. Story and D. Saha, *Lung Cancer*, 2009, **66**, 37-47.

55 I. C. Choong, I. Serafimova, J. Fan, D. Stockett, E. Chan, S. Cheeti, Y. Lu, B. Fahr, P. Pham, M. R. Arkin, D. H. Walker and U. Hoch, *Bioorg. Med. Chem. Lett.,* 2008, **18**, 5763-5765.

56 J. Fan, B. Fahr, D. Stockett, E. Chan, S. Cheeti, I. Serafimova, Y. Lu, P. Pham, D. H. Walker, U. Hoch and I. C. Choong, *Bioorg. Med. Chem. Lett.,* 2008, **18**, 6236-6239.

57 M. S. Squires, R. E. Feltell, N. G. Wallis, E. J. Lewis, D. Smith, D. M. Cross, J. F. Lyons, and N. T. Thompson, *Mol. Cancer Ther.,* 2009, **8**, 324-332.

58 X. Chu, W. DePinto, D. Bartkovitz, S. So, B. T. Vu, K. Packman, C. Lukacs, Q. Ding, N. Jiang, K. Wang, P. Goelzer, X. Yin, M. A. Smith, B. X. Higgins, Y. Chen, Q. Xiang, J. Moliterni, G. Kaplan, B. Graves, A. Lovey and N. Fotouhi, *J. Med. Chem.*, 2006, **49**, 6549-6560.

59 P. L. Toogood, P. J. Harvey, J. T. Repine, D. J. Sheehan, S. N. VanderWel, H. Zhou, P. R. Keller, D. J. McNamara, D. Sherry, T. Zhu, J. Brodfuehrer, C. Choi, M. R. Barvian, and D. W. Fry, *J. Med. Chem.*, 2005, **48**, 2388-2406.

60 D. W. Fry, P. J. Harvey, P. R. Keller, W. L. Elliott, M. Meade, E. Trachet, M. Albassam, X. Zheng, W. R. Leopold, N. K. Pryer and P. L. Toogood, *Mol. Cancer Ther.,* 2004, **3**, 1427-1437.

61 S. Chen, L. Chen, N. T. Le, C. Zhao, A. Sidduri, J. Ping Lou, C. Michoud, L. Portland, N. Jackson, J. Liu, F. Konzelmann, F. Chi, C. Tovar, Q. Xiang, Y. Chen, Y. Wen and L. T. Vassilev, *Bioorg. Med. Chem. Lett.,* 2007, **17**, 2134-2138.

62 L. T. Vassilev, C. Tovar, S. Chen, D. Knezevic, X. Zhao, H. Sun, D. C. Heimbrook and L. Chen, *Proc. Natl. Acad. Sci. USA*, 2006, **103**, 10660-10665.

63 M. Malumbres and M. Barbacid, *Curr. Opin. Genet. Dev.,* 2007, **17**, 60-65.

64 A. Becker, S. Kohfeld, A. Lader, L. Preu, T. Pies, K. Wieking, Y. Ferandin, M. Knockaert, L. Meijer and C. Kunick, *Eur. J. Med. Chem.,* 2010, **45**, 335-342.

65 M. Knockaert, K. Wieking, S. Schmitt, M. Leost, K. M. Grant, J. C. Mottram, C. Kunick and L. Meijer, *J. Biol. Chem.*, 2002, **277**, 25493-25501.

66 K. Wieking, M. Knockaert, M. Leost, D. W. Zaharevitz, L. Meijer and C. Kunick, *Arch. Pharm.,* 2002, **7**, 311-317.

67 D. W. Zaharevitz, R. Gussio, M. Leost, A. M. Senderowicz, T. Lahusen, C. Kunick, L. Meijer and E. A. Sausville, *Cancer Res.*, 1999, **59**, 2566-2569.

68 M. Leost, C. Schultz, A. Link, Y. Wu, J. Biernat, E. Mandelkow, J. A. Bibb, G. L. Snyder, P. Greengard, D. W. Zaharevitz, R. Gussio, A. M. Senderowicz, E. A. Sausville, C. Kunick and L. Meijer, *Eur. J. Biochem.,* 2000, **267**, 5983-5994.

69 J. A. Diehl, M. Cheng, M. F. Roussel and C. J. Sherr, *Genes Dev.,* 1998, **12**, 3499-3511.

70 A. Klaus and W. Birchmeier, *Nature Rev. Cancer*, 2008, **8**, 387-398.

71 K. P. Hoeflich, J. Luo, E. A. Rubie, M. Tsao, O. Jin and J. R. Woodgett, *Nature*, 2000, **406**, 86-90.

72 F. Balkwill, *Nature Rev. Cancer*, 2009, **9**, 361-371.

73 L. Kockeritz, B. Doble, S. Patel and J. R. Woodgett, *Curr. Drug Targets*, 2006, **7**, 1377-1388.

74 T. Lahusen, A. De Siervi, C. Kunick and A. M. Senderowicz, *Mol. Carcinogenesis*, 2003, **36**, 183-194.

75 C. Schultz, A. Link, M. Leost, D. W. Zaharevitz, R. Gussio, E. A. Sausville, L. Meijer and C. Kunick, *J. Med. Chem.,* 1999, **42**, 2909-2919.

76 X. Xie, T. Lemcke, R. Gussio, D. W. Zaharevitz, M. Leost, L. Meijer, C. Kunick, *Eur. J. Med. Chem.,* 2005, **40**, 655-661.

77 C. Kunick, Z. Zeng, R. Gussio, D. Zaharevitz, M. Leost, F. Totzke, C. Schächtele, M. H. G. Kubbutat, L. Meijer and T. Lemcke, *Chem. Bio. Chem.,* 2005, **6**, 541-549.

78 T. Pies, K. Schaper, M. Leost, D.W. Zaharevitz, R. Gussio, L. Meijer and C. Kunick, *Arch. Pharm.,* 2004, **337**, 486-492.

79 C. Kunick, K. Lauenroth, K. Wieking, X. Xie, C. Schultz, R. Gussio, D. Zaharevitz, M. Leost, L. Meijer, A. Weber, F. S. Jørgensen and T. Lemcke, *J. Med. Chem.,* 2004, **47**, 22-36.

80 M. Citron, *Nature Rev. Drug. Dis.*, 2010, **9**, 387-398.

81 I. Melnikova, *Nature Rev. Drug. Dis.*, 2007, **6**, 341-342.

82 K. R. Brunden, J. Q. Trojanowski and V. M. Lee, *Nature Rev. Drug Dis.,* 2009, **8**, 783-793.

83 C. J. Phiel, C. A. Wilson, V. M. Lee and P. S. Klein, *Nature*, 2003, **423**, 435-439.

84 B. De Strooper and J. Woodgett, *Nature*, 2003, **423**, 392-393.

85 Data is taken from *WHO factsheet on diabetes*, 2009, URL: http://www.who.int/mediacentre/factsheets/fs312/en/index.html (accessed 30/8/2010).

86 H. Stukenbrock, R. Mussmann, M. Geese, Y. Ferandin, O. Lozach, T. Lemcke, S. Kegel, A. Lomow, U. Burk, C. Dohrmann, L. Meijer, M. Austen and C. Kunick, *J. Med. Chem.,* 2008, **51**, 2196–2207.

87 C. Kunick, K. Lauenroth, M. Leost, L. Meijer and T. Lemcke, *Bioorg. Med. Chem. Lett.*, 2004, **14**, 413-416.

88 C. Reichwald, O. Shimony, U. Dunkel, N. Sacerdoti-Sierra, C. L. Jaffe and C. Kunick, *J. Med. Chem.,* 2008, **51**, 659–665.

89 A. Dobrov, V. B. Arion, N. Kandler, W. Ginzinger, M. A. Jakupec, A. Rufinska, N. G. von Keyserlingk, M. Galanski, C. Kowol and B. K. Keppler, *Inorg. Chem.*, 2006, **45**, 1945-1950.

90 A. Dobrov, V. B. Arion, N. Kandler, W. Ginzinger, M. A. Jakupec, A. Rufinska, N. G. von Keyserlingk, M. Galanski, C. Kowol and B. K. Keppler, *Inorg. Chem.,* 2007, **46**, 3645-3656.

91 W. F. Schmid, R. O. John, G. Mühlgassner, P. Heffeter, M. A. Jakupec, M. Galanski, W. Berger, V. B. Arion and Bernhard K. Keppler, *J. Med. Chem.*, 2007, **50**, 6343-6355.

92 W. F. Schmid, R. O. John, V. B. Arion, M. A. Jakupec and B. K. Keppler, *Organometallics*, 2007, **26**, 6643–6652.

93 M. F. Primik, G. Mühlgassner, M. A. Jakupec, O. Zava, P. J. Dyson, V. B. Arion and B. K. Keppler, *Inorg. Chem.*, 2010, **49**, 302–311.

94 C. Kunick, *Archiv der Pharmazie*, 1992, **325**, 297–299.

95 T. Opatz and D. Ferenc, *Synthesis*, 2008, 3941-3944.

96 T. Opatz and D. Ferenc, *Org. Lett.*, 2006, **8**, 4473-4475.

97 O. Baudoin, M. Cesario, D. Guénard and F. Guéritte, *J. Org. Chem.*, 2002, **67**, 1199–1207.

98 N. Henry, J. Blu, V. Bénéteau and J. Mérour, *Synthesis*, 2006, 3895-3901.

99 L. Joucla, A. Putey and B. Joseph, *Tetrahedron Lett.*, 2005, **46**, 8177-8179.

100 J. G. Avila-Zárraga, A. Lujan-Montelongo, A. Covarrubias-Zúñiga, M. Romero-Ortega, *Tetrahedron Lett.*, 2006, **47**, 7987-7989.

101 E. M. Beccalli, G. Broggini, M. Martinelli, G. Paladino, E. Rossi, *Synthesis*, 2006, 2404-2412.

102 L. Joucla, F. Popowycz, O. Lozach, L. Meijer and B. Joseph, *Helv. Chim. Acta*, 2007, **90**, 753-763.

103 J. B. Bremner and W. Sengpracha, *Tetrahedron*, 2005, **61**, 5489-5498.

104 F. Popowycz, J.-Y. Mérour and B. Joseph, *Tetrahedron*, 2007, **63**, 8689-8707.

105 Y. M. Choi-Sledeski, R. Kearney, G. Poli, H. Pauls, C. Gardner, Y. Gong, M. Becker, R. Davis, A. Spada, G. Liang, V. Chu, K. Brown, D. Collussi, R. Leadley Jr., S. Rebello, P. Moxey, S. Morgan, R. Bentley, C. Kasiewski, S. Maignan, J.-P. Guilloteau and V. Mikol, *J. Med. Chem.*, 2003, **46**, 681–684.

106 L. Xu, I. R. Lewis, S. K. Davidsen and J. B. Summers, *Tetrahedron Lett.*, 1998, **39**, 5159-5162.

107 S. J. Havens, *J. Org. Chem.*, 1985, **50**, 1763-1765.

108 J. J. Song, J. T. Reeves, F. Gallou, Z. Tan, N. K. Yee and C. H. Senanayake, *Chem. Soc. Rev.*, 2007, **36**, 1120-1132.

109 J. J. Song, Z. Tan, F. Gallou, J. Xu, N. K. Yee and C. H. Senanayake, *J. Org. Chem.*, 2005, **70**, 6512–6514.

110 P. A. Crooks and B. Robinson, *Can. J. Chem.*, 1969, **47**, 2061-2067.

111 F. G. Mann, A. F. Prior and T. J. Willcox, *J. Chem. Soc.*, 1959, 3830-3834.

112 L. L. Melhado, *J. Org. Chem.*, 1981, **46**, 1920-1923.

113 X. Doisy, M. Dekhane, M. Le Hyaric, J. Rousseau, S. K. Singh, S. Tan, V. Guilleminot, H. Schoemaker, M. Sevrin, P. George, P. Potier and R. H. Dodd, *Bioorg. Med. Chem.*, 1999, **7**, 921-932.

114 P. Wu, W. Hsieh, Y. Cheng, C. Wei and P. Chou, *J. Am. Chem. Soc.*, 2006, **128**, 14426-14427.

115 C. Lapeyre, M. Delomenède, F. Bedos-Belval, H. Duran, A. Nègre-Salvayre and M. Baltas, *J. Med. Chem.*, 2005, **48**, 8115–8124.

116 H. R. Snyder, S. Swaminathan and H. J. Sims, *J. Am. Chem. Soc.*, 1952, **74**, 5110–5113.

117 A. J. Verbiscar, *J. Med. Chem.*, 1972, **15**, 149-152.

118 Q. Han, C. Dominguez, P. F. W. Stouten, J. M. Park, D. E. Duffy, R. A. Galemmo, Jr., K. A. Rossi, R. S. Alexander, A. M. Smallwood, P. C. Wong, M. M. Wright, J. M. Luettgen, R. M. Knabb and R. R. Wexler, *J. Med. Chem.*, 2000, **43**, 4398-4415.

119 Z. Zhang, Z. Yang, H. Wong, J. Zhu, N. A. Meanwell, J. F. Kadow and T.Wang, *J. Org. Chem.*, 2002, **67**, 6226-6227.

120 K. Yeung, Z. Qiu, M. E. Farkas, Q. Xue, A. Regueiro-Ren, Z. Yang, J. A. Bender, A. C. Good and J. F. Kadow, *Tetrahedron Lett.*, 2008, **49**, 6250-6253.

121 H. Firouzabadi, N. Iranpoor and H. Hazarkhani, *J. Org. Chem.*, 2001, **66**, 7527-7529.

122 M. M. Faul, T. A. Engler, K. A. Sullivan, J. L. Grutsch, M. T. Clayton, M. J. Martinelli, J. M. Pawlak, M. LeTourneau, D. S. Coffey, S. W. Pedersen, S. P. Kolis, K. Furness, S. Malhotra, R. S. Al-awar and J. E. Ray, *J. Org. Chem.*, 2004, **69**, 2967–2975.

123 G. B. Payne, P. H. Deming and P. H. Williams, *J. Org. Chem.*, 1961, **26**, 659-663.

124 E. Droucheau, A. Primot, V. Thomas, D. Mattei, M. Knockaert, C. Richardson, P. Sallicandro, P. Alano, A. Jafarshad, B. Baratte, C. Kunick, D. Parzy, L. Pearl, C. Doerig and L. Meijer, *Biochimica et Biophysica Acta – Proteins and Proteomics*, 2004, **1697**, 181– 196.

125 M. Malinowski and L. Kaczmarek, *J. Pratk. Chem.,* 1988, **330**, 154-158.

126 A. C. Spivey, T. Fekner, S. E. Spey and H. Adams, *J. Org. Chem.,* 1999, **64**, 9430-9443.

127 Y. Yamane, X. Liu, A. Hamasaki, T. Ishida, M. Haruta, T. Yokoyama and M. Tokunaga, *Org Lett.,* 2009, **11**, 5162-5165.

128 S. F. Vasilevsky, S. V. Klyatskaya and J. Elguero, *Tetrahedron*, 2004, **60**, 6685-6688.

129 F. E. Condon and J. P. Trivedi, *J. Org. Chem.,* 1971, **36**, 1926-1930.

130 G. A. Molander, C.-S. Yun, M. Ribagorda and B. Biolatto, *J. Org. Chem.,* 2003, **68**, 5534-5539.

131 H. B. MacPhillamy, R. L. Dziemian, R. A. Lucas and M. E. Kuehne, *J. Am. Chem. Soc.,* 1958, **80**, 2172-2178.

132 G. Cavallini and V. Ravenna, *Il Farmaco*, 1958, **13**, 105-112.

133 J. DeGraw and L. Goodman, *J. Org. Chem.,* 1962, **27**, 1728-1730.